OUKA
The University of Osaka
Institutional Knowledge Archive

Title	Studies on Cell Dome as a cell culture and evaluation platform for advancing drug development
Author(s)	風間, 遼太郎
Citation	大阪大学, 2025, 博士論文
Version Type	VoR
URL	https://doi.org/10.18910/101690
rights	
Note	

The University of Osaka Institutional Knowledge Archive : OUKA

https://ir.library.osaka-u.ac.jp/

The University of Osaka

Studies on Cell Dome as a cell culture and evaluation platform for advancing drug development

Ryotaro Kazama

MARCH 2025

Studies on Cell Dome as a cell culture and evaluation platform for advancing drug development

A Dissertation Submitted to

THE GRADUATE SCHOOL OF ENGINEERING SCIENCE

OSAKA UNIVERSITY

in Partial Fulfillment of the Requirements for the Degree of

DOCTOR OF PHILOSOPHY IN ENGINEERING

by

Ryotaro Kazama

MARCH 2025

Preface

This dissertation was conducted under the supervision of Professor Shinji Sakai in the Division of Chemical Engineering, Graduate School of Engineering Science, Osaka University, from 2021 to 2025.

The objective of this thesis is to establish and apply a novel bioassay method—a cell culture and assay system—that can handle solutions without cell loss or cell damage, provides a 3D microenvironment for the cells, and can be applied to both adherent and non-adherent cells, with high versatility and reproducibility. This innovative system, named the Cell Dome (1 mm in diameter and approximately 300 μm in height), was evaluated for its ability to culture and assess adherent/non-adherent cells, the effects of the hydrogel shell constituting the Cell Dome, its potential as a lymphoma model, and its application in cell-based transfection arrays.

The author hopes this study will contribute significantly to drug development by providing valuable insights into biological and medical research fields through its use as a reproducible *in vitro* model for disease and tumors.

Ryotaro Kazama

Division of Chemical Engineering

Graduate School of Engineering Science

Osaka University

Toyonaka, Osaka, 560-8531, Japan

Abstract

Drug development is critical for the treatment of diseases, disorders, and tumors, and *in vitro* cell-based models play an important role in this process. The aim of the study of this thesis is to establish and apply a novel bioassay method applicable to the drug development process. This method is designed to handle solutions without causing cell loss or cell damage, provide a 3D microenvironment for cells, handle both adherent and non-adherent cells, and ensure high versatility and reproducibility.

Chapter I describes the importance and challenges of bioassays, *in vitro* cell-based models, and cell-based microarrays, for drug development. It also explains the requirements for effective bioassays.

Chapter II describes the establishment of a novel, standardized cell culture and evaluation system for bioassays, within a dome structure fabricated using a semi-permeable hydrogel shell obtained through horseradish peroxidase (HRP)-mediated hydrogelation. This system, a cell-enclosed hydrogel dome with a hemispherical cavity, was named the Cell Dome (1 mm in diameter and approximately 300 μm in height). In addition, the application of Cell Dome as a platform for the evaluation of non-adherent cell culture was demonstrated. Human leukemia cell line K562 cells, non-adherent cells, enclosed in the Cell Dome were stable for 29 days, with the medium replaced every 2–3 days. The enclosed cells proliferated within the cavity and were stained and differentiated with reagents supplied through the surrounding medium. Furthermore, K562 cells filled with the hemispherical cavities of the Cell Dome (3D microenvironment) exhibited more hypoxia and higher resistance to mitomycin C compared to those cultured in 2D environment. These results indicate that the Cell Dome is a promising tool for standardizing bioassays, offering a convenient and effective platform for the culture and evaluation of non-adherent cells.

Chapter III discusses the usefulness of a Cell Dome in the fabrication of organized

hemispherical cell aggregates of adherent HepG2 cells, a human-hepatoblastoma-derived adherent cell line, with the added advantage of easy observation of the cut surface of the spheroid through glass plates. HepG2 cells formed hemispherical cell aggregates that filled the cavity of the Cell Dome after 18 days of culture and could be cultured for up to 29 days. The central adhesive surface of the hemispherical cell aggregates, expected to have an environment similar to that of the center of the spheroid, could be directly observed through the glass plate. Cells cultured in the Cell Dome for 18 days exhibited higher Pi class glutathione S-transferase enzyme activity, hypoxia-inducible factor-1α gene expression, and resistance to mitomycin C compared to cells cultured in a conventional 2D environment. These results highlight the versatility of the Cell Dome as a bioassay platform for both adherent and non-adherent cells (as described in Chapter II), suggesting its potential as a widely applicable and highly useful standard platform for cell-based assays.

Chapter IV explores the effects of the cell adhesion properties of the Cell Dome's hydrogel shell on the behavior of enclosed cells. Since the hydrogel shell is in direct contact with the enclosed cells, its properties were expected to influence the behavior of the enclosed cells. Hydrogel shells with varying degrees of cell adhesion properties were prepared and the behavior of HeLa-fucci2 cells, a human cervical cancer cell line (HeLa) expressing the cell cycle marker fucci2, was observed. Cells cultured in hydrogel shells with cell adhesiveness proliferated along the inner wall of the hydrogel shell. Conversely, cells in hydrogel shells without cell adhesiveness grew uniformly at the bottom of the cavities. Furthermore, cells cultured in non-adhesive hydrogel shells had a higher percentage of cells in the G1/G0 phase compared to those in adhesive shells and exhibited increased resistance to mitomycin when the cavities became filled with cells. These results indicate the importance of considering the cell adhesiveness properties of the hydrogel shell when selecting materials for Cell Dome preparation.

Chapter V describes the application of the Cell Dome system to the development of a 3D lymphoma model primarily composed of non-adherent cells. Both the human brain lymphoma cell line (TK) and the human B-cell lymphoma cell line (KML-1) grew and filled the cavity, with a hypoxic region in the center of the hemispherical structure. CD19 expression did not change in either cell line, while CD20 expression was slightly upregulated in TK cells and downregulated in KML-1 cells cultured in the Cell Dome compared to those cultured in 2D flasks. In addition, both TK and KML-1 cells in the hemispherical structures exhibited higher resistance to doxorubicin compared to those cultured in 2D flasks. These results demonstrate the effectiveness of Cell Dome in producing lymphoma models and highlight its potential as a platform for accurately elucidating the complex cellular functions of lymphoma-derived cells, offering new avenues for addressing the challenges of lymphoma treatment.

Chapter VI describes the application of the Cell Dome system to develop a gene transfer array that can handle non-adherent cells without requiring them to adhere to adhere to a substrate. The human lymphoma cell line (K562 cells) was used as a model for non-adherent cells to explore suitable hydrogel materials as transfection arrays using the Cell Dome (referred to as Cell Dome-based transfection arrays). Gene transfer to suspended non-adherent cells was successfully achieved in Cell Domes with polyvinyl alcohol (PVA)-Ph/chitosan-Ph composite hydrogel shells. In other words, the Cell Dome with an appropriate hydrogel shell could be used as a transfection array for non-adherent cells in suspension. This novel Cell Dome-based transfection array would be a valuable tool for analyzing the cellular function of non-adherent cells in suspension and holds significant potential for providing important biomedical insights for future research and development.

Overall, this thesis examined the establishment of the Cell Dome system as a novel standardized bioassay method and explores its application. The findings highlight the potential of the Cell Dome system as an *in vitro* cell-based bioassay in the drug development process

and provide important insights for both the biological and medical communities.

Table of Contents

Chapter I

General Introduction **1**
1. Three-dimensional (3D) cell culture and cell-based assays **2**
1-1. Floating culture 3
1-2. Hanging drop 3
1-3. Microcapsule 4
1-4. Spinner culture 4
1-5. Microfluidic device 5
1-6. Scaffold-based 3D culture 6
2. Cell microarray **8**
3. Hydrogel dome studies in Sakai Laboratory at Osaka University **9**
3-1. Hydrogel dome obtained through Ca-alginate cross-inking 9
3-2. Hydrogel dome obtained through horseradish peroxidase (HRP)-mediated hydrogelation 9
4. Overview **10**

Chapter II

Establishment of non-adherent cell-enclosing domes with hydrogel shells via enzymatically mediated hydrogelation **13**
1. Introduction **13**
2. Materials and Methods **15**
2.1 Materials 15
2.2 Cell Dome preparation 16
2.3 Cell Domes stability analysis 17
2.4 Hydrogel permeability analysis 17
2.5 Reagent supply analysis to the enclosed cells 18
2.6 Differentiation analysis inside the Cell Dome 18
2.7 Hypoxia analysis 18
2.8 Drug treatment analysis 19
3. Results and Discussion **19**
3.1 Cell Domes structure and stability 19
3.2 Permeability of hydrogel and enclosed cell analysis 21
3.3 Chemical compounds supply and differentiation analysis 23
3.4 Hypoxia and drug-sensitive analysis 25
4. Conclusion **27**

Chapter III

Cell dome as an evaluation platform for adherent HepG2 cells **29**
1. Introduction **29**
2. Materials and Methods **31**
2.1 Materials 31
2.2 Cell Dome preparation 32

2.3 GSTP1/HIF-1α analysis 33
2.4 Anti-cancer drug-sensitivity analysis 34
2.5 Statistical analyses 35
3. Results and Discussion 35
3.1 Hydrogel permeability 35
3.2 Cell growth in Cell Dome 35
3.3 GSTP1/Hypoxia and drug-sensitive analysis 37
4. Conclusion 40

Chapter IV

Effect of cell adhesiveness of Cell Dome's shell on enclosed HeLa cells 42
1. Introduction 42
2. Materials and Methods 45
2.1 Cell culture and chemical synthesis 45
2.2 Hydrogel sheet preparation 45
2.3 Cell Dome preparation and analysis 46
2.4 Cell cycle analysis 47
2.5 *HIF-1α* gene expression analysis 47
2.6 Chemical sensitivity analysis 47
2.7 Statistical analyses 48
3. Results 48
3.1 Cell behavior on hydrogels 48
3.2 Proliferation of cells cultured within Cell Dome 49
3.3 Cell cycle of cells within Cell Dome 52
3.4 HIF-1α and drug-sensitive analysis 54
4. Conclusion 55

Chapter V

Development of hemispherical 3D models of human brain and B cell lymphomas using a Cell Dome system 56
1. Introduction 56
2. Materials and Methods 57
2.1 Cell culture and chemical synthesis 57
2.2 Cell Dome preparation 58
2.4 Initial cell density analysis 59
2.5 Hypoxia analysis 60
2.6 Flow cytometry 61
2.9 Drug sensitivity analysis 61
2.8 Statistical analyses 61
3. Results and Discussion 62
3.1 Proliferation of enclosed cells in Cell Dome 62
3.2 CD19 and CD20 expression on cells enclosed in Cell Dome 64
3.3 Hypoxia and drug-sensitivity analysis 67
4. Conclusion 70

Chapter VI

Cell Dome-based transfection array for non-adherent suspension cells 72
1. Introduction 72
2. Materials and Methods 73
2.1 Materials 73
2.2 Zeta-potential of hydrogels 74
2.3 Lipofection in the presence of hydrogels 75
2.4 Cell Dome preparation 75
2.5 Transfection in Cell Dome 76
2.6 Statistical analyses 76
3. Results and Discussion 76
3.1 Selection of hydrogel shell material 76
3.2 Cell viability and growth of enclosed cells in Cell Dome 78
3.3 Transfection of cells enclosed in Cell Dome with plasmid DNA 79
4. Conclusion 81

Chapter VII

General Conclusions 82

Suggestions for Future Works 85
References 87
List of Publications 100
Acknowledgments 102

Chapter I

General Introduction

Medicines are widely used worldwide to treat various diseases, and their development is crucial for improving human health. Numerous studies are being conducted to develop new drugs to treat diseases [1]. Drug development is an expensive and time-consuming process, that requires meeting certain characteristics of a drug, such as potency, bioavailability, and non-toxicity [2, 3]. In addition, the process typically costs more than $2 billion, takes more than 10 years, and has a success rate of only about 10% before reaching the clinic [4, 5]. Bioassays are an important tool in drug development for measuring the functional activity of molecules in living organisms, tissues, or living cells [6].

There are two types of bioassays: *in vivo* assays, in which substances are administered directly to experimental animals to evaluate *in vivo* reactions, and *in vitro* assays, in which reactions are reviewed in cells using cultured cells or animal tissue. *In vivo* and *in vitro* assays are essential in drug development [7]; however, they often fail to accurately predict candidate drug in terms of toxicity, specificity, and efficacy [8]. Especially, *in vivo* bioassays have limitations due to their high cost, variability, and the increasing global trend of applying the 3R principle (Replacement, Reduction, and Refinement) in use of animals. Consequently, various *in vitro* cell-based bioassays have been developed and are increasingly used for biological activity analysis. Cells used in these cell-based *in vitro* assays are mainly classified as adherent cells and non-adherent cells. Both types are important research target for analyzing cellar function. Adherent cells are mainly represented by solid tumors and many normal cells, and are important in tumor research and the development of artificial organs. Non-adherent cells, on the other hand, are mainly represented by hematopoietic stem cells, such as lymphocytes and

leukocytes, and are important in the study of lymphoma and leukemia. Cell-based bioassays require a standardized platform that can be applied to both cell types. In addition, such platforms must accurately reproduce the *in vivo* tumor environment to enhance the accuracy of the assays, while also being able easy to handle to ensure high efficiency, reproducibility, and practicality. However, there is no standardized platform that is versatile enough to apply to both adherent and non-adherent cells, while combining high operability and reproducibility. The establishment of such new standardized bioassays and their application is expected to not only improve the accuracy of drug development but also provide important insights into biological and medical fields, helping to better understand cell function for disease treatment.

The following sections discuss the importance of three-dimensional (3D) cell culture in cell-based bioassays and provide an overview of previous 3D cell culture methods. In addition, cell-based microarrays, a versatile approach for assessing the genetic behavior of cells, are discussed. Furthermore, section 3 delves into the research and assignments conducted to date in the Sakai laboratory.

1. Three-dimensional (3D) cell culture and cell-based assays

In general, cell-based bioassays involve two-dimensional (2D) cell culture assays conducted in well plates [9]. While these assays offer advantages such as simplicity, reproducibility, and low cost, the loss of tissue-specific structure and cell-to-cell or cell-to-matrix interactions make it difficult to accurately reproduce biological responses such as those observed in 3D organs and tumors [10, 11]. To address the need for improved productivity in drug development, there has been increasing focus on 3D cell culture and 3D cell-based bioassays [11-13]. Compared to the more simplified 2D cell culture, 3D cell cultures more closely mimic *in vivo* environments, providing a more accurate assessment of cell behavior [11]. For instance, drug responsiveness in 3D cell culture is known to be significantly different from that observed in conventional 2D cell culture [14, 15], and it is known that cancer cells cultured in 3D

environments exhibit enhanced resistance to chemotherapeutic agents and altered gene expression levels that induce such resistance compared to those in 2D environments [16]. The advantages of 3D cell culture assays include the ability to evaluate the safety and efficacy drugs under conditions more similar to *in vivo* systems compared to traditional 2D cell culture assays, which can reduce the dropout rate for new drugs during development [11, 13]. In addition, 3D cell culture allows drugs to be tested directly in the human-based system, eliminating species differences often encountered in preclinical animal models that complicate the interpretation of results [17]. In the following section, a 3D cell culture assay is presented (Table 1-1, and Figure 1-1).

1-1. Floating culture

The floating culture method is a technique in which cells are suspended in a medium and spheroids are produced by cell-cell adhesion (Figure 1-1a). The floating culture method utilizes well plates with non-adherent surfaces [18, 19], round-bottom well plates [20, 21], or specially processed multi-well plates [22, 23]. The advantages of these methods are that they are relatively inexpensive, highly efficient, and simple to perform. Conversely, a major challenge with this technique is that the production of spheroids depends on the adhesive properties of the cells, making it unsuitable for non-adherent cells. Additionally, careful handling during procedures like medium exchange and washing is required to avoid cell loss or damage.

1-2. Hanging drop

The hanging drop method involves suspending droplets in specially designed well plates, where cells are cultured within the droplets that are held in place by surface tension (Figure 1-1b). This technique allows for systematic production of large numbers of spheroid-containing droplets at a time, facilitating 3D cell cultures. Previous work has included the development of 384-well format drop culture plates [24] adapted to high-throughput screening (HTS) equipment and 3D cell culture plates with 384 through-holes surrounded by micro-rings in a

384-well format [25]. However, these plates are highly sensitive to small mechanical effects such as media changes, cell staining, or washing, and cannot be maintained for long periods of time. In addition, it is not applicable for the 3D culture of non-adherent cells, which cannot self-organize into spheroids.

1-3. Microcapsule

Microcapsules are a 3D cell culture technique used to fabricate spheroids by encapsulating cells within spherical capsules made up of a hydrogel membrane (Figure 1-1c). These capsules are typically formed using biocompatible polymers such as alginate and gelatin. The semi-permeable membrane of the microcapsules physically protects the cells while permitting exchange of nutrients and oxygen, allowing for cell proliferation, differentiation, and evaluation of drug response. Previous studies have reported the development of alginate-derivative microcapsules and the use of an integrated coaxial microfluidic device with an electrospray system for fabrication of spheroids [26, 27]. The advantage of microcapsules in 3D cell culture include the ability to produce large number of capsules simultaneously and the physical protection they offer against cell loss. However, since the microcapsules are suspended in the culture medium, solution manipulation including medium exchange and staining is difficult, complicating observation, collection, and evaluation. In addition, direct observation of cells in the center of the spheroid—where unique behavior may occur—is challenging.

1-4. Spinner culture

Spinner culture is a technique for producing spheroids by continuously agitating a suspension of cells in a medium solution (Figure 1-1d). This technique is easy to scale up and large quantities of spheroids can be produced relatively simply and easily [28, 29]. Conversely, a limitation of this technique is that continuous agitation generates shear force that can damage cells, making it unsuitable for cells with weak cell-cell adhesion.

1-5. Microfluidic device

Microfluidic devices are a 3D cell culture technique that utilizes microfluidic channels embedded in a substrate to culture cells and circulate medium (Figure 1-1e). These devices have been developed using various materials, including glass/silicon-based, polymer-based, and paper-based platforms [30]. Microfluidic devices can reproduce complex and dynamic microscale environments that mimic the 3D *in vivo* environments, such as complex chemical gradients, and facilitate studies using small sample volumes. Despite their advantages, microfluidic devices have certain disadvantages. The fabrication of complex microstructures is labor-intensive and expensive, and it is difficult to collect 3D cultured cells for downstream analysis and evaluation.

Table 1-1. Summary of three-dimensional (3D) cell culture and cell-based assays and their advantages and disadvantages.

Model	Description	Advantages	Disadvantages	Reference
Floating culture	Cells are suspended in a medium and spheroids are produced by cell-cell adhesion.	Inexpensive, efficient, simple	Not applicable to non-adherent cells, Requires careful solution handling	[18, 19] [20, 21] [22, 23]
Hanging drop	Droplets are suspended in a specially designed well plates and cells are cultured within the droplets held in place by surface tension.	Produce large numbers of spheroids.	Not applicable to non-adherent cells, Requires careful solution handling	[24, 25]
Microcapsule	Technique for 3D cell culture and spheroid fabrication by encapsulating cells within a spherical capsule consisting of a hydrogel.	Physically protects the cells, producing a large number of capsules.	Difficult to handle the solution due to their suspension in a medium, Difficult to direct observation cells in the center of spheroids.	[26, 27]
Spinner culture	Technique for producing spheroids by continuously agitating a medium solution in which cells are suspended.	Easy to scale up, Easy to fabricate a large number of spheroids, simple.	Cell damage due to shear force of fluid, not applicable to non-adherent cells.	[28, 29]

Microfluidic device	Technique for three-dimensional culture using microfluidic devices with microfluidic channels formed on a substrate to culture cells and return medium.	Reproduce complex and dynamic microscale environments.	Labor intensive, expensive, difficult to collect 3D cultured cells for analysis and evaluation.	[30]

1-6. Scaffold-based 3D culture

The extracellular matrix (ECM) is a structural network located between cells that plays an important role in supporting tissue structure/function and influences cell organization and function. Scaffold-based 3D culture techniques leverage ECM or ECM-mimicking materials to better replicate the *in vivo* microenvironment by facilitating interactions between cells and ECM (Figure 1-1d). For these reasons, scaffold-based 3D culture techniques utilize natural or artificial solid scaffolds to support 3D cell culture.

Matrigel (BD Biosciences) is a commercially available ECM, derived from Engelbress-Holm-Swarm (EHS) mouse tumor cells. Matrigel contains basement membrane proteins like collagen IV, laminin, perlecan, entactin, matrix metalloproteinase-2, and growth factors [31]. Matrigel incorporates basement membrane extracts essential for cell differentiation and allows 3D cell culture under conditions where components necessary for cell signaling are present within organized structures [31, 32]. However, because the ECM is a biological material, Matrigel's exact composition varies from batch to batch, making it less suitable for reproducible high-throughput drug testing due to the non-uniform spheroid size [33].

Natural hydrogels are hydrogels derived from natural polymers such as collagen, hyaluronic acid, and gelatin, and are commonly used as scaffolds for 3D cell culture [34, 35]. The advantage of natural hydrogels is that they can mimic the natural ECM. In addition, by modifying the natural polymers with chemical functional groups, their mechanical properties, pore size, density, stiffness, and other characteristics can also be easily controlled.

Synthetic hydrogels are synthesized by polymerization of synthetic polymers such as

polyvinyl alcohol (PVA) and polyethylene glycol oxide (PEG) [34, 35]. Synthetic hydrogels are advantageous for 3D culture due to their high stability, customizable mechanical properties, and well-defined chemical composition. They also contain active chemical groups (amine, acid, and alcohol functional groups) that facilitate precise chemical modifications to form ECM models with well-defined properties. However, synthetic hydrogels are limited in their ability to promote cell signaling.

Table 1-2. Summary of three-dimensional (3D) cell culture and cell-based assays, with their advantages and disadvantages, especially for scaffold-based 3D culture.

Model	Advantages	Disadvantages	Reference
Matrigel	Incorporate basement membrane extracts essential for cell differentiation, widely available.	Exact composition unknown, not reproducible.	[31-33]
Natural hydrogels	Mimic natural ECM, modification of chemical functional groups to manipulate properties.	Inferior mechanical properties, biodegradable.	[34, 35]
Synthetic hydrogels	High stability and mechanical properties, well-defined structure.	Biocompatibility must be confirmed; lack of promotion of cell signaling.	[34, 35]

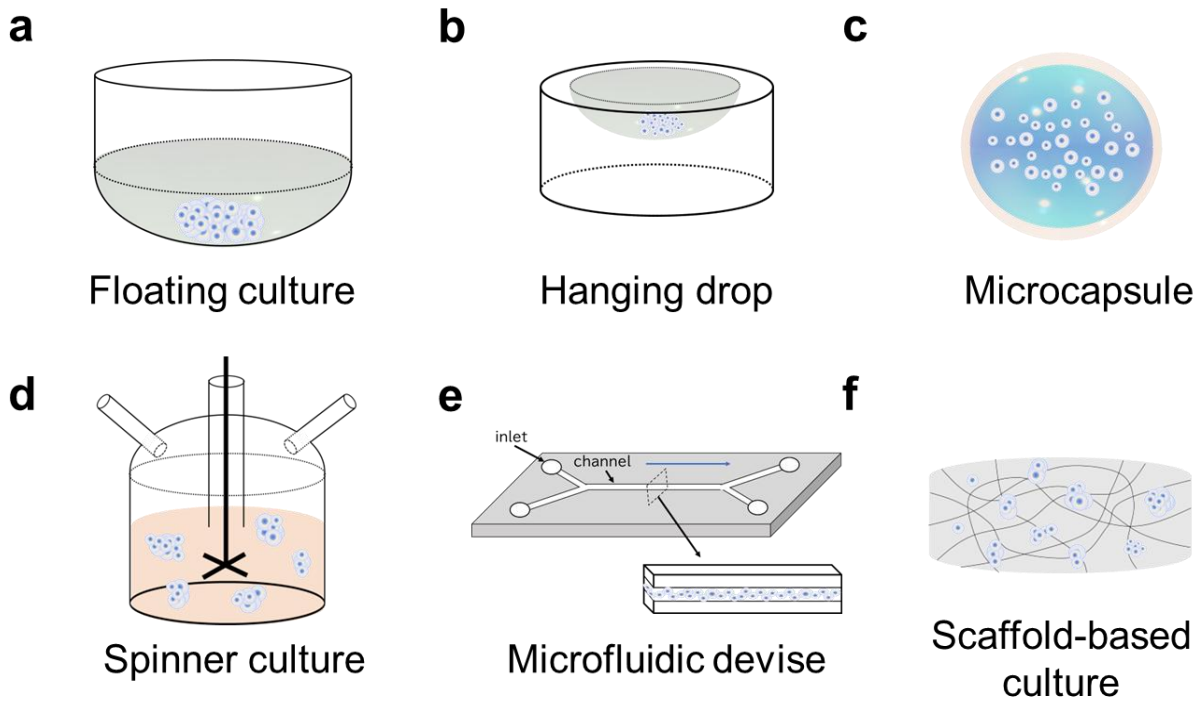

Figure 1-1. Schematic diagram of three-dimensional (3D) cell culture and cell-based assays. (a) Floating culture, (b) Hanging drop, (c) Microcapsule, (d) Spinner culture, (e) Microfluidic device, (f) Scaffold-based culture.

2. Cell microarray

In addition to drug discovery using 2D and 3D cell culture assays, cell-based microarray technology, that allows comprehensive analysis of gene expression levels, is also important for drug development and disease treatment (Figure 1-2). Cell-based microarray is a method in which DNA or genes are deposited onto a glass substrate, upon which cells are cultured to create cell-based arrays, which allows comprehensive evaluation of the genetic behavior of cells based on gene expression [36, 37]. This method is highly efficient and important in biomedical and pharmaceutical research. It can be used to identify drug targets and genes that alter cell behavior and properties. On the other hand, a limitation of this technology is necessary to adhere the cells directly to the spotted DNA or gene, and is thus not possible for non-adherent cells due to their weak cell adhesion properties.

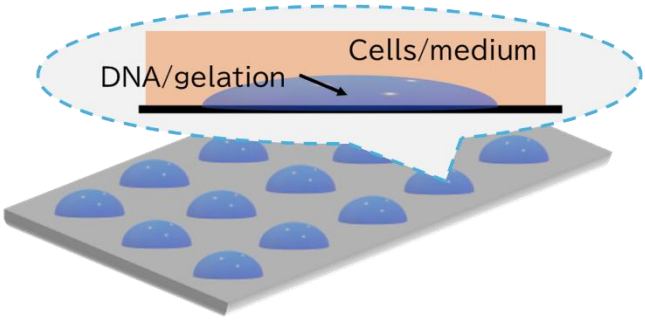

Figure 1-2. Schematic of a cell-based microarray: A method for studying gene function in living cells.

3. Hydrogel dome studies in Sakai Laboratory at Osaka University

Aiming to address the limitations of conventional bioassay methods, the Sakai Laboratory at Osaka University conducted research on hydrogel domes with hemispherical hydrogel membranes, inspired by microcapsule technology. The following sections describe the research and problems addressed so far.

3-1. Hydrogel dome obtained through Ca-alginate cross-inking

Fujiwara [38] reported in his master's thesis the fabrication of hydrogel domes using Ca-alginate crosslinking. In this method, a hemispherical hydrogel membrane is prepared on a glass substrate by forming calcium -alginate crosslinks, and cells are cultured within the membrane. The cells are immobilized by the ionic cross-links formed between the hydrogel membrane and the glass substrate, providing stability for several days. However, the limitation of this method is that it is not possible to perform long-term culture, such as 3D culture, or evaluation and examination over an extended period of time. In addition, the fact that the hydrogel membrane can only be prepared with alginate may prevent the delivery of reagents to the encapsulated cells due to charge interactions.

3-2. Hydrogel dome obtained through horseradish peroxidase (HRP)-mediated hydrogelation

Sato (2019) and Qu (2021) [38, 39] reported on their bachelor and master thesis, respectively, on the fabrication of hydrogel dome obtained by HRP-mediated hydrogelation. In this method,

a hemispherical hydrogel membrane obtained by HRP-mediated hydrogelation was formed on a glass plate, and cells were cultured within the dome. Polymers including alginate, gelatin, and hyaluronic acid modified with phenolic groups (Ph) were used as materials for the hydrogel membrane. It is believed that various polymers modified with Ph groups can be used to create hydrogel membranes for hydrogel domes, offering potential for facilitating improved delivery of reagents to enclosed cells. However, the available studies only provide information on short-term cell culture for a few days using this method, and it remains unclear whether the technique is stable over longer periods and whether it supports long-term cell culture, evaluation, and study. Additionally, no data exist on its application as a bioassay for 3D cell culture or cell microarray. Furthermore, the preparation method and operation are not yet standardized, presenting numerous issues that need to be addressed before this technique can be used as a viable novel bioassay method.

4. Overview

The objective of this study is to establish and apply a novel bioassay method, a cell culture and research system, that can handle solutions without causing cell loss or cell damage, provide a 3D microenvironment for cells, and be applied to both adherent and non-adherent cells, with high versatility and reproducibility.

Chapter II describes the development of a novel, standardized cell culture and evaluation system for bioassays using domes made of semi-permeable hydrogel shells obtained through HRP-mediated hydrogelation. This cell-enclosed hydrogel dome, termed as Cell Dome (1 mm in diameter and approximately 300 μm in height). This chapter specifically focuses on analysis of non-adherent cells, which requires careful manipulation to avoid cell loss or damage during solution manipulation.

Chapter III describes the usefulness of a Cell Dome in the fabrication of organized hemispherical cell aggregates of human-hepatoblastoma-derived HepG2 cells (adherent cells).

The system enables easy observation of the spheroid's cut surface through glass plates. The ability of the Cell Dome to facilitate bioassays for both non-adherent (as described in Chapter II) and adherent cells underscores its potential as a versatile and valuable standard platform for various cell-based assays.

Chapter IV describes the effects of the cell adhesion properties of the Cell Dome's hydrogel shell on the behavior of enclosed cells. The behavior of cancer cell aggregates in 3D cell culture is influenced by cell adherence to their external environment [40, 41]. This chapter explores how differences in the hydrogel shell's adhesion properties influence behavior of cancer cells during cell aggregate formation within the Cell Dome.

Chapter V aims to apply the Cell Dome system to develop a 3D lymphoma model composed mainly of non-adherent cells. Despite its potential to elucidate the resistance to lymphoma therapy and its mechanisms, there are no standardized and reproducible 3D lymphoma models suitable for diverse applications due to their characteristics like weak cell adhesion of the non-adherent cells that mainly comprise lymphoma. Therefore, the development of lymphoma models that better mimic the lymphoma microenvironment is essential to accurately elucidate the complex cellular functions of lymphoma-derived cells and to address the challenges of lymphoma therapy.

Chapter VI describes the application of the Cell Dome system to develop a gene transfer array that can handle non-adherent cells without requiring adhesion to the substrate. This allows gene transfection of non-adherent cells in suspension, a limitation of conventional cell-based microarrays. This novel Cell Dome-based transfection array may offer a valuable tool for analyzing the cellular function of non-adherent cells in suspension and has the potential to provide important biomedical insights, such as identifying disease-causing genes and therapeutic targets.

The results and conclusions of these studies are summarized in the "General Conclusion"

section. In addition, the challenges of this novel Cell Dome system and future research for its application in the drug development process are suggested in the “Future Research” section.

Chapter II

Establishment of non-adherent cell-enclosing domes with hydrogel shells via enzymatically mediated hydrogelation

1. Introduction

Non-adherent or weakly adherent cells, such as hematopoietic cells, lymphocytes, and mesenchymal cells, differ from tissue-constructing adherent cells in functions and gene expression related to intercellular adhesion, migration, invasion, and immunity. Therefore, they are important research targets in biological studies. In cell-based studies and assays, such as functional analyses and drug discovery using imaging, non-adherent or weakly adherent cells require careful handling to avoid cell loss during medium changes and washing steps, unlike adherent cells such as fibroblasts and myoblasts that attach firmly to culture plates [42]. Usually, cytocentrifugation and forced adherence of the cells onto substrates coated with adhesion-inducing molecules are employed to prevent cell loss along with supernatant solutions [43]. However, cytocentrifugation has drawbacks, including inefficiency when handling large numbers of specimens and potential for mild distortion of morphology in the cells of interest [44]. Forced adhesion can also distort cell morphology and cause structural and metabolic changes in cells [45]. Therefore, a system that enables the handling of non-adherent cells with standard solution exchange procedures would be useful for studies involving these cells. In addition, providing a 3D microenvironment for non-adherent cancer cells improves the prediction of chemotherapeutic resistance, compared to cells in 2D culture [46], as observed in adherent cells cultured in 3D systems [47-49]. Karimpoor *et al.* [46] reported that both primary and cell-line leukemia cells cultured in micropores in alginate foam, mimicking the bone marrow microenvironment, showed enhanced myeloid differentiation and reduced sensitivity to antileukemia agents compared to those cultured in 2D environments.

Based on this premise, this chapter aims to establish a standardized system for the culture and study of non-adherent cells that enables the handling of solutions without applying special protocols such as cytocentrifugation and forced cell adhesion, and to provide a 3D microenvironment. To achieve this goal, non-adherent cells were enclosed within hemispherical microdomes on glass plates, consisting of cell-enclosed cavities and semipermeable hydrogel shells obtained through HRP-mediated hydrogelation. HRP-mediated hydrogelation can yield various cell-laden constructs, including fibrous hydrogels [50, 51], microcapsules [52, 53], and 3D-printed hydrogel constructs [54, 55]. This enzymatic process requires hydrogen peroxidase (H_2O_2) as a substrate, but can be optimized to form hydrogel constructs without causing significant damage to the enclosed cells under appropriate conditions [56, 57]. It is expected that the hydrogel shell of microdomes would be permeable to substrates such as oxygen, nutrients, and cell metabolites, supporting the growth of enclosed cells. The semi-permeability of the hydrogel shell allows external stimuli of the enclosed cells, to investigate their chemosensitivity, induce cellular differentiation from the surrounding medium, and stain the cells for imaging applications. Although the molecular permeation properties depend on the preparation conditions, the cells enclosed in the microcapsules prepared through the enzymatic reaction have been demonstrated to grow effectively [58, 59].

Therefore, this chapter describes the establishment of a novel, standardized method for fabricating hemispherical microdomes on glass plates, consisting of cell-enclosed cavities and semipermeable hydrogel shells obtained through HRP-mediated hydrogelation. This construct referred to as the Cell Dome was designed with cavity dimensions of approximately 1 mm in diameter and several hundred micrometers in height (Figure 2-1) [60]. The enzymatic reaction was applied to obtain alginate-based hydrogel shells that were covalently cross-linked and immobilized onto glass plates. Non-adherent cells were enclosed in a Cell Dome on glass plates for further studies. Procedures for enhancing the stability of Cell Domes on glass plates and

the molecular diffusivity of the hydrogel shell were investigated. In addition, the cytocompatibility of the preparation process was assessed by analyzing the growth and behavior of the enclosed cells. Using leukemia cell line K562, as a model of non-adherent cells, the system's suitability was demonstrated by examining cell viability, proliferation, and response to an anti-tumor drug (mitomycin C).

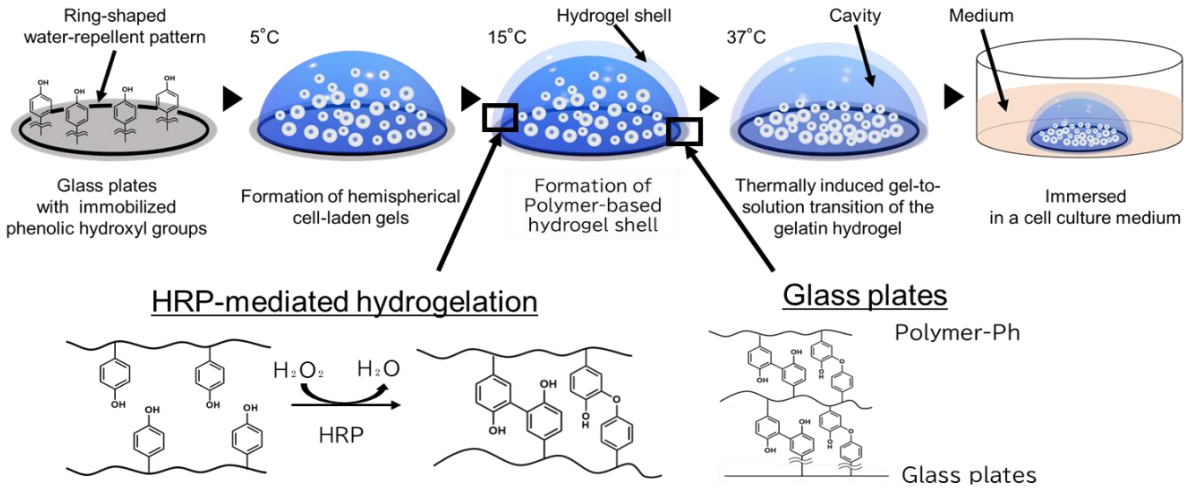

Figure 2-1. Schematic diagram of the fabrication method of Cell Dome enclosing non-adherent cells covered with semipermeable hydrogel shells obtained through horseradish peroxidase (HRP)-mediated hydrogelation. Reprinted (adapted) from [60]. Copyright IOP Science.

2. Materials and Methods

2.1 Materials

Catalase from bovine livers, mitomycin C (MMC), calcium chloride, dimethyl sulfoxide (DMSO), N, N-dimethylformamide (DMF), N-hydroxysuccinimide (NHS), hydrogen peroxide (H_2O_2) aqueous solution (31 wt%), and HRP (180 U/mg) were purchased from Fujifilm Wako Pure Chemical (Osaka, Japan). Water-soluble carbodiimide hydrochloride (WSCD) and tyramine hydrochloride were obtained from Peptide Institute (Osaka, Japan) and ChemImpex International (Wood Dale, IL, USA), respectively. Propidium iodide (PI), CytoRed, Calcein-AM, and FerroOrange were purchased from Dojindo Laboratories (Kumamoto, Japan). Fluorescein isothiocyanate-dextran (FITC-dextran), and gelatin (porcine skin, ~ 300 g bloom,

type A) were purchased from Sigma-Aldrich (St. Louis, MO, USA). Sodium alginate (Kimica I-1G, MW 70 kDa, high guluronic acid content) and poly (lactic-co-glycolic acid) (PLGA) were purchased from Kimica (Tokyo, Japan) and MedChemexpress (NJ, USA), respectively. The hypoxia probe LOX-1 was purchased from Medical & Biological Laboratories (Nagoya, Japan). N-succinimidyl-3(4-hydroxyphenyl)propionate (HPP-NHS) was prepared according to a previous report [61] with slight modifications. Cell Count Reagent SF was purchased from Nacalai Tesque (Kyoto, Japan). RPMI 1640 medium was purchased from Nissui Pharmaceutical (Tokyo, Japan). Sodium alginate and tyramine hydrochloride were conjugated via NHS and WSCD to produce alginate derivatives with phenolic hydroxyl (Ph) moieties (Alginate-Ph, 1.1×10^{-4} mol-Ph/g), as previously reported [62]. In the structure analysis, alginate-Ph labeled with aminofluorescein (AF) (Alginate-Ph-AF, 1.5×10^{-4} mol-Ph/g) was used instead of alginate-Ph. K562 cell, derived from human lymphoma, was purchased from the Riken Cell Bank (Ibaragi, Japan) and cultured in a humidified atmosphere of 5% CO_2/95% air at 37 °C in RPMI 1640 medium with 10% (v/v) fetal bovine serum (FBS). The (3-aminopropyl) triethoxysilane (APS)-coated glass plates (size: 18 mm × 18 mm, thickness: 0.8 mm) with ring-shaped water-repellent patterns (inner diameter: 1 mm, outer diameter: 1.4 mm) arranged in an array of 6 × 6 with 2.5 mm intervals were purchased from Matsunami Glass (Osaka, Japan), and used for each experiment after cutting it to a suitable size, as necessary.

2.2 Cell Dome preparation

To immobilize phenolic hydroxyl groups onto the glass plates, the plates were immersed in DMF containing 2.5% (w/v) HPP-NHS for 24 h. Next, at 5 °C, a phosphate-buffered saline (PBS, pH 7.4) solution (core; 1 μL) containing 50 U/mL HRP, 3.0% (w/v) gelatin, and 1.0×10^6 cells/mL K562 cells was spotted into the ring-shaped water-repellent pattern on the glass plates. After allowing the gelatin-based core gel to stand for 15 min, PBS solution containing 1 mM H_2O_2 and 1.0% w/v% alginate-Ph was added on the gelatin-based core gels at 15 °C.

After 5 min forming an alginate-based hydrogel shell obtained through HRP-mediated hydrogelation, the resultant glass plates were rinsed twice with PBS to remove the remaining solution and immersed in a medium containing 0.5 mg/mL catalase, and incubated for the formation of the hemispherical hollow structure due to the thermally induced gel-to-solution transition of the gelatin hydrogel (Figure 2-1). After 24 h of incubation, the medium was replaced with fresh medium every 2–3 days. The structure of the Cell Dome was analyzed using a confocal laser scanning microscope (C2; Nikon, Tokyo, Japan) by preparing the Cell Dome using alginate-Ph-AF instead of alginate-Ph. The viability of K562 cells was analyzed with live/dead staining using Calcein-AM/PI and observed through a fluorescence microscope (BZ-9000; Keyence, Tokyo, Japan). K562 cells enclosed in the Cell Domes were captured using the fluorescence microscope and further analyzed with an optical coherence tomography (OCT) system using Cell3iMager Estier (CC-9000; Screen, Kyoto, Japan).

2.3 Cell Domes stability analysis

For stability analysis, Cell Domes were prepared using core solutions without cells, as described in section 2.2. In addition, microdomes were prepared under two conditions to investigate their stability. The first condition involved preparing the microdomes using glass plates without immobilized Ph groups, and the second condition involved preparing microdomes with Ca-alginate hydrogel shells. To prepare Ca-alginate hydrogel shell, gelatin-based core solutions were prepared from a PBS solution containing 100 mM calcium chloride and 3.0% (w/v) gelatin. PBS solution containing 1.0 w/v% sodium alginate was then added onto core gels for form Ca-alginate hydrogel shell. The stability of the Cell Domes was evaluated by counting the number of remaining Cell Domes or microdomes at each incubation period.

2.4 Hydrogel permeability analysis

The gels used for permeability analysis were prepared with the same concentration as Cell

Dome: mixing PBS solutions (200 μL) containing 50 U/mL HRP, 1.0 w/v% alginate-Ph, and 10 mM of H_2O_2 in wells of 24 well-plates. The prepared gels were rinsed twice with PBS, immersed in PBS solution containing 0.5 mg/mL FITC-dextran (molecular weight 4,000, 10,000, or 70,000), and incubated at 37 °C for 24 h. The fluorescence recovery after photobleaching (FRAP) method was used to measure the diffusion coefficients, by using a confocal laser scanning microscope, as previously reported [63].

2.5 Reagent supply analysis to the enclosed cells

Before the Cell Dome preparation described in section 2.2, DMSO (0.2 μL) with 50 μg/mL PLGA containing 20 μM CytoRed or Calcein-AM was spotted inside the ring-shaped water-repellent pattern on the glass plates and allowed to dry at 37 °C for 1 h. After the Cell Domes were formed, the enclosed cells were observed at various incubation periods using a fluorescence microscope.

2.6 Differentiation analysis inside the Cell Dome

To induce differentiation to erythroids, the medium surrounding the Cell Dome was replaced with a medium containing 1 mM sodium butyrate after 13 days of culture [64]. After 6 days of culture in the differentiation medium, cell differentiation was observed by staining K562 cells with Hank's balanced salt solution with 20 mM HEPES containing 1 μM FerroOrange, a fluorescent probe that detects intracellular Fe^{2+}. After 30 min of staining, the cells were observed using a fluorescence microscope. Additionally, the enclosed cells were collected by degrading the hydrogel shell with PBS solution containing 1 mg/mL alginate lyase, and the collected cells were analyzed using a flow cytometer (BD Accuri C6; BD, Tokyo, Japan).

2.7 Hypoxia analysis

After the appropriate culture period, Cell Domes were immersed in a medium containing 2 μM hypoxia probe LOX-1 to analyze the hypoxic state of the enclosed cells. After 24 h of incubation, the enclosed cells were rinsed twice with PBS and observed using a fluorescence

microscope. Additionally, the enclosed cells were collected as the same method described in section 2.6 and analyzed using a flow cytometer.

2.8 Drug treatment analysis

After the appropriate culture period, one Cell Dome was immersed in 200 μL of medium, and 20 μL of PBS (pH 7.4) containing 1, 10, 100, 1,000, or 10,000 nM MMC was added, and incubated for 72 h. Then, they were added 20 μL of Cell Count Reagent SF. After 4 h of incubation, the absorbance at 450 nm (with a reference wavelength of 600 nm) was measured using a microplate reader (EPOCH 2; BioTek, CA, USA). Relative activity was calculated by dividing the absorbance with MMC by the absorbance of without MMC and multiplying by 100.

3. Results and Discussion

3.1 Cell Domes structure and stability

To fabricate the Cell Dome with a hydrogel shell and hemispherical cell culture space, I focused on the microcapsule conditioning technique [16, 46, 65]. The gelatin-based core solution was used as a template for the hemispherical cavity, and the hydrogel shell was obtained through HRP-mediated hydrogelation. Ca-alginate hydrogels have commonly been used in studies involving cell-encapsulated microcapsules [66-68]. To ensure stable attachment of the Cell Dome to the glass plate, I applied an enzymatically derived Alginate-Ph hydrogel and aimed to form covalent bonds between the substrate and the hydrogel shell.

In the structure analysis by using the Alginate-Ph-AF hydrogel shell obtained through HRP-mediated hydrogelation, the thickness, and height of the hydrogel shell were 90 μm and 270 μm, respectively (Figure 2-2a).

In the stability analysis, microdomes with Ca-alginate hydrogel shells disappeared from the glass plate after just 1 day of immersion in the medium. Similarly, microdomes with alginate-Ph hydrogel shells (which did not form covalent bonds with the glass plates) all disappeared

from the substrate after 6 days of immersion (Figure 2-2b). In contrast, Cell Domes with alginate-Ph hydrogel shells prepared through HRP-mediated hydrogelation remained securely attached to the glass plates with Ph groups for 6 days, demonstrating high stability (Figure 2-2b). These results indicate that the formation of covalent cross-links between the glass plates and the hydrogel shell by HRP-mediated hydrogelation reaction contributes to the high stability of Cell Dome. Interestingly, microdomes prepared on glass plates without Ph groups in alginate-Ph hydrogel exhibited greater stability than Ca-alginate microdomes. This may be due to covalent cross-linking between alginate-Ph molecules. Sakai et al. [62] previously reported that alginate-Ph microcapsules cross-linked through enzymatic reaction exhibited less swelling than Ca-alginate microcapsules in saline solutions. Ca-alginate hydrogels swell in saline and culture media due to an ion exchange process between calcium ions in the hydrogel and sodium ions in these solutions [69]. This suggests that in addition to the covalent cross-linking between the glass plate and hydrogel shell, the internal covalent cross-linking of Alginate-Ph molecules contributes to the overall stability of the Cell Dome developed in this study.

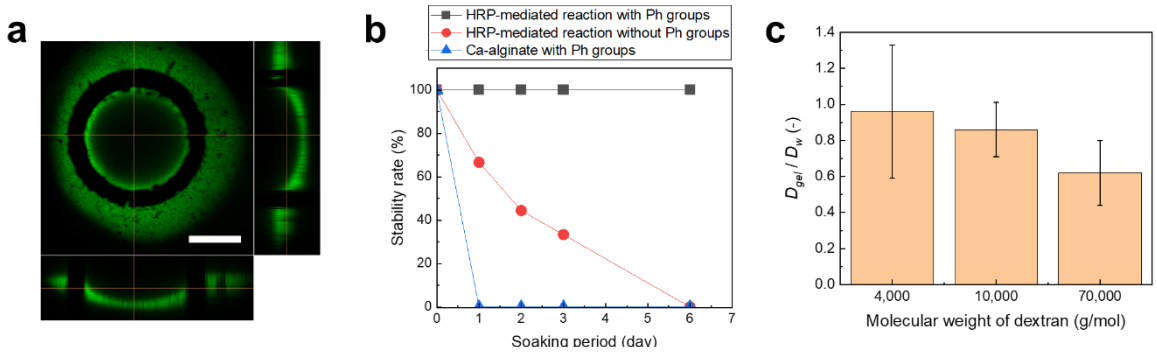

Figure 2-2. (a) Confocal microscope image of the hydrogel shell. Scale bar: 500 µm. (b) The stability of microdomes with Ca-Alginate hydrogel shells (▲), microdomes with Alginate-Ph hydrogel shell prepared through HRP-mediated cross-linking on the glass plates without Ph groups (●), and Cell Domes with Alginate-Ph hydrogel shell prepared through HRP-mediated cross-linking on the glass plates with Ph groups (■) ($n \geq 16$). (c) The diffusion coefficients of FITC-dextrans in Alginate-Ph hydrogel prepared through HRP-mediated hydrogelation. Bars: SD, $n = 5$. Reprinted (adapted) from [60]. Copyright IOP Science.

3.2 Permeability of hydrogel and enclosed cell analysis

The viability of K562 cells immediately after and the day after Cell Dome preparation was 96.7 ± 1.7% and 97.1 ± 0.6%, respectively, the values being comparable to those before enclosure (Figure 2-3a). This indicates that the Cell Dome preparation process does not significantly affect the viability of the enclosed cells.

Next, to investigate substance permeation and diffusion within the Cell Domes, the diffusion coefficient of FITC-dextran in alginate-Ph hydrogels obtained through HRP-mediated hydrogelation was measured using the FRAP method. The relative diffusion coefficients in the hydrogel, compared to diffusion in water were 0.96 ± 0.37, 0.72 ± 0.15 and 0.62 ± 0.18 for FITC-dextran with molecular weights of 4,000, 10,000, and 70,000, respectively (Figure 2-2c). Values closer to 1 indicate efficient diffusion, indicating that the hydrogel shell of the Cell Domes was highly permeable to metabolites, nutrients, and oxygen. Immediately after preparation, K562 cells were observed to be individually present within the hemispherical cavity of the Cell Domes. Over time, as the number of enclosed cells in culture increased, the hemispherical cavity's dark area and intensity of darkness gradually increased, indicating robust cell growth within the Cell Dome (Figures 2-3b–g). This result was also observed from the increase in mitochondrial activity per Cell Dome, which reached a maximum on 10 days of culture and did not increase thereafter (Figure 2-3i). The Cell Domes retained their structural integrity even after 29 days of culture, and within the hemispherical cavity of the Cell Dome, K562 cells demonstrated three-dimensional growth (Figure 2-3h). The slight decrease in mitochondrial activity after 10 days of culture is consistent with findings reported by Zhang *et al.*, who reported a similar transition in mitochondrial activity of K562 encapsulated in microcapsules [70]. They explained that the decrease was due to increased lactate in the cavity caused by increased cell density [70].

The time required to fill the hemispherical cavity with enclosed K562 cells, within the Cell Dome, can be adjusted by varying the initial cell density and the size of the hemispherical cavity. Additionally, the diffusion coefficient of the hydrogel shell was lower than that of water for molecules with a molecular weight of approximately 10,000. This indicates that the required staining time for the enclosed cells would need to be extended compared to systems without Cell Dome. Enhancing the molecular permeability of the hydrogel shell is possible by lowering the polymer concentration, reducing the degree of cross-linking, or reducing the thickness of

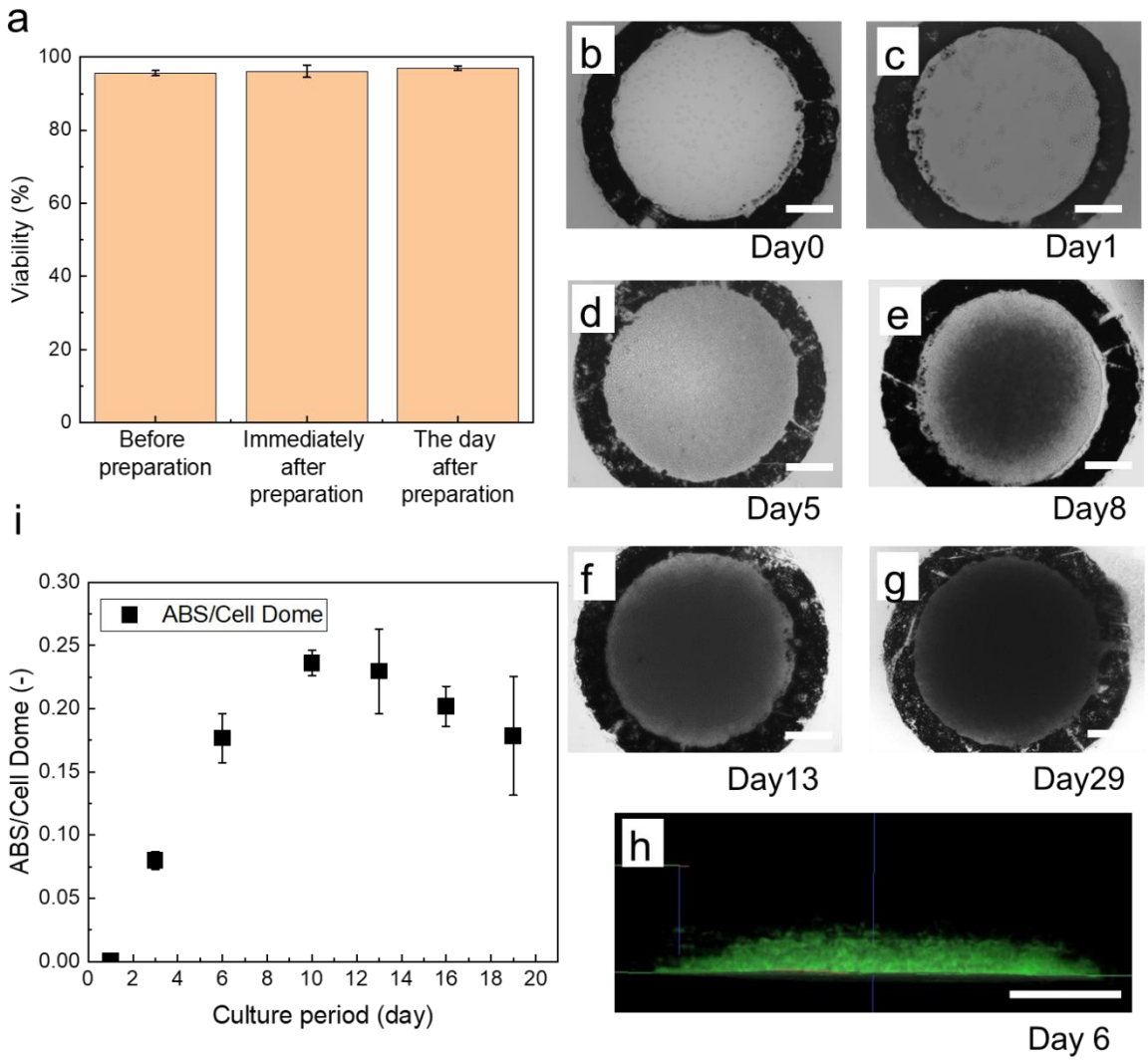

Figure 2-3. (a) Viabilities of K562 cells before, immediately after, and one day after preparation of Cell Domes. (b–g) Growth of K562 cells within the Cell Dome. (h) 3D reconstructed images of the cells in the hemispherical cavities of the Cell Dome after 6 days of culture, visualized using Cell3iMager Estier. (i) Mitochondrial activity transition of cells per Cell Dome over time. Bars in panels a and i represent SD, $n = 5$. Scale bars in panels b–h: 250 µm. Reprinted (adapted) from [60]. Copyright IOP Science.

the hydrogel shell. However, such adjustments must also consider the structural stability of the hydrogel shell to maintain the Cell Dome's integrity. A limitation of the hydrogel shell of Cell Dome in this study is its binding to positively charged molecules, of the charged nature of the alginate-Ph used as the hydrogel shell material [71]. This issue can be addressed by using positively charged polymers such as chitosan, dextran [72], and gelatin [73, 74] in the preparation of the Cell Dome.

3.3 Chemical compounds supply and differentiation analysis

Two types of reagent delivery conditions were investigated to supply chemical compounds to the enclosed cells. (1) delivery of the chemical compound from the bottom of the Cell Dome, and (2) deliver the compound from the surrounding medium in which the Cell Dome is immersed.

To supply chemical compounds to the enclosed cells from the bottom of the Cell Dome, a PLGA solution containing CytoRed or Calcein-AM was spotted onto the glass plate before the Cell Dome preparation. After 1 day of culture, the enclosed cells in each Cell Dome showed red or green fluorescence emitted by CytoRed or Calcein-AM, respectively (Figure 2-4). These fluorescences were also observed after 4 days of incubation, indicating successful compound delivery from the bottom of the Cell Dome. This approach allows for evaluation of various conditions on a single glass plate by spotting different chemical compounds in separate Cell

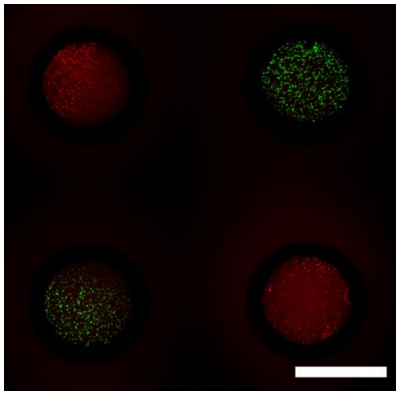

Figure 2-4. Fluorescence microscopic image of the enclosed cells in Cell Domes. Fluorescence signals emitted by Calcein-AM or CytoRed. Scale bar: 1 mm. Reprinted (adapted) from [60]. Copyright IOP Science.

Domes. The methodology extends beyond fluorescent substances to include drugs, enzymes, proteins, and genes, making it a versatile tool for studying compound uptake and cellular responses. In this study, the uptake of compounds by cells in the adjacent Cell Domes was observed after several days of culture. To avoid the effects of compounds enclosed in the adjacent Cell Dome, controlling the charge of the hydrogel shell or using polymeric compounds impermeable to the hydrogel shell would be effective.

Next, I examined the technique of supplying compounds to the enclosed cells from the surrounding medium in which the Cell Dome is immersed. K562 cells differentiate into erythrocytes when exposed to sodium butyrate [64]; hence, I cultured the enclosed cells in a medium containing sodium butyrate for 6 days. To assess differentiation, the enclosed cells

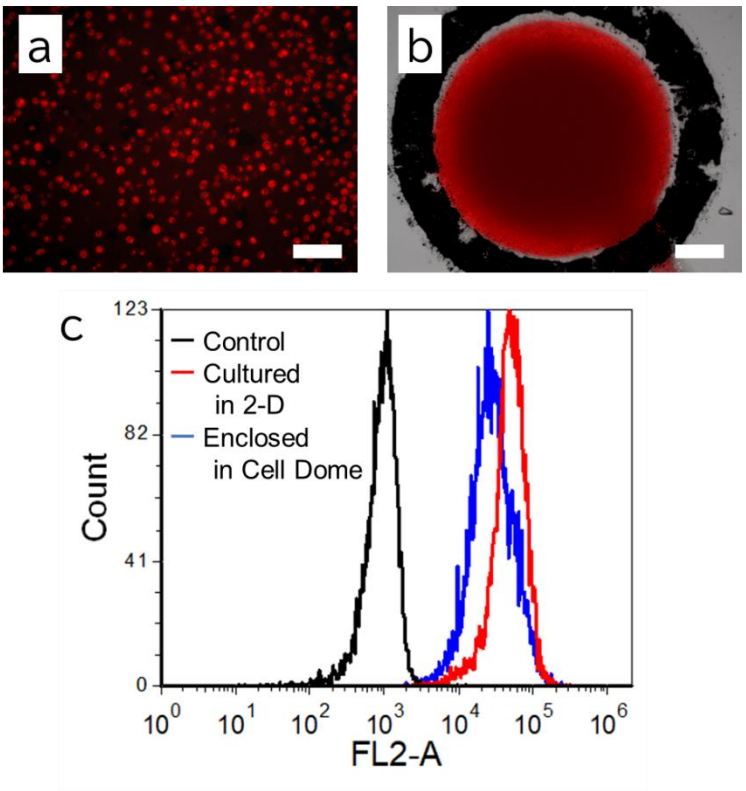

Figure 2-5. (a, b) Fluorescence microscopic images of cells cultured in a 2D environment (a) and cells enclosed within the Cell Dome (b) stained with FerroOrange after incubation in a medium containing sodium butyrate. Scale bars: 250 μm. (c) Fluorescence intensities attributed to the reaction of FerroOrange with Fe^{2+} detected on the cells cultured in 2D (red line) and cells enclosed within the Cell Dome (blue line) in a medium containing sodium butyrate, as well as cells cultured in a medium without sodium butyrate (black line). Reprinted (adapted) from [60]. Copyright IOP Science.

were stained with FerroOrange, which displayed red fluorescence indicative of intracellular Fe^{2+} in erythrocytes, similar to cells cultured in a 2D environment (Figures 2-5a and b). Additionally, flow cytometric analysis revealed higher fluorescence intensity due FerroOrange-Fe^{2+} reaction in cells cultured in a medium containing sodium butyrate compared to those cultured without it (Figure. 2-5c). This indicates that, for the enclosed cells, both staining reagents as well as differentiation-inducing compounds effectively permeate the hydrogel shell of the Cell Dome.

In conclusion, the Cell Dome developed in this study introduces a new bioassay technology that enables good proliferation of enclosed non-adherent cells. Additionally, it facilitates easy evaluation procedures, such as staining, medium exchange, and washing.

3.4 Hypoxia and drug-sensitive analysis

In section 3.3, I demonstrated that it is possible to stain enclosed cells using reagents. In this section, I describe the analysis of the hypoxic state of enclosed cells in the Cell Dome using the hypoxia probe LOX-1, a reagent that stains hypoxic cells. After 13 days of culture, the enclosed cells stained with LOX-1 showed red fluorescence indicative of hypoxia, with the fluorescence intensity being stronger closer to the core of the Cell Dome (Figure 2-6a). This result was also confirmed by flow cytometry, revealing two distinct cell populationa: LOX-1-positive (hypoxic) cells and LOX-1-negative (non-hypoxic) cells (Figure 2-6b). Hypoxic cells were predominantly located at the core of the Cell Dome, while non-hypoxic cells were located closer to the hydrogel shell. This is likely due to oxygen supply from the medium surrounding the Cell Dome. In other words, this result indicates that there is an oxygen concentration gradient in the Cell Dome and that the heterogeneous cell population in the Cell Dome can be easily observed under a microscope because of the hemispherical structure of the Cell Dome. The utility of cancer cell spheroids in drug development studies is widely known [47, 48], especially their ability to adapt metabolically to microenvironmental stress induced by

diffusion gradients of oxygen and nutrients [48, 75]. As various cancer cells including K562 cells are known to exhibit hypoxic conditions [76, 77], I hypothesized that cells cultured within the Cell Dome might develop drug resistance. Indeed, examination of the chemosensitivity of K562 cells cultured in the Cell Dome demonstrated that cells cultured 13 days after enclosure were more resistant to MMC than those in the 2D or in the Cell Dome for just 1 day (Figure 2-6c). In addition, the cells cultured in 2D and those within Cell Dome for 1 day showed similar responses to MMC, indicating that the alginate-Ph hydrogel shells allowed effective

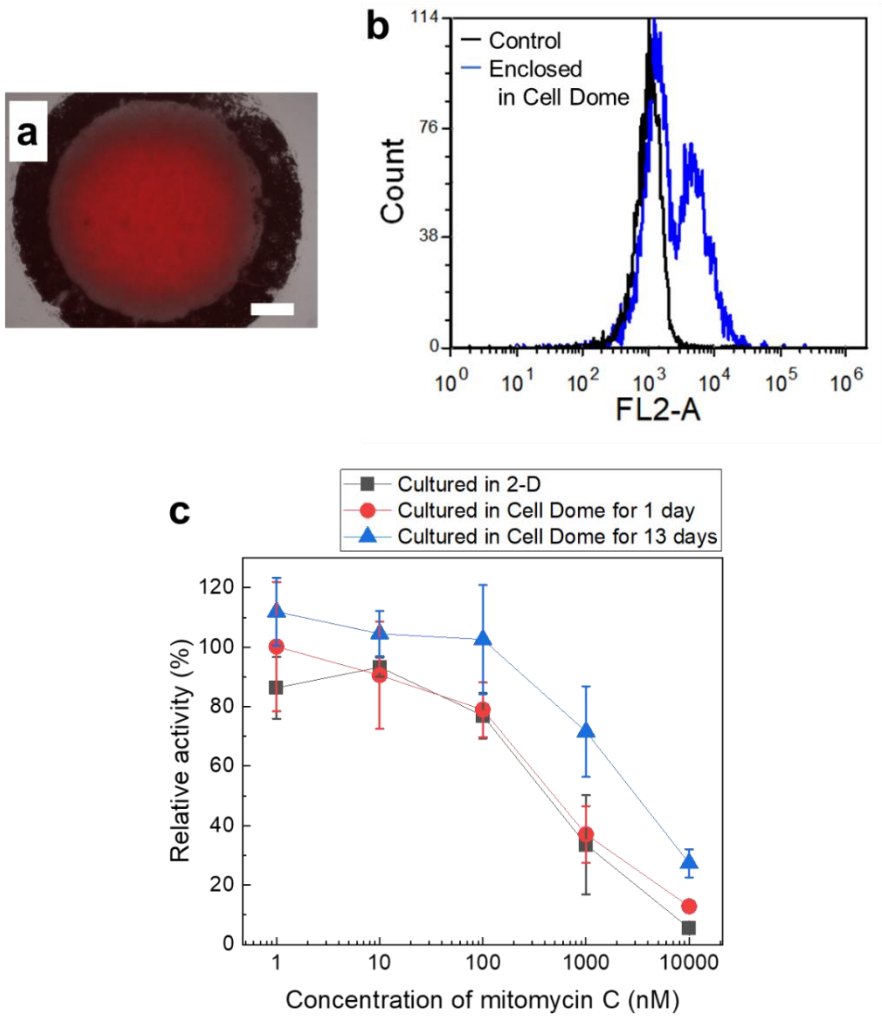

Figure 2-6. (a) Fluorescence microscopic image of the cells in the Cell Dome stained with the hypoxia probe LOX-1 after 13 days of culture. Scale bar: 250 µm. (b) Fluorescence intensities from the reaction of hypoxia probe LOX-1 in cells collected from Cell Domes (blue line) and cells cultured in 2D (black line). (c) Drug response to mitomycin C in cells cultured in 2D (■) and those enclosed for 1 day (●) and 13 days (▲). Bars: SD, n = 5. Reprinted (adapted) from [60]. Copyright IOP Science.

penetration of MMC. These results indicate that cells enclosed within Cell Dome acquired drug-resistance induced by hypoxia and have the potential to be used as a highly reproducible tool for drug screening.

4. Conclusion

The purpose of this study was to establish a standardized system that enables handling of non-adherent cells for imaging-based studies and assays, including application on cell culture plates, and to evaluate the usefulness of this novel system. The hydrogel shell of the Cell Dome demonstrated its ability to allow staining reagents to permeate into the cavity containing the cells, enabling effective staining and subsequent microscopic observation. These capabilities were confirmed through studies using the Fe^{2+} detector FerroOrange (Figure 2-4), the hypoxia probe LOX-1 (Figure 2-5), and fluorescent live/dead staining using Calcein AM and PI (Figure 2-3a). Enclosed cells successfully differentiated in response to sodium butyrate, similar to cells in 2D culture (Figure 2-4), and exhibited measurable response to anticancer drugs supplied via the culture medium (Figure 2-5c) This highlights the effectiveness of the Cell Dome in diverse cell-based studies. The system also enabled the easy collection of enclosed cells for flow cytometric analysis, as demonstrated with K562 cells stained with fluorescent probes (Figures 2-5c and 2-6b). This was achieved by immersing the alginate-Ph hydrogel shell in a solution containing alginate lyase for 5 min, effectively degrading the shell. Furthermore, the Cell Dome does not disintegrate its hydrogel shell, allowing direct microscopic observation of the cells in the core, an important feature in cancer research.

In conclusion, the Cell Dome system established in this study offers a significant improvement in the culture, manipulation of non-adherent cells, making it a promising standardized platform for the manipulation and evaluation of non-adherent cells.

Some portion of this thesis, including text and figures, have been previously published in the journal article “Development of non-adherent cell-enclosing domes with enzymatically cross-linked hydrogel shell” by Kazama *et al.*, published in *Biofabrication*, 2023, 15, 015002 (Reference No. 60). These sections are reproduced here with permission from IOP Science.

Chapter III

Cell dome as an evaluation platform for adherent HepG2 cells

1. Introduction

Various cancer models have been actively studied for new drug testing and cell behavior evaluation in drug development [78, 79]. Solid cancer models using human-derived cells have been reported, including predictive models [80], colorectal cancer models [81], and breast cancer models [82, 83]. Solid tumors are often composed of adherent cells, and liver-derived cells are among those used in such models.

Liver-derived cells are widely used in research, including metabolite profiles and drug development [84], because it is important to investigate hepatotoxicity, hepatic metabolism, and absorption/excretion of candidate drugs in the liver [85]. The cell line most commonly used to study hepatotoxic mechanisms of drugs and toxins is HepG2 cells [86, 87]. Since there are differences in the functional, transcriptomic, and proteomic levels between HepG2 cells cultured in 2D and primary human hepatocytes [88, 89], HepG2 cells do not fully reflect all hepatic functions *in vivo*, although they are easier to handle than primary human hepatocytes and their responses are more reproducible [84, 90].

In general, 2D substrates are widely used as a cell culture method and cell evaluation system for HepG2 cells, because of their simplicity, reproducibility, and low cost [91, 92]. However, for drug development and mechanistic studies, evaluation using HepG2 cells cultured in 3D rather than those cultured in 2D is garnering attention, because cells cultured in 3D provide better biological models compared with those cultured in 2D [93-95]. HepG2 cells cultured in 3D exhibit enhanced expression of phase II drug metabolism enzymes and transporters [94, 96, 97]. Phase II enzymes are involved in the detoxification and activation of many xenobiotics and transporters involved in their absorption and excretion. The elevation of their expression

in HepG2 cells to match the levels found in primary hepatocytes is crucial for drug discovery and pharmacokinetic research.

Based on the previous studies, various 3D HepG2 cell culture systems have been developed, such as microwells [98, 99], hanging drops [100], and microcapsules [53, 101]. Previous 3D systems have been used to produce spherical spheroids. In HepG2 cells, the cells at the center of the spheroids become hypoxic, leading to an increase in the expression of hypoxia-inducible factor-1α (HIF-1α), which is involved in various processes such as drug metabolism [75, 77, 102]. Until now, observing cells at the center of spheroids has traditionally used protocols such as fixation/sectioning or confocal laser scanning [103, 104].

In chapter II, I introduced a culture/research system known as the Cell Dome which is1 mm in diameter and approximately 300 μm in height. The system was established to culture non-adherent cells in 3D microenvironment [60]. The Cell Dome is a hemispherical microdome fabricated on a glass plate, with cells enclosed in a cavity surrounded by a hemispherical hydrogel shell. The hemispherical hydrogel structure containing cells was created through the thermal sol-gel transition of gelatin, followed by HRP-mediated hydrogelation, and the hydrogel shell was then immobilized onto the glass plate.

The aim of this chapter was to evaluate the usefulness of the Cell Dome in the fabrication of organized hemispherical cell aggregates of HepG2 cells, an adherent cell line, enabling easily observation of the cut surface of the spheroid through glass plates. A platform that allows the straightforward observation and evaluation of HepG2 cells cultured in 3D would be valuable for drug development. The versatility of the Cell Dome, which can be applied to both non-adherent cells (as described in Chapter II) and adherent cells, highlights its potential for a wide range of cell-based assays, positioning it as a highly useful and standardized platform. The proliferation and behavior of HepG2 cells enclosed in Cell Dome, including the cellular compatibility of the preparation process, changes in Pi-class Glutathione S-Transferase

(GSTP1) activity, associated HIF-1α gene expression, and tolerance to antitumor drugs (mitomycin C), were compared to those of cells cultured in 2D [105].

2. Materials and Methods

2.1 Materials

The glass plates (thickness: 0.8 mm, size: 18 mm × 18 mm), coated with aminosilane and printed with water-repellent patterns in a ring shape (outer/inner diameter: 1.4/1.0 mm) were purchased from Matsunami Glass Ind., Ltd. (Osaka, Japan). Alginate lyase from *Flavobacterium sp*., trypsin from porcine pancreas, type B gelatin from bovine skin (ca. 250 g bloom), type A gelatin from porcine skin (ca. 300 g bloom), and fluorescein isothiocyanate-dextran (FITC-dextran) were purchased from Sigma-Aldrich (St. Louis, MO, USA). N-hydroxysuccinimide (NHS), mitomycin C, horseradish peroxidase (HRP, 180 units/mg), catalase from bovine liver, H_2O_2 aqueous solution (31 wt.%), and N,N-dimethylformamide (DMF) were purchased from Fujifilm Wako Pure Chemical Industries (Osaka, Japan). Propidium iodide (PI), dihydrate (EDTA·2NA) disodium salt, and ethylenediamine-N,N,N',N'-tetraacetic acid were sourced from Dojindo (Kumamoto, Japan). Calcein-AM was purchased from Nacalai Tesque Inc. (Kyoto, Japan). Water-soluble carbodiimide hydrochloride (WSCD·HCl) and 3-(4-hydroxyphenyl) propionic acid were sourced from the Peptide Institute (Osaka, Japan) and Tokyo Chemical Industry (Tokyo, Japan), respectively. Sodium alginate (Kimica I-1G, Mannuronic acid/Guluronic acid ratio ≈ 0.7), tyramine hydrochloride, and 3-(4-hydroxyphenyl) propionic acid were obtained from Kimica (Tokyo, Japan) and Chem-Impex Inter-national (Wood Dale, IL, USA), respectively. The primers used for real-time PCR analysis were purchased from Eurofins Genomics (Tokyo, Japan). 3-(4-Hydroxyphenyl)propionic acid N-hydroxysuccinimide ester (HPP-NHS) was synthesized as previously described [106]. Gelatin-Ph (2.4×10^{-4} mol-Ph/g) and alginate-Ph (1.1×10^{-4} mol-Ph/g) were synthesized using type B gelatin or sodium alginate with tyramine hydrochloride

or 3-(4-hydroxyphenyl) propionic acid via WSCD·HCl/NHS chemistry, as previously described [62, 107].

HepG2 cells were purchased from the Riken Cell Bank (Ibaraki, Japan) and cultured in Dulbecco's Modified Eagle's Medium (DMEM; Nissui, Tokyo, Japan) containing 10% (v/v) FBS in an atmosphere humidified with 5% CO_2 and 95% air at 37 °C.

2.2 Cell Dome preparation

Cell Domes for enclosing HepG2 cells, which serve as a model for adherent cells, were prepared based on a previously reported method [60]. The core solution (1 μL, PBS containing 1.2×10^6 cells/mL HepG2 cells, 3.0% (*w*/*v*) type A gelatin, and 50 U/mL HRP) was spotted into a ring-shaped hydrophobic pattern on the glass plates, on which phenolic hydroxyl groups had been immobilized via HPP-NHS. After allowing it to stand at 5 °C for 15 min, 10 μL of the shell solution (PBS containing 1 mM H_2O_2, 1.0 w/v% gelatin-Ph, and 0.5 w/v% alginate-Ph) was added onto the core solution. After the formation of hydrogel shell gel at 15 °C for 5 min, the resultant glass plates with Cell Dome were washed with PBS to remove the residual shell solution, immersed in the medium containing 0.5 mg/mL catalase, with the medium being replaced with fresh one after 1 day of incubation (Figure 3-1). HepG2 cells completely filled the hemispherical cavities within the Cell Dome, hemispherical cell aggregates cultured for 18 days were used primarily for analysis. Cells cultured in a 2D dish were used as controls for comparison. The HepG2 cells within the Cell Dome were observed using a fluorescence microscope (BZ-9000, Keyence, Tokyo, Japan) and viability analysis was evaluated using a fluorescence live/dead assay with Calcein AM/PI staining. The diffusion properties of the hydrogel shell surrounding the HepG2 cells were evaluated by fluorescence recovery after photobleaching (FRAP) using optical coherence tomography (Cell3iMager Estier, Screen, Kyoto, Japan). FITC-dextran with molecular weights of 4,000 and 70,000 was used to measure diffusion coefficient of the hydrogel shell using a confocal laser scanning microscope (C2,

Nikon, Tokyo, Japan) based on previous work [63]. Hydrogels for the measurements were prepared with PBS containing 1.0% (w/v) gelatin-Ph, 0.5% (w/v) alginate-Ph, 50 U/mL HRP, and 1 mM H_2O_2, and was immersed in PBS containing 0.5 mg/mL FITC-dextran at 37 °C overnight. The permeability of the hydrogel shell was evaluated by the diffusion coefficient of FITC-dextran in the hydrogel relative to those in water.

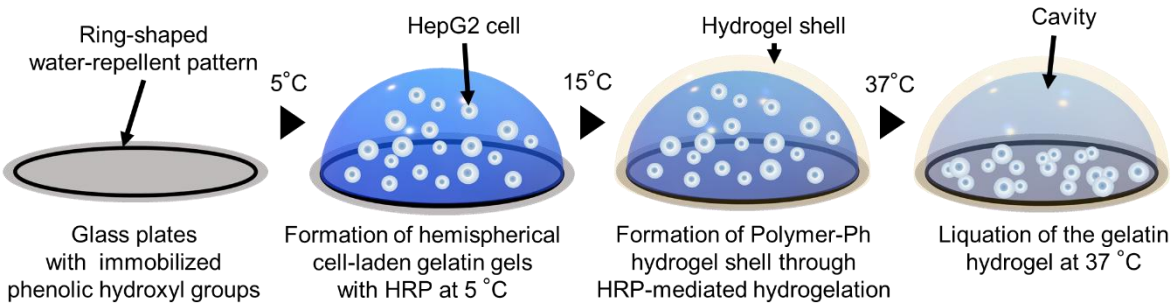

Figure 3-1. Schematic drawing of Cell Dome preparation process on glass plates. Cells are enclosed in a cavity consisting of hemispherical hydrogel shells. Reprinted (adapted) from [105]. Copyright MDPI.

2.3 GSTP1/HIF-1α analysis

GSTP1 enzyme activity and hypoxic response to HepG2 cells within the Cell Dome were analyzed using fluorescence-based assays and real-time PCR. To assess GSTP1 enzyme activity, the Cell Domes were immersed in Hanks' equilibrium salt solution of 20 mM HEPES (pH 7.4, HBSS) containing 10 μM MK571 and 2.5 μM GSTP1 Green (Funakoshi, Tokyo, Japan) for 30 min at 37 °C. After two washes in HHBS, GSTP1 enzyme activity was observed and analyzed using fluorescence microscopy and flow cytometry (Accuri C6, BD Biosciences, Tokyo, Japan). For flow cytometric analysis, single HepG2 cells were collected by immersing the Cell Dome in PBS containing 1 mg/mL alginate lyase for 5 min to disassemble the hydrogel shell, followed by trypsin treatment.

For hypoxia analysis, the Cell Domes were immersed in PBS containing 2.0 μM Hypoxia Probe Solution: LOX-1 (MBL, Nagoya, Japan) for 24 h at 37 °C. Following incubation, the Cell Domes were washed twice with PBS, and the HepG2 cells were stained with LOX-1 and

observed under a fluorescence microscope.

Relative amounts of *HIF-1α* mRNA were determined by real-time PCR. HepG2 cells were harvested from the Cell Dome following enzymatic digestion with alginate lyase and trypsin, and total cellular RNA was extracted using the CellAmp Direct TB Green RT-qPCR Kit (Takara Bio, Shiga, Japan) according to the manufacturer's instructions. Reverse transcription of RNA to single-stranded cDNA was performed at 37 °C for 30 min, followed by enzyme inactivation at 85 °C for 5 sec. From the resulting cDNA template, target sequences were amplified and quantified by real-time PCR using specific primers for *HIF-1α* (reference gene: *GAPDH*, Table 3-1). The PCR reactions involved an initial denaturation step at 95 °C for 30 s, followed by 40 cycles of at 95 °C for 5 s and 60 °C 10 s. Threshold cycle (Ct) values were obtained using a real-time PCR system (CFX Connect™, Bio-Rad Laboratories, California, USA). Relative mRNA content was calculated using the ΔΔCt method (n = 3).

Table 3-1. Primer used for detecting *HIF-1α* gene expression. Reprinted (adapted) from [105]. Copyright MDPI.

Gene	Primer Forward	Primer Reverse	Reference
GAPDH	5′-GGA GTC CCT GCC ACA CTC AG-3′	5′-GGC CCC TCC CCT CTT CA-3′	[108]
HIF-1α	5′-TGC ATC TCC ATC TCC TAC CC-3′	5′-CCT TTT CCT GCT CTG TTT GG-3′	[109]

2.4 Anti-cancer drug-sensitivity analysis

The glass plates with one Cell Dome were immersed in a 200 μL of medium containing 1, 10, 100, and 1,000 nM MMC and incubated for 72 h. Then, 20 μL of Cell Count Reagent SF (Nacalai Tesque, Kyoto, Japan) was then added was added to each well and incubated for 4 h. To evaluate mitochondrial activity, the absorbance of the supernatant at 450 nm was measured with a UV-VIS spectrophotometer (UV-2600, Shimadzu, Kyoto, Japan). "Relative activity" was determined by comparing the mitochondrial activity of treated cells (absorbance of the supernatant) in the Cell Dome after adding MMC to that of untreated control cells (no MMC addition).

2.5 Statistical analyses

All data were presented as the mean ± standard deviation (SD). Statistical analyses were performed to evaluate the significance of differences between groups. Student's *t*-test was used for comparisons between two datasets. One-way analysis of variance (ANOVA) followed by Tukey's post hoc analysis was used for comparisons among three or more datasets.

3. Results and Discussion

3.1 Hydrogel permeability

The hydrogel shell of Cell Dome was fabricated using a polymer blend of gelatin-Ph and alginate-Ph hydrogels obtained through HRP-mediated hydrogelation. These materials are highly cytocompatible [110], and HRP-mediated hydrogelation has been used to prepare cell-containing hydrogels, such as structures fabricated by 3D bioprinting [54, 55] and microcapsules [53, 111]. The diffusion coefficients of FITC-dextran in the hydrogel shell were determined to be 0.91 ± 0.18 (molecular weight 4,000) and 0.58 ± 0.14 (molecular weight 70,000), expressed relative to the diffusion coefficients in water. Permeability is inferred from values closer to 1, indicating the hydrogels exhibit high permeability to low molecular weight compounds. In other words, the results indicate that the gelatin-Ph and alginate-Ph composite hydrogels obtained through HRP-mediated hydrogelation are highly permeable to low molecular weight compounds. This is a very important factor for supplying oxygen and nutrients to the enclosed cells in the Cell Dome for their optimal growth and proliferation.

3.2 Cell growth in Cell Dome

The development of organized cell structures by using adherent cells are very useful for research as bioassays, including drug discovery [88, 96, 112]. Various techniques have been employed to obtain organized cells, including the hanging drop method [100], ultra-low adherent dishes [113], microwells [98, 99], and spinner flasks [114]. Although the size and shape of spheroids can affect the outcome and efficiency of drug discovery [115, 116], it is

difficult to control them using these methods, especially when cultured with appropriate media exchange. Therefore, a 3D culture system that can control the size and shape of organized cells is warranted [116].

In 3D culture of adherent cells using Cell Dome, enclosed HepG2 cells were initially dispersed as individual cells immediately after enclosure, and began to form aggregates after 1 day of culture (Figures 3-2b, and -2c). The area occupied by cells increased with increasing

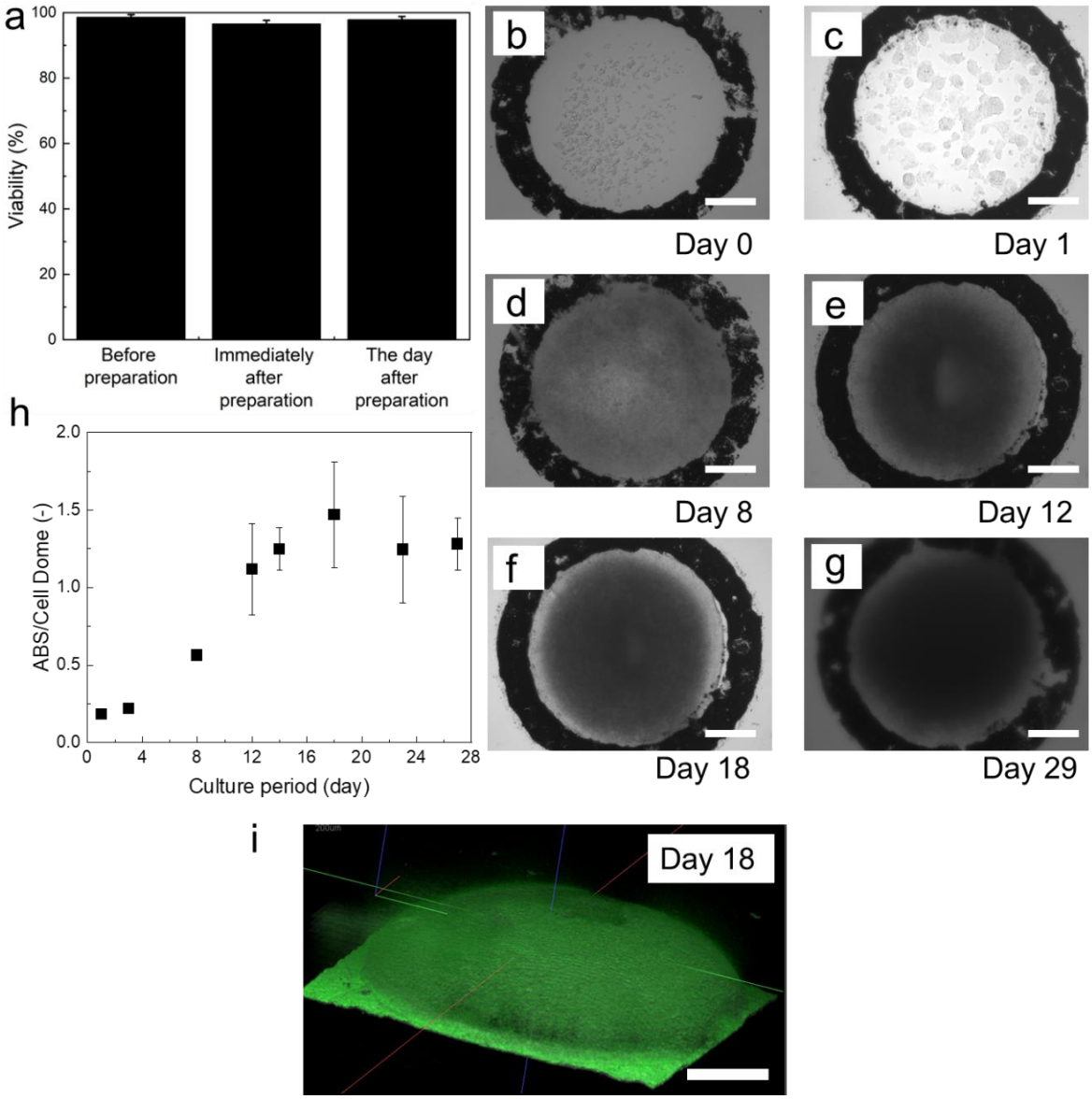

Figure 3-2. (a) HepG2 viabilities before enclosing and, immediately and one day post-enclosure. (b–g) HepG2 cell growth in Cell Dome, (h) mitochondrial activity corresponding to the number of living cells per Cell Dome, (i) optical coherence tomography image of HepG2 cells after 18 days of culture. Bars in a and h represent SD, n = 5; Scale bars in (b–g) and (i): 250 μm. Reprinted (adapted) from [105]. Copyright MDPI.

duration of culture, with cells filling the hemispherical cavity after 18 days of culture, after which the Cell Dome maintained its shape for 29 days of culture (Figures 3-2b-g and -2i). This result was also confirmed by mitochondrial activity analysis, which showed that enclosed cells proliferated within the Cell Dome and formed hemispherical cell aggregates that filled the cavity of the Cell Dome by the 18 days of culture (Figure 3-2h).

The successful long-term culture of HepG2 cells within the Cell Dome can be attributed to the good permeability and stability of the hydrogel shell. The hydrogel shell of the Cell Dome is highly permeable to the oxygen and nutrients necessary for the survival and proliferation of the enclosed cells, while also enabling the removal of cellular metabolites from Cell Dome to the surrounding medium. Due to its high stability, the Cell Dome containing HepG2 cells maintained its shape even after the hemispherical cavity is filled with cells, producing cell aggregates that were uniform in size. Toxicity testing and drug development require long-term, low-level exposure to test compounds, yet conventional screening systems, such as primary human hepatocytes cultured in 2D, can survive only a few days [88, 117]. The application of this Cell Dome system, which can culture cells for long periods of time, would facilitate a variety of studies to be evaluated over an extended period of time, which could be valuable for drug development. The period during which enclosed cells fill the hemispherical cavities can be controlled by adjusting the concentration of initially enclosed cells and the size of the Cell Domes. Furthermore, the size of the hemispherical cell aggregates can be controlled by controlling the size of the cavity.

3.3 GSTP1/Hypoxia and drug-sensitive analysis

Glutathione S-transferases (GSTs) are multifunctional enzymes that play important roles in cellular detoxification [85]. Upon binding to compounds, such as anti-cancer drugs, GSTs facilitate their excretion by multidrug resistance-associated protein (MRP) transporters. Among GSTs, Pi class GST (GSTP 1) is highly expressed in various cancer types and contributes

significantly to the acquisition of drug resistance in cancer cells [118, 119]. The green fluorescence intensity observed in the enclosed cells showed high GSTP1 activity was higher than that observed in 2D cultured cells (Figure 3-3). Furthermore, flow cytometric analysis of cells collected from the Cell Dome and stained with GSTP1 Green showed a small peak just before the fluorescence peak, suggesting the presence of a GSTP1 activity gradient due to the oxygen concentration gradient in hemispherical cell aggregates (Figure 3-3).

Hypoxia is a common feature in tumors *in vivo*, arising from oxygen concentration gradient, that lead to low oxygen levels in tumor core [48, 75]. Hypoxic cells overexpress HIF-1, which upregulates the expression of genes that contribute to drug resistance [120]. In hypoxia analysis of enclosed cells in the Cell Dome, HepG2 cells at the center of hemispherical cell aggregates emitted red fluorescence indicating hypoxia, after 18 days of culture (Figure 3-4a). In addition, HIF-1α expression of cells collected from the Cell Dome was 4.8 ± 1.0-fold higher than that of cells in 2D culture (Figure 3-4b). These results indicate that the center of hemispherical cell aggregates is hypoxic and that an oxygen concentration gradient exists within the Cell Dome.

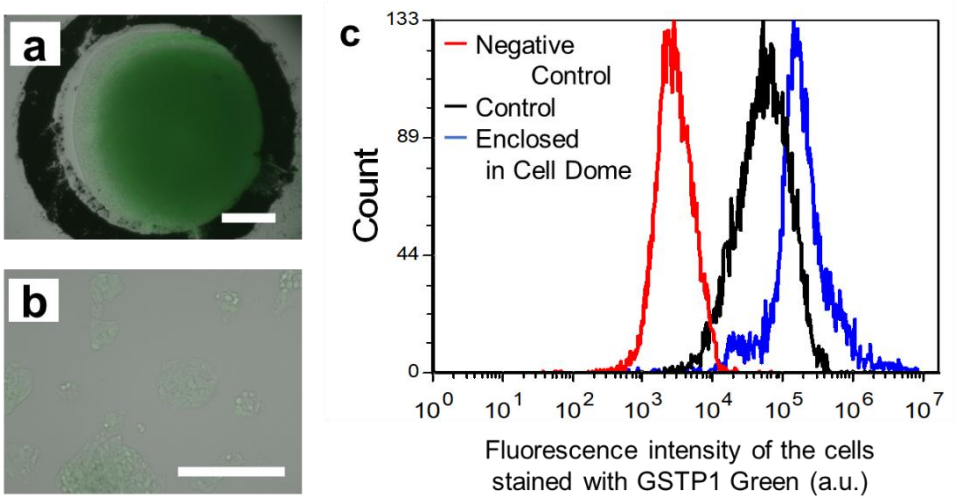

Figure 3-3. (a, b) Fluorescence observation of HepG2 cells in Cell Domes after 18 days of culture (a) and 2D-cultured cells on a tissue culture dish (b) both stained with GSTP1 Green. Scale bars: 250 μm. (c) Flow cytometry analysis data of the cells not stained with GSTP1 Green (red line: Negative Control) and stained with GSTP1 Green enclosed in Cell Domes after 18 days of culture (blue line) and 2D-cultured cells on a tissue culture dish stained with GSTP1 Green (black line: Control). $*p < 0.05$ vs. 2D-cultured cells with and without staining GSTP1 Green. Reprinted (adapted) from [105]. Copyright MDPI.

An attractive feature of the Cell Dome is that the hydrogel shell can be degraded by a mild reaction, which allows for easy collection of enclosed cells, allowing cells to be evaluated using flow cytometry (Figure 3-3c) and real-time PCR (Figure 3-4b). In addition, spheroids formed

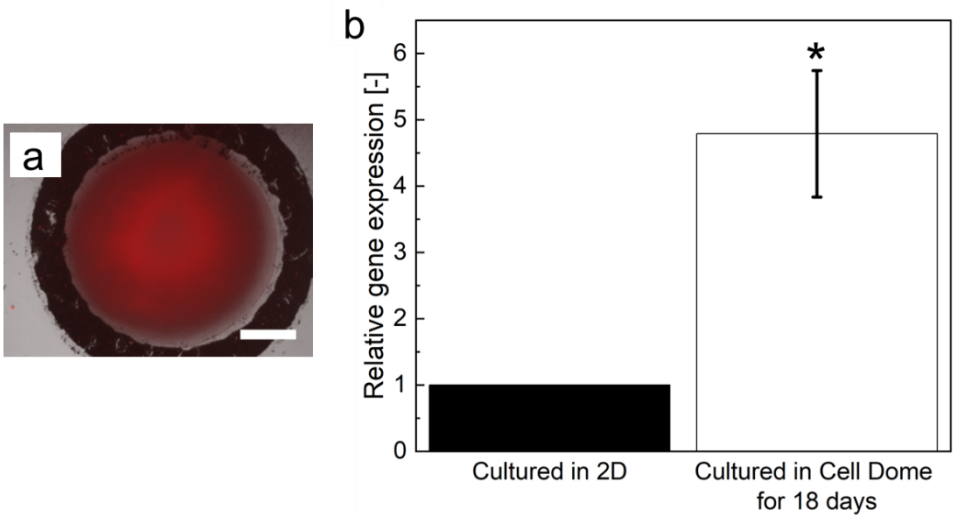

Figure 3-4. (a) Fluorescence observation of HepG2 cells cultured in Cell Domes at 18 days and stained with LOX-1. Scale bar: 250 μm. (b) *HIF-1α* gene expressions in 2D-cultured HepG2 cells on a tissue culture dish and those cultured in Cell Domes for 18 days. Each value was normalized by the means of data in the 2D-cultured cells. Bars: SD, (n = 3). *p < 0.05 vs. 2D-cultured cells on a tissue culture dish. Reprinted (adapted) from [105]. Copyright MDPI.

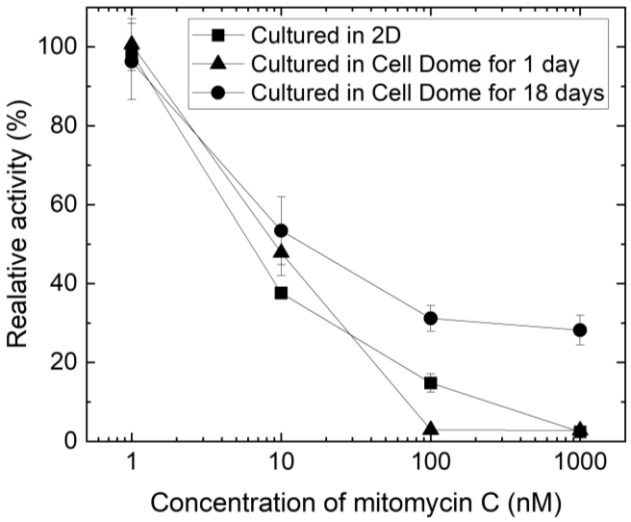

Figure 3-5. Relative activity of 2D-cultured cells on a tissue culture dish (■), the cells in Cell Dome after 1 day of culture (▲), and hemispherical cell aggregates formed in Cell Dome after 18 days of culture (●). Bars: SD, n = 3~5, *p < 0.05 vs. 2D-cultured cells and those in Cell Dome after 1 day of culture, **p < 0.05 vs. cultured in 2D-cultured cells. Reprinted (adapted) from [105]. Copyright MDPI.

by other methods often require confocal imaging to observe and analyze the hypoxic region at their centers, [23, 103, 104]. Conversely, the Cell Dome, due to its hemispherical structure, allows conventional fluorescence microscopy to be used for observation and evaluation of the hypoxic region in the center of cell aggregates adhering to the glass surface.

Based on the elevated GSTP1 enzyme activity and *HIF-1α* gene expression in hemispherical aggregates of HepG2 cells, it was expected that HepG2 hemispherical cell aggregates were resistant to antitumor drugs. Therefore, MMC was used to evaluate the chemical sensitivity of the cell aggregates. Enclosed cells in the Cell Dome after 1 day of culture and 2D-cultured cells showed comparable relative activity. In contrast, hemispherical cell aggregates formed after 18 days of culture in the Cell Dome showed higher relative activity compared to that in 2D-cultured cells (Figure 3-5). Similar results were reported previously for HepG2 cells cultured in 3D culture systems using microwells and 3D cell culture hydrogels [99, 121, 122]. These results indicate that hemispherical aggregates of HepG2 cells fabricated using Cell Dome were resistant to MMC. Increased expression of genes such as ATP-binding cassette transporter G2 (*ABCG2*), multidrug resistance (*MDR*; *ABCB1*), and MRP (*ABCC1*) would contribute to the acquisition of drug resistance in the enclosed cells [123, 124].

4. Conclusion

In Chapter II, I had targeted non-adherent cells and established the Cell Dome system to facilitate their culture and evaluation. In this chapter, the applicability of the Cell Dome to adherent cells was investigated.

Organized tumor cells obtained by culturing tumor cells in 3D better reflect the pathophysiology of tumor tissue compared to 2D cultures [48, 125]. This is due to the increased cell-cell interactions in 3D cultures, which closely mimic the complex cellular arrangements found in tumor tissues *in vivo*. Additionally, 3D cultures establish biochemical concentration gradients that replicate the *in vivo* environment, including oxygen gradients. Observation and

analysis of cells within hypoxic regions due to oxygen concentration gradients is important in tumor research because these cells play an important role in tumorigenesis [77, 120, 126].

In this study, HepG2 cells were used as a model of adherent cells and cultured in a Cell Dome to form hemispherical cell aggregates, which adhered to glass plates. Cells at the center of the glass adhesion surface of the hemispherical cell aggregates exhibited specific characteristics attributed to hypoxia, which could be observed without the use of confocal laser imaging microscopy. These results demonstrate the feasibility of the Cell Dome as an evaluation platform for adherent cells.

Some portion of this thesis, including text and figures, have been previously published in the journal article “Cell Dome as an Evaluation Platform for Organized HepG2 Cells” by Kazama *et al.*, published in *Cells*, 2023, 12, 69 (Reference No. 105). These sections are reproduced here with permission from MDPI.

Chapter IV

Effect of cell adhesiveness of Cell Dome's shell on enclosed HeLa cells

1. Introduction

Various methods for fabricating cell aggregates, including microcapsules [127, 128] and hanging drops [24, 129] have been extensively studied as three-dimensional (3D) culture techniques to mimic in vivo tumor microenvironments [130, 131]. In chapters II and III, I described the Cell Dome system, a novel standardized bioassay system, for fabricating hemispherical cell aggregates using adherent/non-adherent cells [60, 105]. Cell Dome is a cell-laden dome structure with a diameter of 1 mm and a height of approximately 300 μm. This system prevents cell loss during various solution manipulations such as medium exchange, washing, and staining, and allows the core of cell aggregates, that exhibit characteristic behaviors, to be observed. It encompasses cells within a cavity covered by a hemispherical hydrogel shell that is immobilized on a glass plate. To construct Cell Dome, I initially prepared a hemispherical gelatin gel containing cells through a temperature-dependent sol-to-gel transition of an aqueous gelatin solution placed on a glass plate. Subsequently, the hydrogel shell is fabricated by crosslinking polymers with phenolic hydroxyl groups (Ph) via a horseradish peroxidase (HRP)-mediated hydrogelation reaction (Figure 4-1a).

This unique hemispherical hydrogel shell provides a 3D microenvironment for the enclosed cells. Importantly, the immobilization of the Cell Dome on a glass plate facilitates easy handling during procedures such as media exchange, staining, and washing. In chapter II, I employed an alginate derivative possessing Ph moieties (Alg-Ph) as the hydrogel shell material for the 3D culture together with evaluation of the human lymphoma cell line, K562 [60]. In

chapter III, I additionally used a combination of Alg-Ph and a gelatin derivative possessing Ph moieties (Gel-Ph) as the hydrogel shell material for the 3D culture and evaluation of a hepatoblastoma-derived cell line, HepG2 [105]. Since the hydrogel shell is fabricated via HRP-mediated hydrogelation, a diverse range of polymers possessing Ph moieties, including alginate [111], gelatin [59, 74], and their combinations [110], can be employed to create hydrogels. These polymers and the enzymatic hydrogelation system have also been utilized in the fabrication of cell-laden microcapsules [59, 111], injectable matrices [74], and 3D bioprinting applications [110]. Although the cells within Cell Dome are in contact with the inner walls of the hydrogel shell, the impact of the cell adhesiveness of hydrogel materials on cellular behavior within Cell Dome remains unexplored.

Gelatin, derived from various animal collagens sourced from porcine [132, 133], bovine [134], and fish [135] tissues, is known for its biocompatibility and biodegradability [136, 137]. Gelatin contains an arginine-glycine-asparagine (RGD) sequence that promotes cell adhesion and proliferation [138, 139], and shares chemical properties with the extracellular matrix (ECM) of natural tissues [136, 137]. Owing to these characteristics, hydrogels containing gelatin have been extensively employed in tissue engineering applications [140, 141]. Liu *et al.* [107] reported that cells adhered and proliferated well on hydrogels fabricated from a blend of Gel-Ph and Alg-Ph. Moreover, microcapsules made from crosslinked alginate-gelatin hydrogels demonstrated enhanced cell adhesion, proliferation, and migration compared to those composed solely of alginate [142-145].

In this chapter, I aimed to investigate the impact of the cell adhesiveness of the hydrogel shells in the Cell Dome system on the behavior of the enclosed cells [146]. In the cell aggregation process, in addition to cell-cell adhesion, adhesion between cells and the external environment of the cell is involved in the cellular behavior including formation and function of cancer cell aggregates [40, 41]. Therefore, for understanding the differences in cancer cell

behavior, analysis of formation of cell aggregates in the Cell Dome is important. I fabricated hydrogel shells of varying adhesiveness—those lacking cell adhesiveness (Ad(-)-Cell Dome) and those promoting it (Ad(+)-Cell Dome)—using either Alg-Ph alone or a combination of Gel-Ph and Alg-Ph, through HRP-mediated hydrogelation (Figures 4-1a, and -1b). I investigated cell adhesion and proliferation within these hydrogel shells using human cervical cancer cell lines that express fucci2, a marker for cell cycle progression (HeLa-fucci2). Additionally, I evaluated cell cycle progression, the gene expression of the hypoxia-inducible factor (HIF-1α), and the chemosensitivity of cells cultured in both types of Cell Domes.

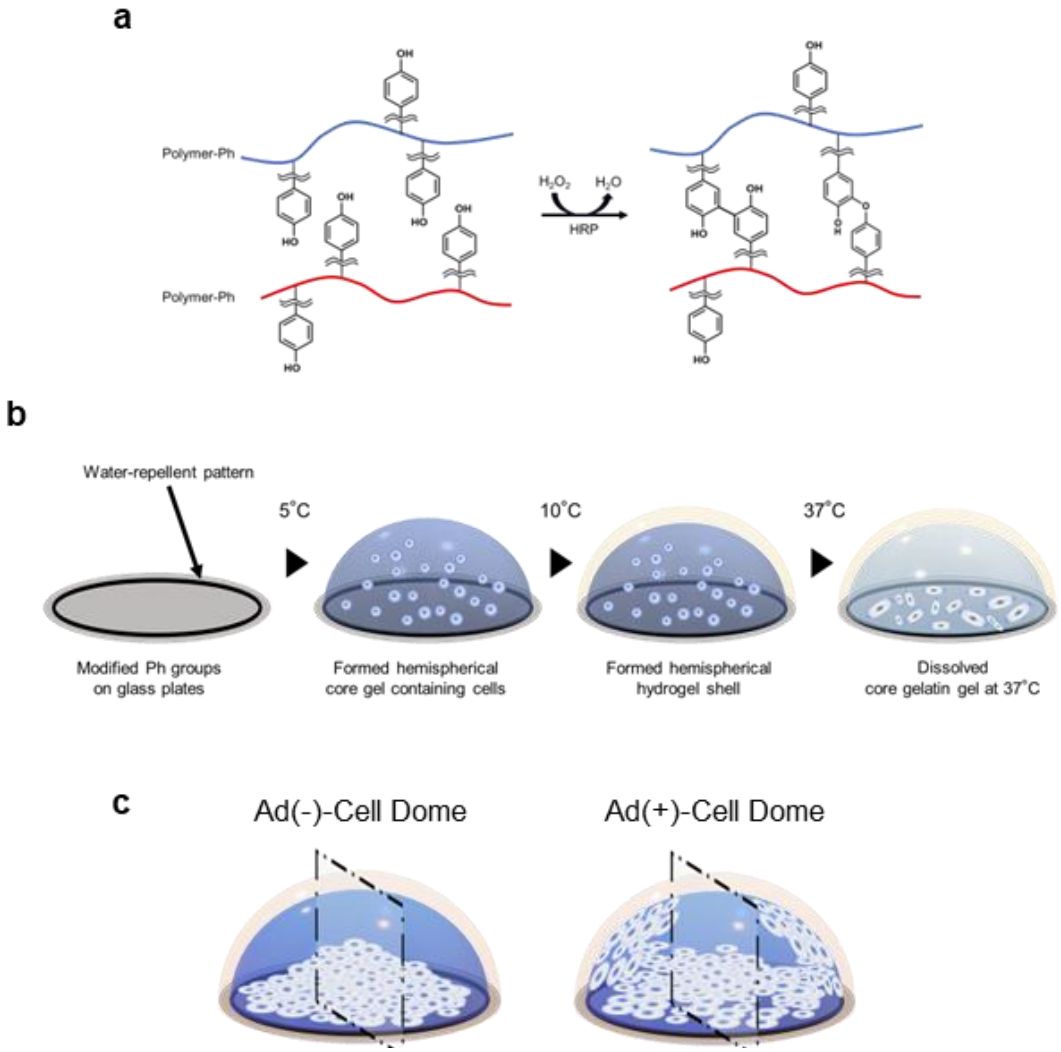

Figure 4-1. (a) Schematic illustration of the reaction in HRP-mediated hydrogelation of Alg-Ph and a mixture of Gel-Ph and Alg-Ph. (b) Schematic diagram of the preparation methods of Cell Dome enclosing HeLa-fucci2 cells. (c) Schematic diagram of the preparation of frozen section. Reprinted (adapted) from [146]. Copyright © 2024 The Society for Biotechnology.

2. Materials and Methods

2.1 Cell culture and chemical synthesis

HeLa-fucci2 cells [147] were obtained from the Riken Cell Bank (Ibaraki, Japan) and cultured in a humidified environment of 5% CO_2/95% air, at 37 °C with a in DMEM (Nissui, Tokyo, Japan) supplemented with 10% (v/v) FBS (Peak Serum, CO, USA).

Alg-Ph (2.7×10^{-4} mol-Ph/g) was synthesized by the reaction of Sodium alginate (I-1G, viscosity = 100-200 mPa-s at 1%, mannuronic acid/gluronic acid ratio ≈ 0.7, Kimica, Tokyo, Japan) and tyramine hydrochloride (ChemImpex International, Illinois, USA) via water-soluble carbodiimide hydrochloride (EDC·HCl; Peptide Institute, Osaka, Japan) and N-hydroxysuccinimide (NHS; Fujifilm Wako Chemical, Osaka, Japan) [62].

Gela-Ph (7.8×10^{-4} mol-Ph/g) was also synthesized by the reaction of gelatin type B from bovine skin (approximately 250 g bloom; Sigma-Aldrich, St. Louis, MO, USA) and 3-(4-hydroxyphenyl) propionic acid (Tokyo Chemical Industries, Tokyo, Japan) via EDC-HCl and NHS) [107].

2.2 Hydrogel sheet preparation

PBS (500 μL, pH 7.4) containing 50 U/mL HRP, 1 mM H_2O_2 (31% [w/w]; Fujifilm Wako Chemical), and 1.0% (w/v) Alg-Ph or a mixture of 1.0% (w/v) Gel-Ph and 0.5% (w/v) Alg-Ph were added to a 24-well plate to form the hydrogel sheet.

After washing twice with PBS, the medium containing 0.5 mg/mL catalase from bovine liver (Fujifilm Wako Chemical) and 0.5×10^5 cells/mL HeLa-fucci2 cells were added to the hydrogel sheets. After 1 day of culture, the cells were observed using a fluorescence microscope (BZ-9000; Keyence, Tokyo, Japan), and the cell area and cell aspect ratio were analyzed using ImageJ software [148]. The cell area and cell aspect ratio are the area occupied by cells on a 2D culture dish or hydrogel per image and the ratio of the major axis to the minor axis of the cell, respectively.

2.3 Cell Dome preparation and analysis

The Cell Domes were prepared according to the procedure described in a previous study [60, 105]. Briefly, a core solution (PBS, 1 μL) containing 3.0% (w/v) gelatin type A from porcine skin (approximately 300 g bloom; Sigma-Aldrich), 1.0 $\times 10^6$ cells/mL HeLa-fucci2 cells, and 50 U/mL HRP was placed inside the water-repellent rings (inner/outer diameter: 1/1.4 mm) printed on phenolic hydroxyl groups-modified glass plate. After allowing it to stand at 5 °C for 15 min, a 10 μL shell solution (PBS containing 1 mM H_2O_2 and 1.0% [w/v] Alg-Ph or a mixture of 1.0 [w/v] Gel-Ph and 0.5% [w/v] Alg-Ph) was added onto the hemispherical core gel. After hydrogel shell formation (at 15 °C for 5 min), the resultant glass plate with the Cell Dome was washed with PBS and cultured in a medium containing 0.5 mg/mL catalase. Following 24 h of cultivation, the medium was replaced with a fresh one (Figure 4-1b). The viability of HeLa-fucci2 cells enclosed within the Cell Dome was analyzed by live/dead staining using Calcein AM (Nacalai Tesque, Kyoto, Japan) and DAPI (Nacalai Tesque, Kyoto, Japan) and using fluorescence microscopy. The hydrogel shell was degraded using alginate lyase (24 units/mg; Nagase Chemtex Corporation, Osaka, Japan) and the enclosed cells were dissociated using trypsin/EDTA. The single cells were then collected for cell count analysis using the Countess II FL (Thermo Fisher Scientific, MA, USA).

Frozen sections of cells cultured within the Cell Domes were prepared as follows: Cell domes cultured for 6 days were first immersed in 4% paraformaldehyde solution (Fujifilm Wako Pure Chemicals) for 1 h, then in 5% sucrose solution (Fujifilm Wako Pure Chemicals) for 1 h. After washing twice with PBS, they were quickly frozen in liquid nitrogen with Tissue-Tek® O.C.T. compound (Sakura Finetek Japan K.K., Tokyo, Japan) and sliced into 15 μm sections using a cryomicrotome (2800 Frigocut E, Reichert-Jung, Germany) (Figure 4-1c). The resulting frozen sections were observed under a fluorescence microscope.

2.4 Cell cycle analysis

In the HeLa-fucci2 cell line, nuclei emit red fluorescence during the G1/G0 phase and green fluorescence during the S/G2/M phase [147]. The enclosed cells were collected using the same procedure described in the "Cell Dome preparation and Analysis" section. Based on the red (mCherry-hCdt1) or green (mVenus-hGem) fluorescence emitted by the fucci2 cell cycle marker system, the G1/G0 phase of cell cycle of the collected cells was analyzed by counting red fluorescent cells using Countess II FL.

2.5 *HIF-1α* gene expression analysis

The enclosed cells after 6, 8, and 11 days of culture were collected in the same manner as described in the "Cell Dome preparation and analysis" section, total RNA was extracted from the collected cells, and single-stranded cDNA was synthesized from the extracted total RNA. Thermal Cycler Dice® Real Time System II (Takara Bio) was used to analyze relative expression levels of *HIF-1α* mRNA (beta 2-microglobulin (*B2M*): reference gene) by RT-qPCR using the CellAmp Direct TB Green RT-qPCR Kit (Takara Bio, Shiga, Japan). Data analysis was performed using the ΔΔCt method, with Ct values calculated by the second derivative maximum method; specific primers for *B2M* and *HIF-1α* are shown in Table 4-1.

Table 4-1. The primers for detecting *B2M,* and *HIF-1α* mRNA gene expression. Reprinted (adapted) from [146]. Copyright © 2024 The Society for Biotechnology.

Gene	Primer Forward	Primer Reverse	Reference
B2M	5′-AGG ACT GGT CTT TCT ATC TCT TGT -3′	5′-ACC TCC ATG ATG CTG CTT ACA-3′	[149]
HIF-1α	5′-TGC ATC TCC ATC TCC TAC CC-3′	5′-CCT TTT CCT GCT CTG TTT GG-3′	[109]

2.6 Chemical sensitivity analysis

After 11 days of culture, Cell Domes were exposed to a cell culture medium containing 100, and 1,000 nM of mitomycin hydrochloride (Fujifilm Wako Chemical) for a period of 48 h. Subsequent to a rinse with PBS, Cell Domes were incubated for 3 h in 200 μL of cell culture medium supplemented with 20 μL of Cell Count Reagent SF (Nacalai Tesque), which is used

to assess cellular mitochondrial activity. The level of mitochondrial activity was quantified by measuring the absorbance at wavelengths of 450 and 600 nm, where the latter serves as a reference wavelength, using a microplate reader (EPOCH 2; BioTek, CA, USA), in accordance with the manufacturer's guidelines. The relative mitochondrial activity was calculated as the activity in the presence of mitomycin hydrochloride relative to that in its absence.

2.7 Statistical analyses

Numerical results were presented as mean ± SD. ANOVA with post-hoc Tukey HSD was used for the statistical analyses.

3. Results

3.1 Cell behavior on hydrogels

The aim of this study was to fabricate and evaluate Cell Dome with hydrogel shells having different cell adhesion capacities using various hydrogel materials. The ECM influences cell behavior during cell adhesion [150-152]. Gel-Ph and Alg-Ph, the materials used in this study for the preparation of hydrogel shells, are highly cytocompatible [138, 153], and HRP-mediated hydrogelation reactions are frequently used to produce cell-containing structures [26, 154]. Gelatin, with its inherent chemical similarity to the extracellular microenvironment [136, 137] and cell adhesion properties [138, 139], is widely used in cell culture applications. To evaluate the cell adhesion properties of the hydrogel materials used, hydrogel sheets were fabricated with each material, and cell growth was assessed. HeLa-fucci2 cells seeded on gel-Ph and alg-Ph composite hydrogel sheets adhered and proliferated, while cells seeded on alg-Ph-only hydrogels adhered to the hydrogel sheets, but did not proliferate (Figures 4-2a-c). The latter also showed reduced cell area and lower cell aspect ratios compared to cells grown in composite hydrogels and in 2D culture dishes (Figures 4-2d and 2e). It was unexpected that cells adhered to alg-Ph-only hydrogel sheets. This could be explained by the enhanced adsorption of cell adhesion proteins, which results from the increased hydrophobicity generated

during the cross-linking of the Ph groups by HRP-mediated hydrogelation (36). These results allowed me to evaluate two hydrogels with different cell adhesion and cell proliferation properties on the hydrogel surface.

3.2 Proliferation of cells cultured within Cell Dome

The viability of HeLa-fucci2 cells cultured in Ad (-)-Cell Dome and Ad (+)-Cell Dome for 1 day was 90.8 ± 2.6% and 92.8 ± 4.6%, respectively, which are similar to the values observed before and 30 min after enclosure (Figure 4-3a). This indicates that the Cell Dome preparation process does not significantly affect the enclosed cells, which is consistent with the results of previous studies [60, 105].

The purpose of this study was to determine the extent to which the cell adhesion properties of

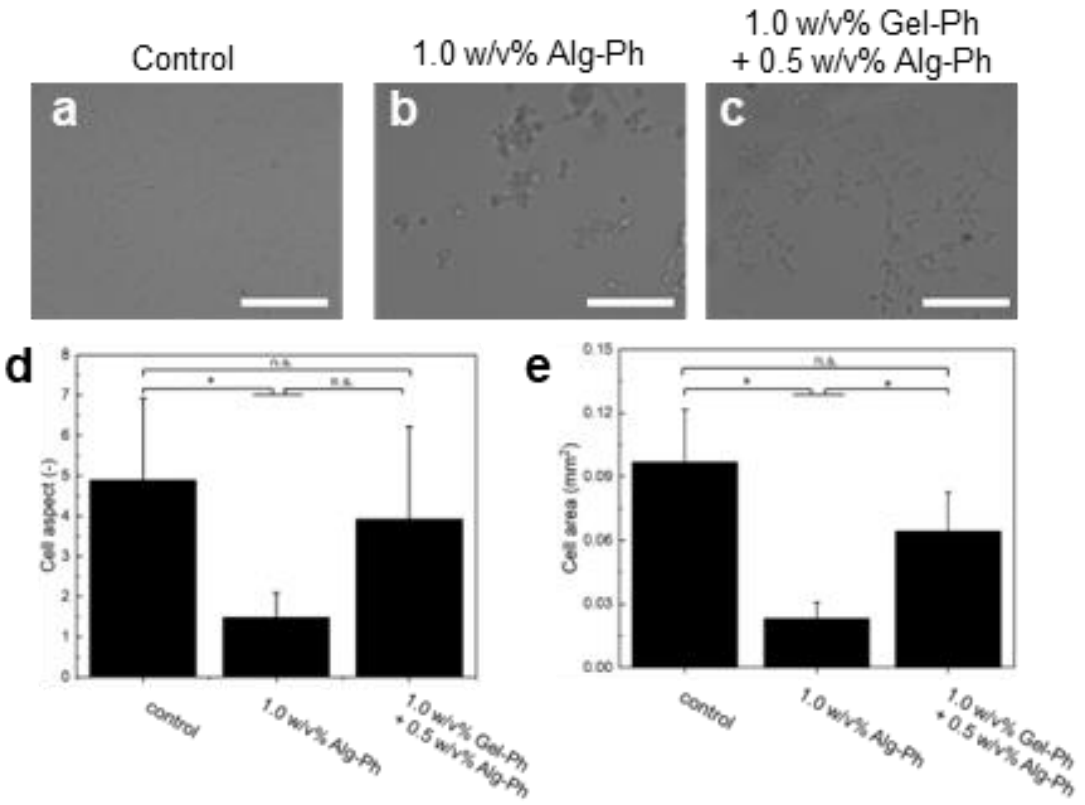

Figure 4-2. Proliferation of HeLa-fucci2 cells cultured for 1 day on 1.0 w/v% Alg-Ph hydrogel and the mixed hydrogel of 1.0 w/v% Gel-Ph and 0.5 w/v% Alg-Ph obtained through HRP-mediated hydrogelation reaction. (a-c) Microscopic images of HeLa-fucci2 cells on two types of materials (Scale bars = 200 μm). (d) Cell area of HeLa-fucci2 cells on two types of materials (n = 10, $*p < 0.05$, Bars: SD). (e) Cell aspect rate of HeLa-fucci2 cells on two types of materials (n > 100, $*p < 0.05$, Bars: SD). Reprinted (adapted) from [146]. Copyright © 2024 The Society for Biotechnology.

the hydrogel shells of the Cell Dome affect cell behavior. In the process of cancer cell aggregation, adhesion between the cell and the external environment is involved in cell behavior, including the formation and function of cancer cell aggregates [40, 41]. Since cells cultured in the Cell Dome are in direct contact with the inner wall of the hydrogel shell, the adhesive properties of the material are expected to have a significant impact on cell behavior. The cells enclosed in both Ad (-)-Cell Dome and Ad (+)-Cell Dome proliferated well (Figures 4-3c and -3d). The number of cells per Cell Dome also showed good cell proliferation, with the incubation period increasing, reaching a peak at 11 days of culture and remaining relatively stable thereafter (Figure 4-3b). This would be the effect of efficient diffusion of nutrients and oxygen into the cells due to high permeability of the hydrogel shell. Previous studies have confirmed that the hydrogel shells of both Ad (-)-Cell Dome and Ad (+)-Cell Dome are permeable to low molecular weight compounds [60, 105].

In the Ad (-)-Cell Dome, the enclosed cells adhered to the glass plate and showed 3D proliferation (Figure 4-3e). After 9 days of cultivation, a prominent dark area indicating cell aggregates appeared at the center of the Ad (-)-Cell Dome (Figure 4-3c). Similarly, the cells enclosed in the Ad (+)-Cell Dome adhered to the glass plate after enclosure (Figure 4-3d). As the incubation period progressed, these cells grew along the inner wall of the hydrogel shell (Figure 4-3e). After 5 days of cultivation, a prominent dark area showing cell aggregates appeared on the inner wall of the hydrogel shell (Figures 4-3d and -4). The dark areas indicative of cell aggregates were also confirmed by gray value analysis in Figure 4-3d, and these dark areas were distinct near the hydrogel shell (Figures 4-4a and -4b). After 11 days of culture, cells cultured in both Ad (-)- and Ad (+)- Cell Domes completely occupied the hemispherical cavities, forming hemispherical cell aggregates (Figures 4-3b-d). In addition, histological analysis revealed that after 6 days of culture, cells cultured in the Ad (-)-Cell Dome were primarily localized on the glass plate at the bottom of the Cell Dome (Figure 4-3e). In contrast,

cells in the Ad (+)-Cell Dome were distributed along both, the inner wall of the hydrogel shell and the glass plate at the bottom of the Cell Dome (Figure 4-3e). Furthermore, fluorescence microscopy based on the fucci2 cell cycle marker system showed that the cells cultured in the Ad (-)-Cell Dome were evenly distributed at the bottom of the Cell Dome (Figure 4-4c). On the other hand, cells in the Ad (+)-Cell Dome showed red and green fluorescence, indicating that the cells are close to the hydrogel shell (Figure 4-4c). In addition, out-of-focus cells in the Ad (+)-Cell Dome were observed, indicating that the cells were close to the hydrogel shell

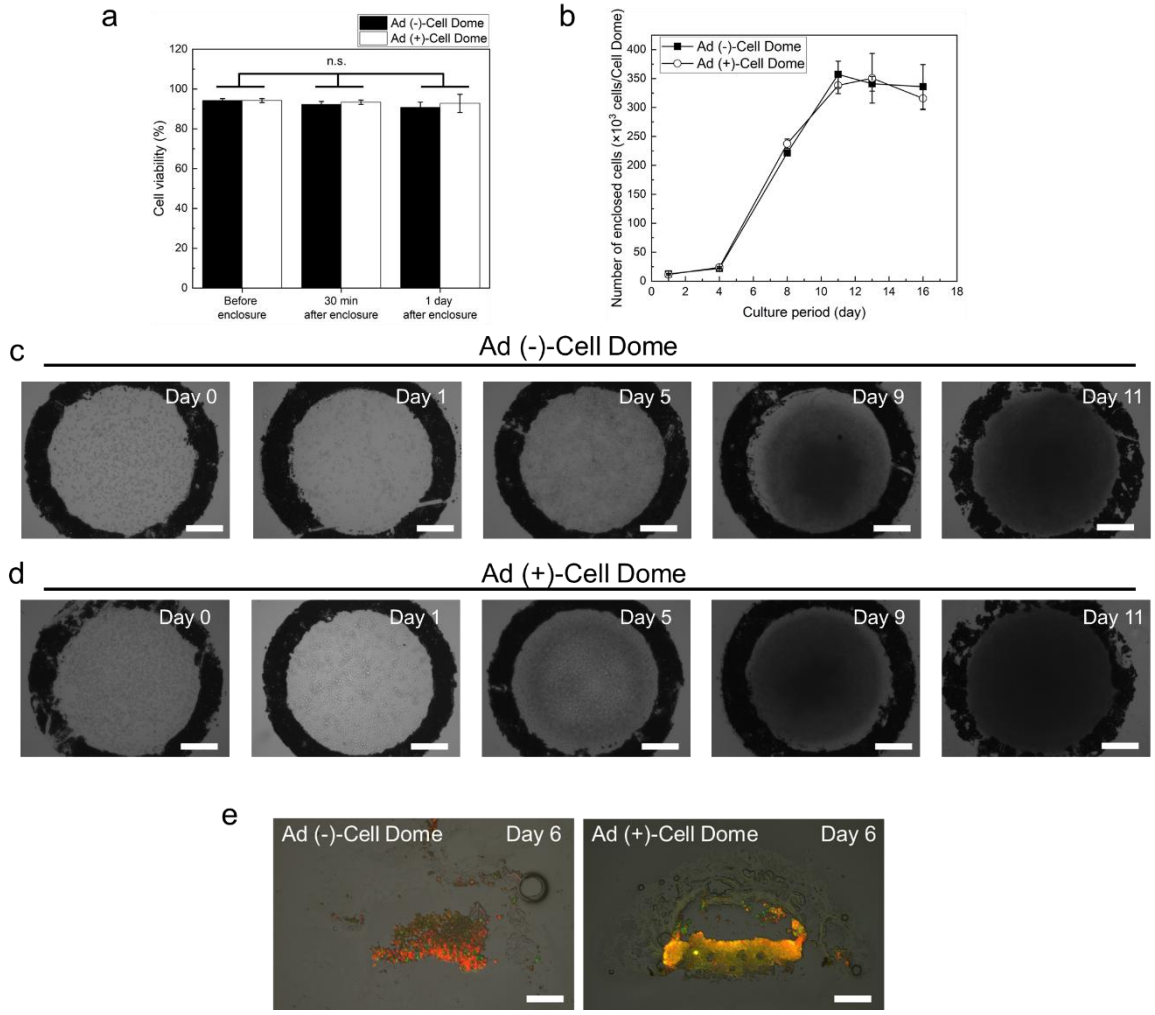

Figure 4-3. (a) Viabilities of HeLa-fucci2 cells before, 30 min, and 1 day after enclosure, respectively (n = 5, * p < 0.05, Bars: SD). (b and c) The microscopic images of HeLa-fucci2 cells cultured within (b) Ad(-)-Cell Dome and (c) Ad(+)-Cell Dome (Scale Bars: 250 μm). (d) The number of cells within Cell Dome (n = 3, Bars: SD). (e) Fluorescence images of the frozen section consisting of HeLa-fucci2 cells cultured within Ad(-)-Cell Dome and Ad(+)-Cell Dome for 6 days (Scale Bars: 250 μm). Reprinted (adapted) from [146]. Copyright © 2024 The Society for Biotechnology.

(Figure 4-4c). These results indicate that the cell proliferation behavior is influenced by the presence or absence of the cell adhesion properties of the hydrogel shell forming the Cell Dome.

3.3 Cell cycle of cells within Cell Dome

The cellular microenvironment has a profound effect on the cell cycle [151], and especially in the case of cancer cells, the cell cycle is crucial for studying both tumor growth and its

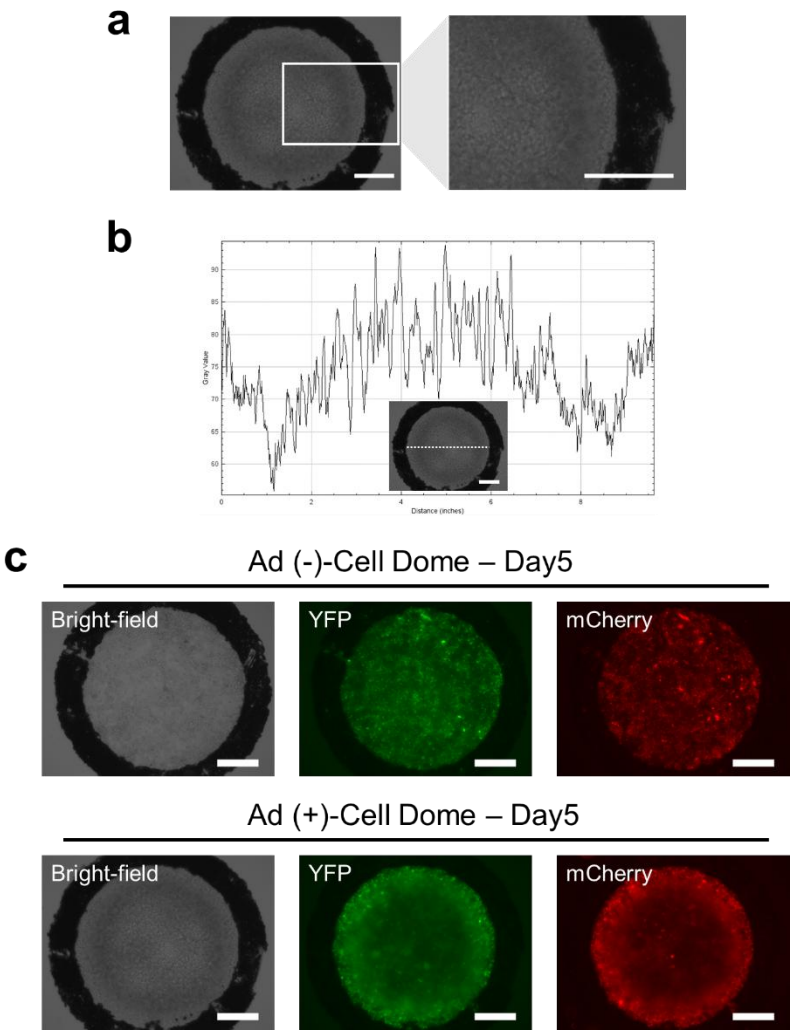

Figure 4-4. (a) Microscopic images of HeLa-fucci2 cells cultured within Ad(+)-Cell Dome for 5 days (Scale bars: 250 μm). (b) The graph showing the gray values of microscopic images of HeLa-fucci2 cells cultured within Ad(+)-Cell Dome for 5 days (Scale bars: 250 μm). Image analysis was performed using ImageJ. (c) Fluorescence images of HeLa-fucci2 cells cultured for 5 days within Ad(-)-Cell Dome or Ad(+)-Cell Dome (Scale bars: 250 μm). Fluorescent images were analyzed based on red fluorescence (mCherry-hCdt1) or green fluorescence (mVenus-hGem), emitted by the fucci2 cell-cycle marker system. Reprinted (adapted) from [146]. Copyright © 2024 The Society for Biotechnology.

suppression [155, 156]. The G1/G0 phase ratio of cells cultured for 3 days in Ad (-)- and Ad (+)-Cell Domes was 35.7 ± 2.4% and 33.0 ± 3.6%, respectively (Figures 4-4). On 5, 7, and 9 days of culture, the percentage of cells in the G1/G0 phase increased significantly in the Ad (-)-Cell Domes compared to the Ad (+)-Cell Domes (Figure 4-5); cells in G1/G0 phase were widely distributed at the bottom of the Cell Domes (Figure 4-3e). These results suggest that the size of cell aggregates in the Ad (-)-Cell Dome was larger than in the Ad (+)-Cell Dome, suggesting that a higher percentage of cells in the G1/G0 phase were present during cell growth in the Ad (-)-Cell Dome. The number of cells in both types of Cell Domes was nearly identical (Figure 4-3b), and the fact that the Ad (-)-Cell Dome could not adhere to the hydrogel shell and grew only on the glass plate supports this hypothesis (Figure 4-3). As the cell spheroid grows, the cells inside, lacking sufficient nutrients, enter a non-proliferative state or G0 phase [157]. By day 11 of culture, the percentages of cells in the G1/G0 phase of both types of Cell Domes had nearly converged, and remained stable thereafter (Figure 4-5). The fact that the percentage of cells in the G1/G0 phase remained relatively stable after the cavity in the hemispherical hydrogel shell was filled, suggests that the limited hemispherical cavity in the Cell Dome physically prevents cell proliferation and exhibits similar cell cycle levels regardless of the cell adhesiveness of the hydrogel shell.

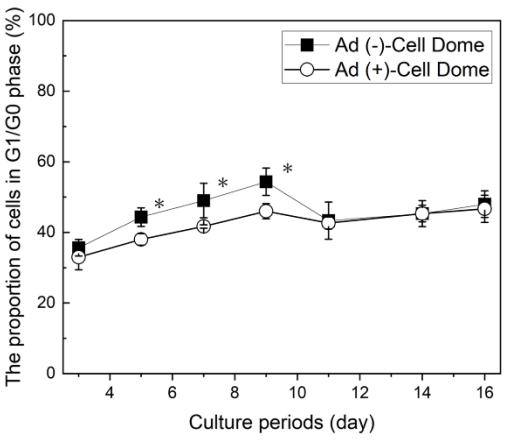

Figure 4-5. Proportion of HeLa-fucci2 cells in the G1/G0 phase cultured within Ad(-)-Cell Dome and Ad(+)-Cell Dome ($n = 3$, $*p < 0.05$, Bars: SD). Reprinted (adapted) from [146]. Copyright © 2024 The Society for Biotechnology.

3.4 HIF-1α and drug-sensitive analysis

A hypoxic microenvironment is a hallmark of many solid tumors [158, 159] and promotes tumor invasion, metastasis, upregulation of multidrug resistance proteins, angiogenesis, and decreased efficacy of antitumor drugs [158, 159]. Hypoxic conditions increase *HIF-1α* gene expression levels [160, 161]. *HIF-1α* gene expression in HeLa-fucci2 cells cultured for 11 days in Ad(-)-Cell Dome and Ad(+)-Cell Dome was 5.4 ± 1.6-fold and 3.3 ± 1.2-fold higher, respectively, compared to cells cultured in 2D culture dishes (Figure 4-6a). These results are consistent with previous studies on K562 or HepG2 cells cultured within the Cell Dome [60, 105], suggesting the presence of an oxygen concentration gradient within both Cell Dome types. No significant differences in HIF-1α expression levels between cells cultured for 6 and 8 days in both types of Cell Dome, and cells cultured in 2D dishes could be attributed to the good permeability of the hydrogel shell (Figure 4-6a).

Upregulation of *HIF-1α* gene expression also affects energy metabolism, angiogenesis, drug resistance, and tumor invasion [158, 162, 163], and the adhesion of cancer cells to the ECM affects drug resistance [164, 165]. The cells cultured in either Cell Domes showed markedly

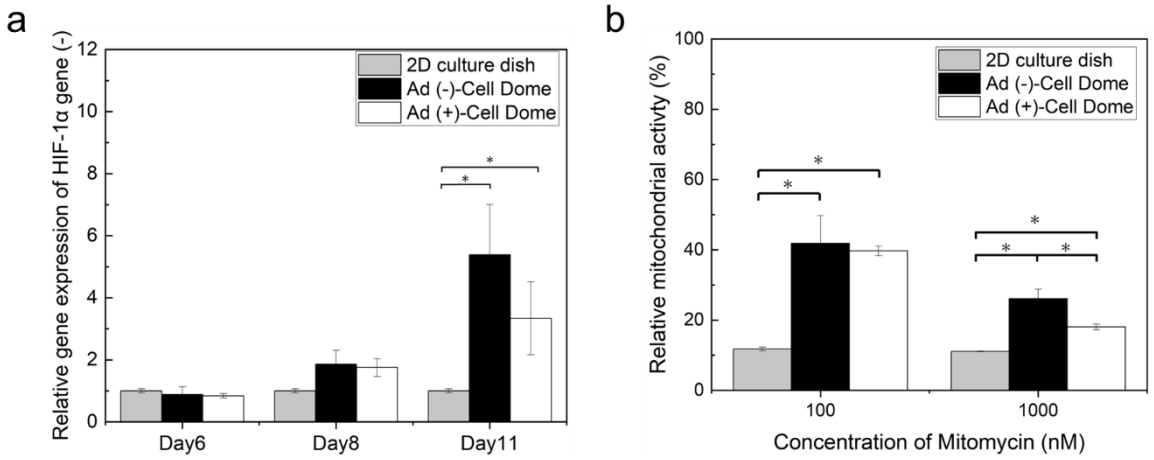

Figure 4-6. (a) Gene expression level of *HIF-1α* in HeLa-fucci2 cells cultured on 2D culture dishes, cultured within Ad(-)-Cell Dome, and Ad(+)-Cell Dome ($n = 3$, $^*p < 0.05$, Bars: SD). (b) The relative mitochondrial activity of Hela-fucci2 cells cultured on 2D culture dishes, cultured within Ad(-)-Cell Dome, and Ad(+)-Cell Dome for 11 days. ($n = 5$, $^*p < 0.05$, Bars: SD). Reprinted (adapted) from [146]. Copyright © 2024 The Society for Biotechnology.

increased relative mitochondrial activity compared to those within the 2D dish (Figure 4-6b). Liu *et al.* reported that under hypoxic conditions, induction of autophagy via HIF-1α has a protective effect on HeLa cells, contributing to drug resistance [166]. When exposed to 1,000 nM mitomycin hydrochloride, cells cultured in the Ad(-)-Cell Dome showed slightly higher activity than those in the Ad(+)-Cell Dome. Although integrin-mediated cell-matrix adhesion improves cellular resistance to drugs [167, 168], this contrasting result would be due to cell adhesion and the rigidity of the hydrogel shell. Zustiak *et al.* found that the stiffer the 3D matrix, the higher the drug resistance, and the integrin-based cell-matrix interactions have been reported to mitigate the effect of 3D matrix stiffness [169]. These findings could be attributed to the higher relative mitochondrial activity of cells cultured in the Ad (-)-Cell Dome than in the Ad (+)-Cell Dome at a mitomycin concentration of 1,000 nM.

4. Conclusion

In summary, the cell adhesiveness of the hydrogel shell material significantly influenced cell proliferation patterns within the Cell Dome, which in turn affected the cell cycle and drug resistance of the enclosed cellular populations. These findings provide new insights into the effect of the hydrogel shell's cell-adhesive properties on the enclosed cancer cell behavior, including cell cycle dynamics and drug resistance. This study represents the first report on the hydrogel shell of the Cell Dome, highlighting its numerous advantages over conventional spheroid fabrication methods. The results emphasize the importance of careful selection of the hydrogel shell materials with appropriate cell-adhesive properties for optimal Cell Dome construction.

Some portion of this thesis, including text and figures, have been previously published in the journal article “Effect of cell adhesiveness of Cell Dome shell on enclosed HeLa cells” by Kazama *et al.*, published in *Journal of Bioscience and Bioengineering*, 2024, 137 (4), 313-320 (Reference No. 146). These sections are reproduced here with permission from © 2024 The Society for Biotechnology.

Chapter V

Development of hemispherical 3D models of human brain and B cell lymphomas using a Cell Dome system

1. Introduction

Lymphoma, a type of blood cancer is classified into two main types: Hodgkin lymphoma and non-Hodgkin lymphoma. Non-Hodgkin lymphoma encompass a wide range of diseases, from indolent to highly aggressive malignancies, with 80–90% being of B-cell origin [170]. 2D models of lymphoma-derived B-cells have been used to elucidate their cellular function in hematology/oncology and in drug screening for new drug development [171, 172]. However, 2D models cannot mimic cellular interactions in the lymphoma microenvironment and may not provide an accurate understanding of the cellular function of lymphoma-derived cells and the efficacy of anti-cancer compounds [171, 173]. Thus, the development of lymphoma models that better mimic the lymphoma microenvironment is needed to accurately elucidate the complex cellular functions of lymphoma-derived cells and to address challenges related to lymphoma treatment.

3D culture methods have gained much attention in the study of tumor cell biology under conditions that closely resemble *in vivo* cell behavior, compared to 2D culture methods [11, 174]. 3D culture methods such as hanging drops [25, 129] and microwells [175] have been mainly used for solid tumor analysis. However, lymphoma-derived cells are generally non-adherent cells, represented by hematopoietic cells and lymphocytes, making them more complex to handle, culture, and evaluate in 3D culture compared to adherent cells comprising solid tumors. Therefore, it is challenging to fabricate 3D structures mimicking the 3D lymphoma microenvironment *in vivo*, and the area of 3D culture in lymphoma is still

underexplored, with only few published reports [171, 176]. Although microwells [177] and optical tweezers [178] allow a 3D culture of lymphoma-derived cells, they require gentle solution manipulation during culture, analysis, and evaluation due to weak cell-to-cell adhesion of non-adherent cells. Therefore, there are no standardized and reproducible 3D lymphoma models available for various applications, despite their potential to elucidate resistance to lymphoma therapies and their underlying mechanisms. In chapter II, I established a cell culture and evaluation system called a Cell Dome which is a dome with a hemispherical cavity (1 mm in diameter and almost 300 μm in height) that provides a 3D space for cell growth of enclosed cells [60]. One major advantage of the Cell Dome is that it can be applied to non-adherent cells cultured in suspension.

This chapter presents the fabrication of a hemispherical 3D lymphoma model using the Cell Dome system with the hemispherical cavity [179]. The Cell Dome offers distinct advantages over existing 3D culture techniques, including improved handling of non-adherent cells, ease of operation and reproducibility, and the ability to mimic *in vivo* microenvironment more accurately. I used the human brain lymphoma cell line (TK cells) and the human B cell lymphoma cell line (KML-1 cells) as models to study cellular behavior in the Cell Domes, including cell proliferation, cellular hypoxia, and drug sensitivity. I also examined CD19 and CD20 expressions, biomarkers for immunotherapy targeting lymphomas which are mainly B cell-derived [180-182], on cells cultured in the Cell Dome. Cell Dome for fabricating lymphoma models is a promising tool for studying lymphoma behavior in 3D culture and could provide valuable insights for drug development in lymphoma treatment.

2. Materials and Methods

2.1 Cell culture and chemical synthesis

The human brain lymphoma cell line (TK cells: JCRB1206, JCRB Cell Bank, Ibaraki, Japan) and human B cell lymphoma cell line (KML-1 cells, JCRB Cell Bank) were cultured in RPMI

1640 medium (Nissui, Tokyo, Japan) with the addition of 20% FBS (Gibco, NY, USA) in a fully humidified atmosphere of 5% CO_2 at 37 °C.

Alg-Ph (2.7×10^{-4} mol-Ph/g) was synthesized by the reaction of sodium alginate (I-1G, viscosity = 100-200 mPa-s at 1%, mannuronic acid/gluronic acid ratio ≈ 0.7, Kimica, Tokyo, Japan) and tyramine hydrochloride (ChemImpex International, Illinois, USA) via water-soluble carbodiimide hydrochloride (EDC·HCl; Peptide Institute, Osaka, Japan) and N-hydroxysuccinimide (NHS; Fujifilm Wako Chemical, Osaka, Japan) [62].

Gela-Ph (7.8×10^{-4} mol-Ph/g) was also synthesized by the reaction of gelatin type B from bovine skin (approximately 250 g bloom; Sigma-Aldrich, St. Louis, MO, USA) and 3-(4-hydroxyphenyl) propionic acid (Tokyo Chemical Industries, Tokyo, Japan) via EDC-HCl and NHS) [107].

2.2 Cell Dome preparation

The Cell Domes were prepared according to the procedure described in a previous study [105]. Briefly, a 1 μL core solution (PBS containing 3.0 w/v% gelatin type A from porcine skin [approximately 300 g bloom; Sigma-Aldrich], 1.2×10^7 cells/mL TK or KML-1 cells, and 50 U/mL HRP [140 units/mg; Fujifilm Wako Chemical]) was placed inside the water-repellent rings (inner/outer diameter: 1/1.4 mm) printed on phenolic hydroxyl groups-modified glass plate. After allowing it to stand at 5 °C for 15 min, a 10 μL shell solution (PBS containing 1 mM H_2O_2, 1.0 w/v% gel-Ph, and 0.5 w/v% alg-Ph) was added onto the hemispherical core gel. After hydrogel shell formation (15 °C for 5 min), the resultant glass plate with Cell Dome was washed with PBS and cultured in a medium containing 0.5 mg/mL catalase. After 24 h of cultivation, the medium was replaced with a fresh one (Figure 5-1). FITC-labeled gela-Ph was used instead of gela-Ph for structural analysis of the Cell Dome. Images of TK and KML-1 cells cultured in the Cell Dome were captured at appropriate incubation period times using a fluorescence microscope (BZ 9000; Keyence, Tokyo, Japan). The hydrogel shell was degraded

using alginate lyase (24 units/mg; Nagase Chemtex Corporation, Osaka, Japan) and the enclosed cells were dissociated with trypsin/EDTA. The single cells were then collected for cell count analysis using the Countess II FL (Thermo Fisher Scientific, MA, USA).

Frozen sections of cells cultured within the Cell Domes were prepared as follows: Cell Domes cultured for 10 days were first immersed in 4% paraformaldehyde solution (Fujifilm Wako Pure Chemicals) for 1 h, then in 5% sucrose solution (Fujifilm Wako Pure Chemicals) for 1 h. After washing twice with PBS, they were quickly frozen in liquid nitrogen with Tissue-Tek® O.C.T. compound (Sakura Finetek Japan K.K., Tokyo, Japan) and sliced into 15 μm sections using a cryomicrotome (2800 Frigocut E, Reichert-Jung, Germany). The resulting frozen sections were stained with hematoxylin/eosin and observed under a fluorescence microscope.

2.4 Initial cell density analysis

PBS containing 3.0% (w/v) gelatin from porcine skin, 1.5×10^8 cells/mL of TK or KML-1 cells, and 50 U/mL HRP were used as a core solution to fabricate the Cell Domes in the same manner as described in the "Cell Dome preparation" section. This Cell Dome fabricated with

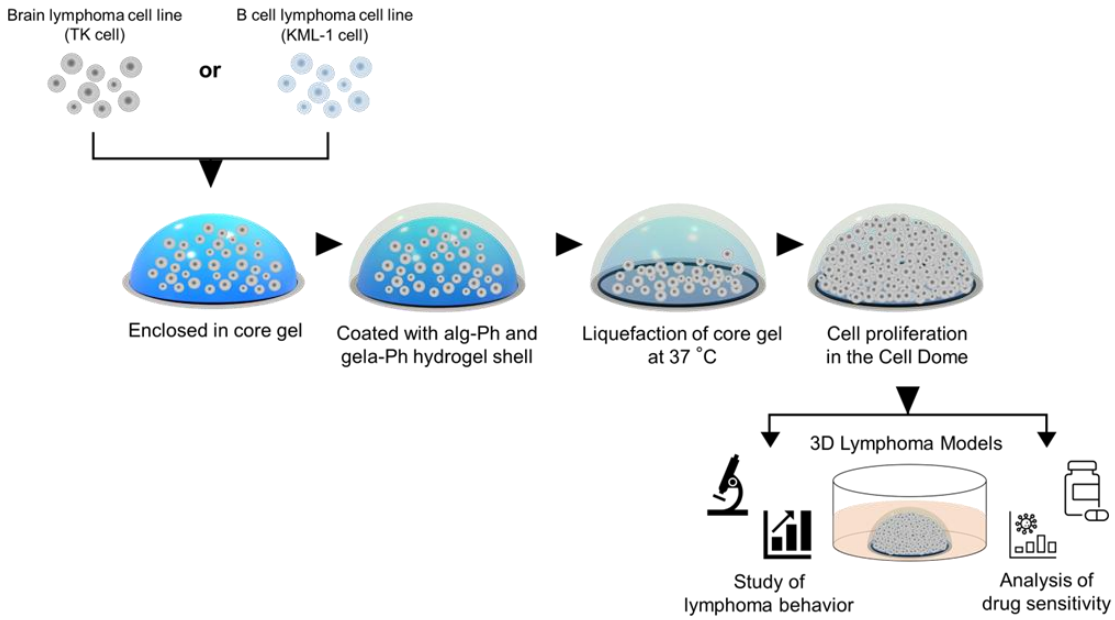

Figure 5-1. Schematic diagram of the Cell Dome preparation process. The process includes the preparation of the core gel with horseradish peroxidase (HRP), followed by the formation of the hydrogel shell with alg-Ph and gela-Ph through HRP-mediated hydrogelation, and finally, the immersion in a medium containing catalase for cell culture. Reprinted (adapted) from [179]. Copyright MDPI.

an initial cell density of 1.5×10^8 cells/mL was named a “High-density-Cell Dome”. Images and a number of TK and KML-1 cells cultured in the High-density-Cell Dome were analyzed in the same manner as described in the “Cell Dome preparation” section.

2.5 Hypoxia analysis

Cell Domes with cells incubated for 10 days and High-density-Cell Domes with cells incubated for 3 days were immersed in PBS containing 2.0 μM Hypoxia Probe Solution LOX-1 (MBL, Nagoya, Japan) for 24 h at 37 °C. Following incubation, the cells were washed twice with PBS and stained with LOX-1. They were observed under a fluorescence microscope and the relative amounts of *HIF-1α* mRNA in the enclosed cells collected from Cell Dome were determined by real-time PCR using specific primers,. Total cellular RNA was extracted using the CellAmp Direct TB Green RT-qPCR Kit (Takara Bio, Shiga, Japan) according to the manufacturer's instructions, and single-stranded cDNA was prepared by reverse transcription PCR reaction at 37 °C for 30 min followed by enzyme inactivation at 85 °C for 5 sec using DNase-treated RNA using PrimeScript™ FAST RT reagent Kit with gDNA Eraser (Takara Bio). From the resulting cDNA template, target sequences were amplified and quantified by real-time PCR using specific primers *HIF-1α* (reference gene: 18S ribosomal RNA [18s rRNA], Table 5-1). The PCR reactions involved an initial denaturation step at 95 °C for 30 s, followed by 40 cycles of at 95 °C for 5 s and 60 °C 10 s using TB Green® Premix Ex Taq™ II FAST qPCR (Takara Bio). Threshold cycle (Ct) values were obtained using a real-time PCR system (Thermal Cycler Dice® Real Time System II, Takara Bio). Relative mRNA content were determined using the ΔΔCt method, with calculations based on the 2nd Derivative Maximum approach (n=3).

Table 5-1. Primer used for detecting gene expressions. Reprinted (adapted) from [179]. Copyright MDPI.

Gene	Primer Forward	Primer Reverse	Reference
18s rRNA	5′-CCC GAC CCG GGG AGG TAG TG-3′	5′-GCC GGG TGA GGT TTC CCG TG-3′	[183]
HIF-1α	5′-TGC ATC TCC ATC TCC TAC CC-3′	5′-CCT TTT CCT GCT CTG TTT GG-3′	[109]

2.6 Flow cytometry

The cells cultured for 2, 7, and 10 days in the Cell Domes and the cells cultured for 3 days in the High-density-Cell Domes were collected as described in the "Cell Dome preparation" section. The collected cells were immersed in PBS (500 μL) with Hu Fc Block (5 μL, Becton, Dickinson and Company, NJ, USA) at 4 °C for 30 min. The cells were then immersed in PBS (500 μL) containing 2 μM propidium iodide (Dojindo, Kumamoto, Japan) and anti-CD19 mouse-mono (HIB19) APC (5 μL, Gene Tex, CA, USA) or anti-CD20 monoclonal antibody (2H7) FITC (5 μL, ThermoFisher, MA, USA) at 4 °C for 1 h. After washing with PBS twice, the cells were analyzed by flow cytometry (Accuri C6; BD Biosciences, Tokyo, Japan). The 2D-cultured cells with and without treatment with the antibodies were used as a positive and negative control, respectively.

2.9 Drug sensitivity analysis

After 10 days of culture in the Cell Dome or 3 days of culture in the High-density-Cell Dome, Cell Domes were exposed to a cell culture medium containing 10, 100, and 1,000 nM of doxorubicin (DOX; Fujifilm Wako Chemical) for a period of 72 h. The cells were stained with CalceinAM (Dojindo) and propidium iodide, collected as described in the "Preparation of Cell Dome" section, and cell viability was determined using the fluorescence microscope.

2.8 Statistical analyses

Statistical analyses of two or more data sets in this study were performed using Student's *t*-test or one-way ANOVA with Tukey's post hoc analysis. Values are expressed as mean ± SD.

3. Results and Discussion

3.1 Proliferation of enclosed cells in Cell Dome

The composite hydrogel of alg-Ph and gela-Ph used as the hydrogel shell of the Cell Dome has high cytocompatibility and good permeability to low molecular weight compounds [60, 105]. The hemispherical cell growth cavity of the Cell Dome was 283 ± 19 μm high and the hydrogel shell was 104 ± 16 μm thick (Figure 5-2a, n = 3), providing a hemispherical 3D growth space for the enclosed cells. Both TK and KML-1 cells grew well within the Cell Dome, and after 10 days of culture, they filled the hemispherical cavity and maintained their shape (Figures 5-2b and 2c). Proliferation was also confirmed by measuring the number of enclosed cells (Figure 5-2e), which increased over time, reaching a peak after 10 days of incubation and remaining almost constant thereafter (Figure 5-2e). In the High-density-Cell Dome too, both TK and KML-1 cells proliferated as the culture period progressed. These results are consistent with our previous report on K562 cells, a similar non-adherent cell cultured in the Cell Dome [60]. Compared to traditional 3D culture methods such as microwells [177] and optical tweezers [178], the Cell Dome system allows for the preparation of uniform hemispherical cavities enclosing the cells, facilitating critical operations such as solution manipulation and cell collection. These findings indicate that the Cell Dome system is suitable for 3D culture of non-adherent cells derived from lymphomas and provides reproducible and uniformly sized 3D cultured cells, which is essential for evaluation. Surprisingly, cell proliferation behavior differed by cell type in the High-density-Cell Dome. For TK cells, after 3 days of culture, dark areas were seen throughout the interior of the High-Density Cell Dome, indicating that cells were growing uniformly in 3D within the hemispherical cavity. In contrast, for KML-1 cells, after 3 days of culture a dark area in the center of the High-density-Cell Dome was observed indicating that the cells were proliferating in 3D in the center of the hemispherical cavity. (Figure 5-3a). Proliferation was also confirmed by measuring the number of enclosed cells, and

the number of cells cultured for 3 days in the High-density-Cell Dome was less than the number of cells cultured for 10 days in the Cell Dome and slightly more than the number of cells

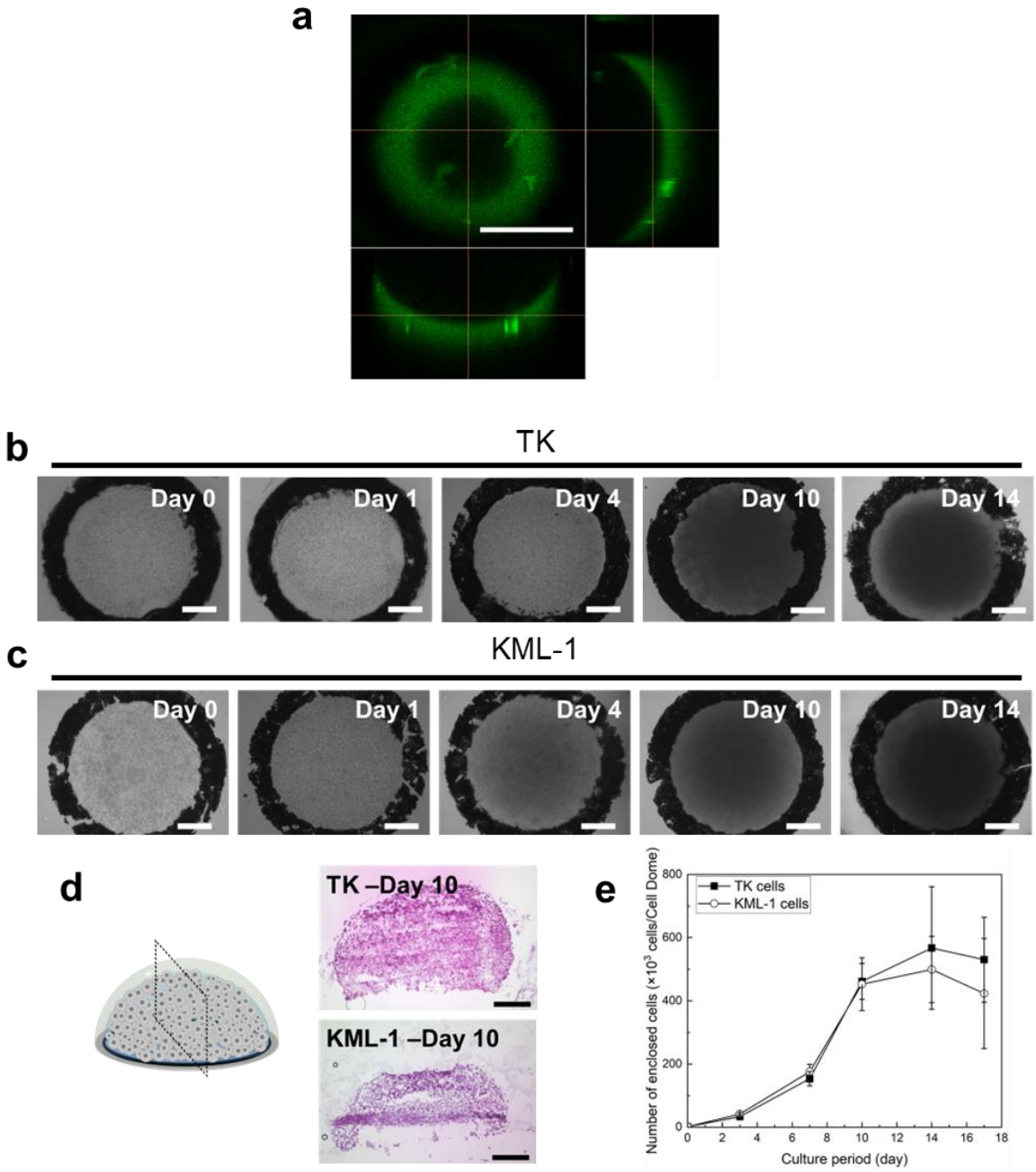

Figure 5-2. (a) Confocal microscope microscopic images of the Cell Dome fabricated using a mixture of alg-Ph and gela-Ph as the hydrogel shell material. The image shows the uniform hemispherical structure of the Cell Dome. Scale bar in panel b represents = 500 µm. (b, c) Microscopic images of TK (b) and KML-1 (c) cells cultured in the Cell Dome. (d) Histological section images of TK and KML-1 cells cultured in the Cell Dome for 10 days, showing cell distribution within the cavities. (e) Absorbance values attributed to mitochondrial activities of TK and KML-1 cells in the Cell Dome. Scale bars in panels a, b, and c represent 250 µm. Bars in panel d represent the SD ($n = 3$). Reprinted (adapted) from [179]. Copyright MDPI.

cultured for 7 days in the Cell Dome (Figures 5-2e and 5-3c). This could be attributed to differences in doubling time and proliferation rate of the cell types. Furthermore, in this study, lymphoma-derived cells cultured in the Cell Dome could be fixed and processed directly to produce tissue sections. This approach overcomes a common challenge in major hematologic tumor models, where weak cell-to-cell connections are often disrupted during processing.

3.2 CD19 and CD20 expression on cells enclosed in Cell Dome

CD19 and CD20 are specific markers for B cells in lymphoma and serve as biomarkers for immunotherapy targeting B cell-derived diseases [180, 182]. Therefore, investigating CD19 and CD20 expression on lymphoma-derived cells in 3D cultures can provide important insights for developing drugs targeting these biomarkers. In both TK and KML-1 cells cultured in the Cell Dome, there were no significant differences in CD19 expression levels compared to those cultured in 2D flasks (Figure 5-4a and Table 5-2, $p > 0.05$). CD19 expressions on TK and KML-1 cells cultured for 3 days in the High-density-Cell Domes were similar to those cultured in 2D flasks and in the Cell Domes for 10 days (Figure 5-4b and Table 5-2, $n = 3$, $p > 0.05$). Muz *et al.* reported that CD19 expression on multiple myeloma cells differentiated from B cells was not affected by hypoxia [184]. In contrast, CD20 expression levels differed during 3D culture

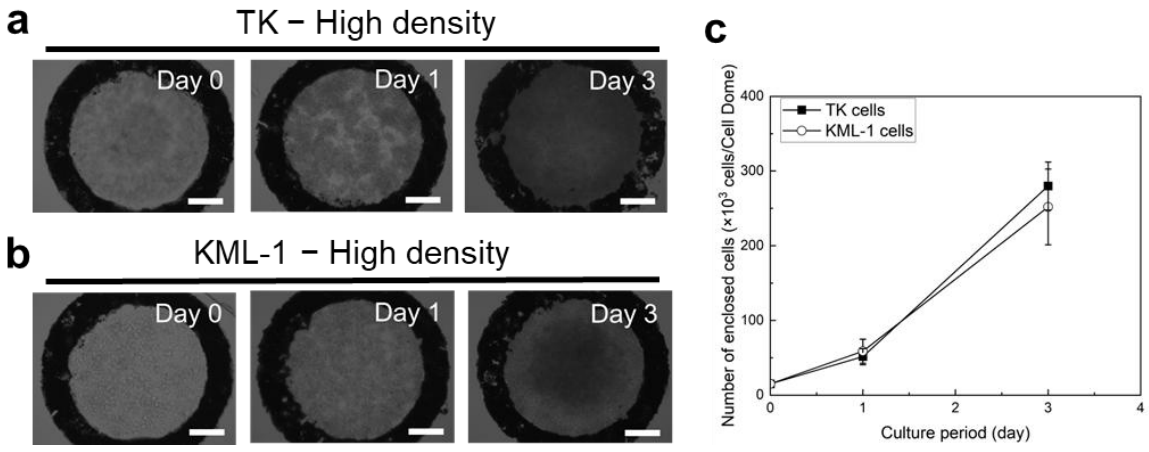

Figure 5-3. Microscopic images of TK (a) and KML-1 (b) cells cultured in the High-density-Cell Dome. (c) Absorbance values attributed to mitochondrial activities of TK and KML-1 cells in the High-density-Cell Dome. Scale bars in panels a and b represent 250 μm. Bars in panel c represent the SD ($n = 3$). Reprinted (adapted) from [179]. Copyright MDPI.

depending on the cell type. Flow cytometry analysis of CD20 expression on TK cells cultured in the Cell Domes for 2, 7, and 10 days showed two peaks, indicating both, higher and similar expression levels to those cultured in 2D flasks (Figure 5-4a and Table 5-3). The lower peak increased with the incubation periods and reached nearly the same percentage as the higher peak at 10 days of culture. The flow cytometry analysis of CD20 expression on TK cells cultured in the High-density Cell Domes for 3 days also showed two peaks, with similar peaks as those cultured in Cell Domes for 2 and 7 days (Figure 5-4a and Table 5-3). In contrast, CD20 expressions on KML-1 cells cultured for 2, 7, and 10 days in the Cell Domes showed a single peak that gradually decreased with increasing culture periods (Figure 5-4a and Table 5-3, n = 3, $^{*}p < 0.05$). CD20 expression on KML-1 cells after 10 days of culture in the Cell Domes showed lower expression levels than those cultured in 2D flasks (Figure 5-4a and Table 5-3, n = 3, $^{*}p < 0.05$). CD20 expression on KML-1 cells cultured in the High-density-Cell Domes for 3 days also showed one peak, indicating lower expression levels than those cultured in 2D flasks, with slightly higher peak height than those cultured in the Cell Domes for 10 days

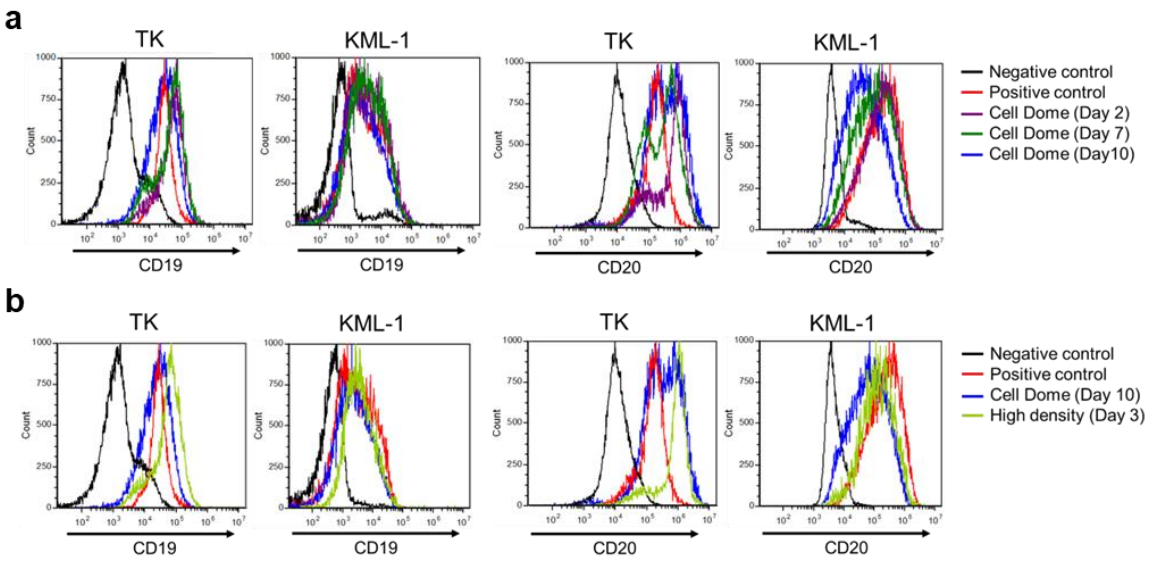

Figure 5-4. Flow cytometry analysis of CD19 and CD20 expression on 2D-cultured TK or KMl-1 cells immunostained without anti-CD19 or CD20 (negative control), with anti-CD19 or -CD20 (positive control), (a) Cell Dome-cultured cells for 2, 7, and 10 days immunostained with anti-CD19 or -CD20, and (b) High-density-Cell Dome-cultured cells for 3 days immunostained with anti-CD19 or -CD20. Reprinted (adapted) from [179]. Copyright MDPI.

(Figure 5-4b and Table 5-3, n = 3). Although the detailed mechanisms underlying the differences in CD20 expression levels based on cell type have not been elucidated, the upregulation of CD20 expression on TK cells cultured in the Cell Dome could be due to hypoxia. Ahmed *et al.* reported that HIF-1α might regulate CD20 expression in lymphoma [185]. To further investigate the potential regulation of CD20 expression by hypoxia, future studies should include the use of hypoxia inhibitors or siRNA targeting *HIF-1α* to directly assess its role in modulating CD20 levels. Additionally, examining downstream signaling pathways activated under hypoxic conditions could provide deeper mechanistic insights into how hypoxia influences CD20 expression in different lymphoma cell types. In this study, the presence of two peaks in flow cytometry analysis of CD20 expression on TK cells cultured in the Cell Dome (Figure 5-4a and Table 5-3), indicating both similar and higher expression levels compared to those cultured in 2D flasks, suggests that hypoxic conditions in the Cell Dome upregulated the CD20 expression on TK cells. On the other hand, the proportion of Cell Dome-cultured cells expressing CD20 at levels similar to those of 2D cultured-cells increased with extended incubation periods (Figure 5-4). This downregulation of CD20 on TK cells could result from mechanical stress and changes in the integrin signaling network caused by 3D culture [186]. The downregulation of CD20 was also observed on KML-1 cells cultured in the Cell Dome, where CD20 expression was gradually downregulated with increasing culture periods, likely due to the increased 3D cell-cell interactions [186]. Some B cell lymphoma patients are resistant to anti-CD20 targeting agents, including rituximab [187]. The mechanisms behind resistance to anti-CD20 agents have remained largely unknown but may involve downregulation or loss of CD20 expression [188, 189]. The results of this study may help elucidate CD20 regulation in lymphoma, as multiple mechanisms may be involved in CD20 regulation [190], and the Cell Dome would be beneficial for future experiments investigating this regulation, which is important for lymphoma treatment.

Table 5-2. Mean fluorescence intensities of TK or KML-1 cells, cultured in a 2D flask without immunostaining, the immunostaining 2D cultured cells with anti-CD19, and the immunostaining cells cultured in Cell Domes or High-density-Cell Domes with anti-CD19 (*n* = 3). Reprinted (adapted) from [179]. Copyright MDPI.

Sample	Mean intensity of surface CD19 Expression on TK cells [a.u.]	Mean intensity of surface CD19 expression on KML-1 cells [a.u.]
2D flask without anti-CD19	$0.9 \pm 0.4 \times 10^4$	$0.4 \pm 0.1 \times 10^3$
2D flask with anti-CD19	$3.4 \pm 1.0 \times 10^4$	$2.5 \pm 1.0 \times 10^3$
For 2 days in Cell Domes with anti-CD19	$3.2 \pm 0.4 \times 10^4$	$3.1 \pm 0.4 \times 10^3$
For 7 days in Cell Domes with anti-CD19	$2.0 \pm 0.5 \times 10^4$	$3.0 \pm 0.3 \times 10^3$
For 10 days in Cell Domes with anti-CD19	$2.1 \pm 0.5 \times 10^4$	$2.2 \pm 0.4 \times 10^3$
For 3 days in High-density Cell Domes with anti-CD19	$4.6 \pm 0.2 \times 10^4$	$3.8 \pm 0.4 \times 10^3$

Table 5-3. Mean fluorescence intensities of TK or KML-1 cells, cultured in a 2D flask without immunostaining, the immunostaining 2D cultured cells with anti-CD20, and the immunostaining cells cultured in Cell Domes or High-density-Cell Domes with anti-CD20 (*n* = 3). Reprinted (adapted) from [179]. Copyright MDPI.

Sample	Mean intensity of surface CD20 expression on TK cells [a.u.]	Mean intensity of surface CD20 expression on KML-1 cells [a.u.]
2D flask without anti-CD20	$5.0 \pm 2.0 \times 10^4$	$0.4 \pm 0.1 \times 10^4$
2D flask with anti-CD20	$19.4 \pm 1.2 \times 10^4$	$18.5 \pm 6.2 \times 10^4$
For 2 days in Cell Domes with anti-CD20	$46.3 \pm 17.4 \times 10^4$	$15.7 \pm 0.3 \times 10^4$
For 7 days in Cell Domes with anti-CD20	$28.5 \pm 5.2 \times 10^4$	$8.9 \pm 0.4 \times 10^4$
For 10 days in Cell Domes with anti-CD20	$35.2 \pm 6.7 \times 10^4$	$5.0 \pm 1.3 \times 10^4$
For 3 days in High-density Cell Domes with anti-CD20	$93.8 \pm 4.1 \times 10^4$	$12.1 \pm 1.7 \times 10^4$

3.3 Hypoxia and drug-sensitivity analysis

Hypoxia is a typical feature of the tumor microenvironment [191] and is closely associated with drug resistance, increased aggressiveness, accelerated metastatic potential, and tumor progression [191, 192]. Tumor cells, including malignant lymphomas, that are hypoxic, overexpress HIF-1α [120], which is considered a poor prognostic factor [193, 194]. After 10 days of culture, both TK and KML-1 cells in the cell dome stained with hypoxia probe solution showed red fluorescence, indicating hypoxia in the center of the cell dome, whereas cells in

2D flasks did not show red fluorescence (Figure 5-5a and 5-5b). *HIF-1α* gene expression was 12.7 ± 7.3-fold and 9.1 ± 2.6-fold higher in TK and KML-1 cells, respectively, when cultured in cell domes for 10 days than when cultured in 2D flasks (Figure 5-5d, $n \geq 3$, $^{*}p < 0.05$). In TK cells cultured in the High-density Cell Dome for 3 days, cells stained with the hypoxia probe solution also showed red fluorescence throughout the High-density Cell Dome, indicating hypoxia. In KML-1 cells cultured for 3 days in the High-density-Cell Dome, staining with the hypoxia probe solution revealed red fluorescence in the center of the Cell Dome, indicating hypoxia. This pattern was similar to that observed in cells cultured for 10 days in the Cell Dome (Figures 5-5b and -5c). Gene expression of *HIF-1α* was 4.3 ± 0.7-fold and 10.6 ± 6.8-fold higher in TK and KML-1 cells, respectively, when cultured for 3 days in the High-density Cell Dome compared to cells cultured in 2D flasks (Figure 5-5d, $n \geq 3$). To the best of our knowledge, these is the first report reproducing hypoxia and oxygen concentration gradients in 3D cultures of lymphoma-derived cells. Pangarsa *et al.* [195] reported that hypoxia, as with many solid tumors, was present in diffuse large B cell lymphoma (a type of lymphoma) and emphasized the need for further research on its role as a potential pathogenic or prognostic marker in this type of blood cancer. This Cell Dome system, which recapitulates hypoxia, may help elucidate the role of hypoxia in lymphomas.

Hypoxia and upregulated HIF-1α in hypoxia promote tumor cell survival and chemotherapy resistance in many malignancies [196, 197], upregulate the expression of multidrug resistance proteins, and are a major cause of multidrug resistance. DOX, one of the effective lymphoma therapeutics and widely evaluated and used in combination therapy of lymphoma malignancies, was used to assess drug sensitivity [198, 199]. Both TK and KML-1 cells cultured in the Cell Dome for 10 days and in the High-density-Cell Dome for 3 days showed significantly higher cell viability compared to those in 2D flasks (Figures 5-5e and -5f, $n = 3$, $^{*}p < 0.05$). When exposed to 10 nM of DOX, the cells cultured in the Cell Dome for 10 days exhibited

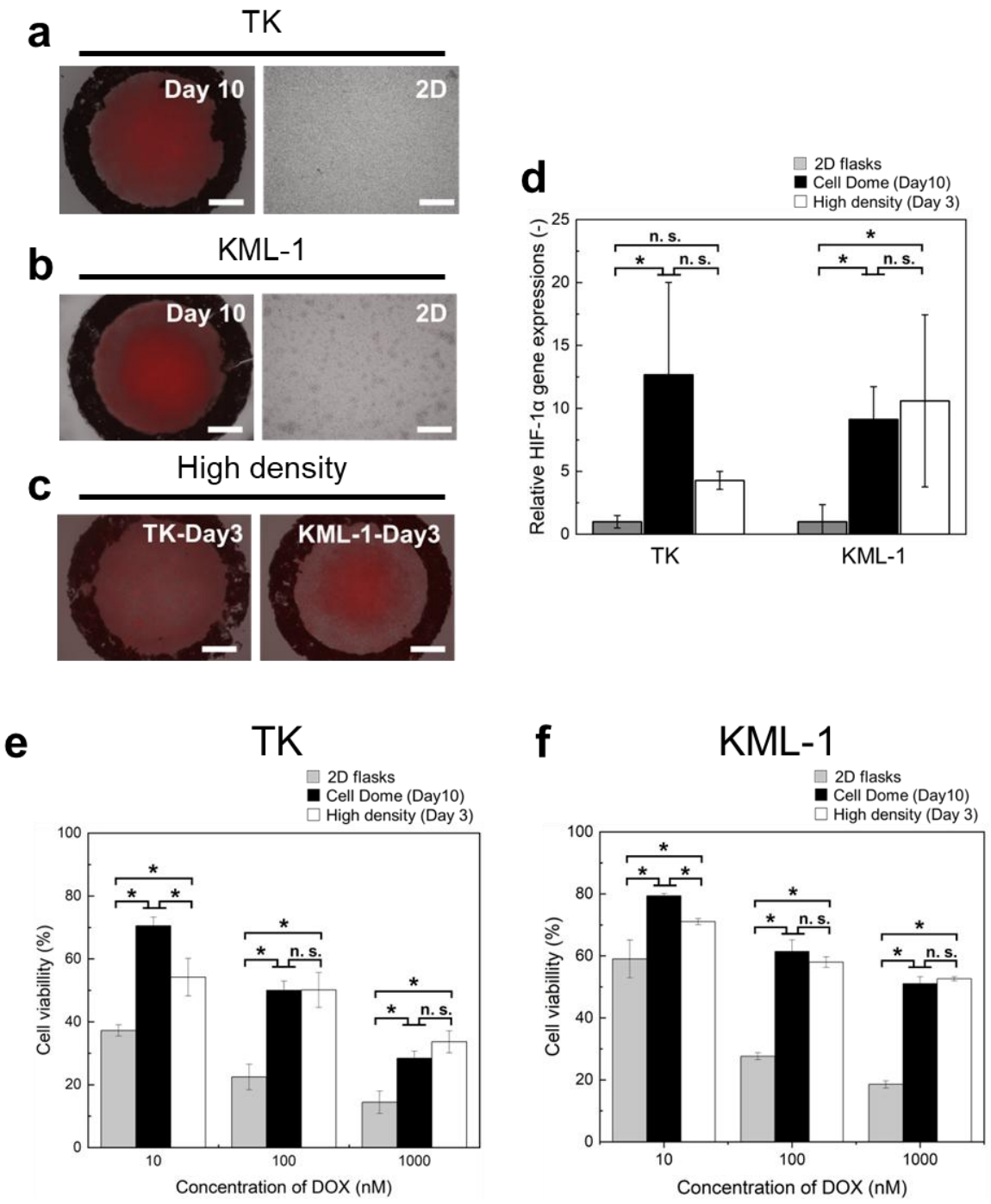

Figure 5-5. (a-c) Fluorescence microscope images of TK (a) or KML-1 (b) cells cultured in the Cell Dome for 10 days and in a 2D flask, stained with Hypoxia Probe solutions. Red fluorescence indicates hypoxic conditions. (c) Fluorescence microscope images of TK or KML-1 cells cultured in the High-density-Cell Dome for 3 days stained with Hypoxia Probe solutions. Red fluorescence indicates hypoxic conditions. (d) Relative gene expression of *HIF-1α* in TK or KMl-1 cells cultured for 10 days in the Cell Dome and for 3 days in the High-density-Cell Dome. Scale bars in panels a, b, and c represent 250 μm. Bars in panel d represent the SD ($n \geq 3$, *$p < 0.05$, n.s: $p>0.05$). (e, f) Viability of TK (e) or KML-1 (f) cells cultured in the Cell Dome for 10 days, in the High-density-Cell Dome for 3 days, and in 2D flasks, exposure to 10, 100, and 1000 nM doxorubicin (DOX). Bars represent the SD ($n = 3$, *$p < 0.05$, n.s: $p>0.05$). Reprinted (adapted) from [179]. Copyright MDPI.

significantly higher cell viability compared to those cultured in the High-density-Cell Dome for 3 days (Figures 5-5e and -5f, $n = 3$, $*p < 0.05$). This suggests that lymphoma-derived cells acquired drug resistance due to hypoxia induced by 3D culture. Mechanisms such as multidrug resistance proteins would influence the acquisition of drug resistance. Further research into these mechanisms, including the role of multidrug resistance proteins, could provide a deeper understanding of how lymphoma-derived cells acquire drug resistance when cultured in the Cell Dome. Since the 2D culture system cannot effectively replicate the environment that induces multidrug resistance [200, 201], the drug resistance to DOX in the cells cultured in the Cell Dome reflects the characteristics of *in vivo* lymphoma microenvironment. This suggests that this 3D lymphoma model utilizing the Cell Dome could be a useful platform for the development of new drugs for lymphoma treatment.

4. Conclusion

In summary, a 3D lymphoma model was developed by culturing lymphoma-derived TK and KML-1 cells using the Cell Dome system. The central cells in the Cell Dome were hypoxic, exhibiting an oxygen concentration gradient. CD19 expression remained unchanged in both cell lines when cultured in the Cell Dome compared to those in 2D flasks. CD20 expression was slightly upregulated in TK cells and downregulated in KML-1 cells cultured in the Cell Dome compared to 2D cultures. Furthermore, both TK and KML-1 cells in the Cell Dome exhibited higher resistance to DOX compared to those cultured in 2D flasks. In addition, by significantly increasing the initial cell density during the Cell Dome preparation process, cells that behave nearly identically to those cultured in the Cell Dome can be rapidly harvested, allowing rapid evaluation of lymphoma models using the Cell Dome system. The study in this chapter demonstrated the utility of the Cell Dome in a 3D lymphoma model and would provide valuable insights for studying lymphoma behavior and developing new drugs for lymphoma treatment.

Some portion of this thesis, including text and figures, have been previously published in the journal article “Development of Hemispherical 3D Models of Human Brain and B Cell Lymphomas Using On-Chip Cell Dome System” by Kazama *et al.*, published in *Bioengineering*, 2024, 11 (12), 1303 (Reference No. 179). These sections are reproduced here with permission from MDPI.

Chapter VI

Cell Dome-based transfection array for non-adherent suspension cells

1. Introduction

Understanding the functions of genes and proteins expressed in cells, as well as identifying gene products with specific properties is an important issue in biology and pathology. Cell-based microarrays are valuable tools for analyzing cellular functions and are gaining interest as for various cell biology applications, including drug discovery, toxicology, functional genomics, stem cell research, and tissue engineering [37, 202-204]. Ziauddin *et al.* developed cell-based microarrays by printing different complementary DNA at specific positions on glass slides, followed by culturing adherent HEK293 cells on them [36]. Only adherent cells are suitable for use in conventional cell-based microarrays owing to the requirement of cells to adhere to the substrate. This restriction excludes non-adherent cells, such as hematopoietic cells and lymphocytes, which are crucial targets in the biological and medical research. Kato et al. reported preparation of cell-based microarrays of a non-adherent human lymphoma cell line (K562 cells) by fixing the cells to a glass slide using immobilized plasmid DNA [205]. However, the forced adhesion of cells induces metabolic and structural changes in the cells due to distorted cell morphology [206]. Additionally, to prevent cell migration and cross-contamination within the array, it is typically necessary to maintain a fixed distance between spots and pattern the glass substrates, often by preparing hydrophobic or hydrophilic surfaces [202, 207-209].

Therefore, the study of this chapter aimed to develop a gene transfection array that can handle non-adherent cells without immobilizing them onto substrates. To achieve this goal, I

applied the Cell Dome technique, which enables the culture and evaluation of non-adherent cells suspended in solution [60]. Cell Dome is a hemispherical dome (1 mm diameter, about 300 μm height) with a hydrogel shell (about 90 μm-thick) enclosing cells in the hemispherical cavity. The hydrogel shell is obtained through HRP-mediated hydrogelation on cell-enclosing hemispherical gelatin hydrogel [60, 105, 146]. HRP-mediated hydrogelation has already been used to fabricate several cell-laden structures, such as microcapsules [53, 111], hydrogel fibers [51], and hydrogel sheets [107, 210]. In the study presented in this chapter, polyvinyl alcohol (PVA) and chitosan derivatives were used as hydrogel shell materials. PVA and PVA-based hydrogels are widely used in biomedical fields due to their biocompatibility [211, 212]. Chitosan and chitosan-based hydrogels are used in the pharmaceutical and medical fields due to their biodegradability, biocompatibility, and antibacterial properties [213-215]. Composite hydrogels of these polymers have high biocompatibility and are used in biomedical applications [216, 217]. Because Cell Domes are immobilized on transparent glass plates, non-adherent cells can be cultured, handled, and evaluated with the same ease as adherent cells [60]. In addition, multiple Cell Domes can be fabricated on the same plate [60].

The study in this chapter proposes Cell Dome as a novel gene transfection array, i.e., Cell Dome-based transfection array allowing for the transfection of non-adherent cells in suspension, a limitation of conventional cell-based microarrays [218]. Hydrogel shell materials for gene transfer within the Cell Dome were investigated and the transfection effect of non-adherent cells in suspension enclosed in Cell Dome was examined. This novel Cell-Dome transfection array would be a valuable tool for analyzing the cellular function of non-adherent cells in suspension and could provide important biomedical insights.

2. Materials and Methods

2.1 Materials

Tyramine hydrochloride and water-soluble carbodiimide hydrochloride (EDC-HCl) were

obtained from ChemImpex International (Wood Dale, IL, USA), the Peptide Institute (Osaka, Japan). Calcein-AM and Propidium iodide (PI) were purchased from Dojindo Laboratories (Kumamoto, Japan). Chitosan (Chitosan LL; average molecular weight: 50–100 kDa, deacetylation: 80%) was purchased from Yaizu Suisankagaku Industry (Shizuoka, Japan).

PVA derivative with carboxyl moieties (PVA-COOH; AF-17, viscosity of 4% solution: 30 mPa·s, degree of hydrolysis: >96.5% mol) and sodium alginate (I-1G; mannuronic acid/guluronic acid ratio ≈ 0.7, MW 70 kDa) were obtained from Japan Vam & Poval Co., Ltd. (Osaka, Japan), Kimica (Tokyo, Japan). RPMI 1640 medium was purchased from Nissui Pharmaceutical (Tokyo, Japan). 3-(4-hydroxyphenyl) propionic acid (HPP) and gelatin (type A from porcine skin) were purchased from Sigma-Aldrich (MO, USA). K562 cells were obtained from the Riken Cell Bank (Ibaraki, Japan) and cultured in RPMI 1640 medium containing 10% (v/v) FBS under a humidified atmosphere (5% CO_2/95% air) at 37 °C. FBS was purchased from Gibco (NY, USA). N-hydroxysuccinimide (NHS), H_2O_2 (31% w/w), catalase (from bovine liver; 8,000 U/mg), and HRP (200 U/mg) were purchased from Fujifilm Wako Chemicals (Osaka, Japan). Lipofectamine 3000 was purchased from Thermo Fisher Scientific (MA, USA). The mCherry expression plasmid (pCAG-HAmCherry) was prepared as previously described [219]. PVA-Ph and alginate-Ph were synthesized from PVA-COOH and sodium alginate, respectively, and tyramine hydrochloride using EDC-HCl and NHS based on the previous reports [62, 220]. Chitosan-Ph was synthesized from chitosan and HPP using EDC-HCl and NHS based on the previous report [215]. The phenolic hydroxyl group content in PVA-Ph, alginate-Ph, and chitosan-Ph was 4.9×10^{-4}, 2.7×10^{-4}, and 1.2×10^{-4} mol Ph/g, respectively.

2.2 Zeta-potential of hydrogels

For preparing the hydrogels, PBS (pH 7.4) containing 50 U/mL HRP and 1.0 w/v% alginate-Ph, 2.0 w/v% PVA-Ph, or the mixture of 2.0 w/v% PVA-Ph and 2.0 w/v% chitosan-Ph was

placed in a mold ($10 \times 30 \times 3$ mm^3) and exposed to air containing 16 ppm H_2O_2 for 30 min. A zeta potential measurement system (ELSZ-2000ZS; Otsuka Electronics, Osaka, Japan) was used to measure hydrogel surface charges.

2.3 Lipofection in the presence of hydrogels

In the wells of a 6-well plate, a mixture containing 1 mM H_2O_2, 50 U/mL HRP, and PBS containing 1.0 w/v% alginate-Ph, 2.0 w/v% PVA-Ph, or a combination of 2.0 w/v% PVA-Ph and 2.0 w/v% chitosan-Ph was prepared to form the hydrogels (100 µL) through HRP-mediated hydrogelation. After washing twice with PBS, the medium containing 1.0 mg/mL catalase, 1.0×10^7 cells/mL K562 cells, and the Lipofectamine/pDNA complex was added to the wells. Lipofectamine/pDNA complex was prepared by mixing P3000™ reagent, Lipofectamine™ 3000 reagent, and pDNA (pCAG-HAmCherry) according to the manufacturer's instructions. After 48 h of incubation, a fluorescence microscope (BZ-9000; Keyence, Tokyo, Japan) was used to observe K562 cells.

2.4 Cell Dome preparation

The Cell Domes were prepared according to the procedure described in a previous study [11-13]. Briefly, a core solution (PBS, 1 µL). containing 3.0 w/v% gelatin type A from porcine skin (approximately 300 g bloom), 1.0×10^7 cells/mL K562 cells, and 50 U/mL HRP. was placed inside the water-repellent rings (inner/outer diameter: 1/1.4 mm) printed on phenolic hydroxyl groups modified glass plate. After allowing it to stand at 5 °C for 15 min, a shell solution (PBS, 10 µL) containing 1 mM H_2O_2, 2.0 w/v% PVA-Ph, and 2.0 w/v% chitosan-Ph was added onto the hemispherical core gel. After hydrogel shell formation at 15 °C for 5 min, the resultant glass plate with Cell Dome was washed with PBS and cultured in a medium containing 0.5 mg/mL catalase. Images of TK and KML-1 cells cultured in the Cell Dome were captured at appropriate times during the incubation period using the fluorescence microscope, and viability analysis was measured using a fluorescence live/dead assay stained with Calcein AM/PI.

2.5 Transfection in Cell Dome

Prior to Cell Dome preparation as described in "Cell Dome preparation" section, antibiotic and serum-free medium (0.2 μL) containing 0.6 w/v% gelatin and 2.0 mg/mL catalase with Lipofectamine/pDNA complexes (0.013 μL of P3000™ reagent, 0.020 μL of Lipofectamine™ 3000 reagent, and 6.7 ng of pDNA-mCherry) was spotted inside the water-repellent ring pattern on the glass plates and allowed to stand for 15 min at room temperature (Figure 6-1). The concentration of lipofectamine/pDNA complex, cell, and catalase were optimized for this experiment. After 72 h of incubation, the cells cultured in the Cell Domes were observed under a fluorescence microscope.

2.6 Statistical analyses

Data are presented as mean ± SD. Comparisons between three or more datasets were performed using a ANOVA with Tukey's post-hoc analysis. Statistical significance was set at $*p < 0.05$.

3. Results and Discussion

3.1 Selection of hydrogel shell material

In the Cell Dome-based transfection array newly proposed in this study, the Lipofectamine/pDNA complex, which is spotted onto the bottom surface, is released into the Cell Dome, which contains non-adherent cells in suspension, enabling gene transfer. Since the Lipofectamine/pDNA complex is a cationic liposome, it is expected to form an electrical bond with the hydrogel shells and adsorb, preventing efficient gene transfer. To address this concern,

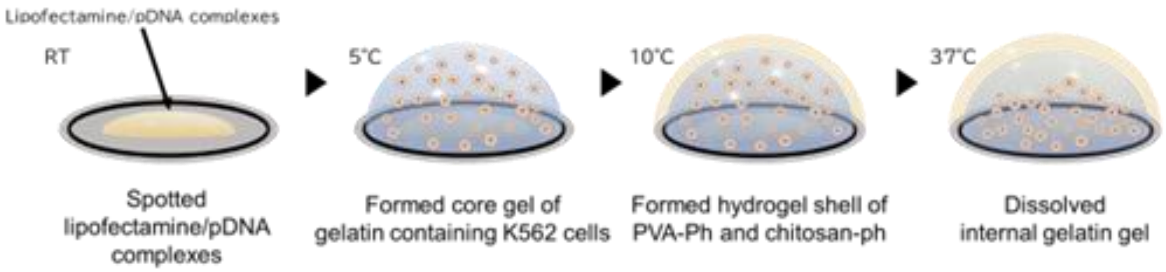

Figure 6-1. Schematic of the Cell Dome preparation process. Reprinted (adapted) from [218]. Copyright © 2024 Elsevier B.V.

I measured the zeta potential of the polymer-Ph hydrogel, a candidate material for the hydrogel shell, and investigated materials with a cationic surface charge. The surface charges of the alginate-Ph and PVA-Ph hydrogels were -46.0 ± 6.5 mV and -20.4 ± 4.0 mV, respectively, while the surface charge of the PVA-Ph/chitosan-Ph composite hydrogel was 3.8 ± 2.5 mV (Figure 6-2a). Attempts were made to develop Cell Domes using only chitosan-Ph as the material for the hydrogel shell, but due to the fragility of the hydrogel, the structure could not be maintained. Considering the increased transfection efficiency due to the cationic charge of the polymer (PVA-Ph/chitosan-Ph composite hydrogel), positively charged polymers such as polylysine [221, 222] and cationic cellulose [223, 224] could also be used for efficient transfection, but the stability of the hydrogel shell need to be considered.

Next, gene transfer using a Lipofectamine/pDNA complex was performed in the presence of the three hydrogels whose surface charges were measured. The transfection efficiency of K562 cells in medium without hydrogel was 3.7 ± 1.8% (n = 3, Figure 6-2c), while cells in medium containing hydrogels formed from PBS containing alginate-Ph or PVA-Ph showed significantly lower transfection efficiency (n = 3, Figures 6-2b, -2d, and -2e, $*p < 0.05$). Conversely, the transfection efficiency of cells in a medium containing PVA-Ph/chitosan-Ph combined hydrogel was not significantly different from that of cells in a medium without hydrogel (n = 3, Figures 6-2b and -2f, $*p > 0.05$). This suggests that the cationic charge of the PVA-Ph/chitosan-Ph composite hydrogel prevented the adsorption of the lipofectamine/pDNA complex to the hydrogel, thereby increasing transfection efficiency in K562 cells. Based on these findings, Cell Domes with PVA-Ph/chitosan-Ph composite hydrogel shells were predicted to be effective for the transfection of lipofectamine/pDNA complexes and were thus used as hydrogel shell materials of the Cell Dome-based transfection array.

3.2 Cell viability and growth of enclosed cells in Cell Dome

In this study, PVA-Ph/chitosan-Ph composite hydrogel was used for the first time as the hydrogel shell of the Cell Dome. The viability of K562 cells before, immediately after, and the day after enclosure in Cell Domes with PVA-Ph/chitosan-Ph composite hydrogel shell were 80.2 ± 4.5%, 75.2 ± 2.8%, and 82.0 ± 5.9%, respectively, with no significant differences between them (Figures. 6-3a-d, $p^* > 0.05$). Additionally, the cells enclosed in the Cell Dome proliferated with increasing periods of culturing, and by day 7 of culture, a black area indicating high cell density was observed (Figures. 6-3e-h). These results indicate that Cell Domes

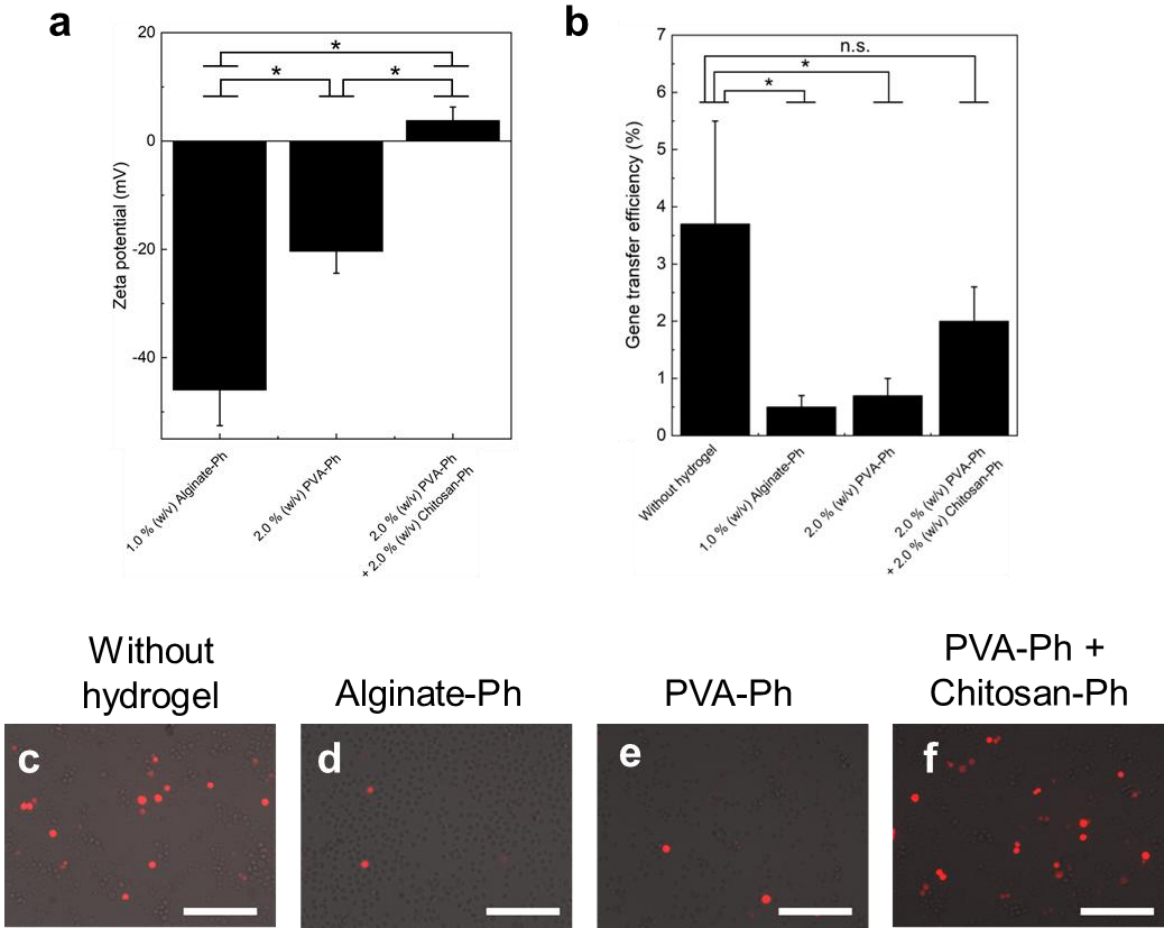

Figure 6-2. (a) Zeta potential of 1.0% w/v alginate-Ph, 2.0% w/v PVA-Ph, and 2.0% w/v PVA-Ph/2.0% w/v chitosan-Ph composite hydrogels prepared through HRP-mediated hydrogelation (n = 3, bars: SD, $^*p < 0.05$). (b) The transfection efficiency of the cells in media without and with hydrogels (n = 3, bars: SD, $^*p < 0.05$). (c-f) K562 cells transfected with Lipofectamine/pDNA complexes in medium (c) without hydrogel, and with the hydrogel prepared using (d) 1.0% w/v alginate-Ph, (e) 2.0% w/v PVA-Ph, (f) 2.0% w/v PVA-Ph and 2.0% w/v chitosan-Ph composite (Scale bars: 200 μm). Reprinted (adapted) from [218]. Copyright © 2024 Elsevier B.V.

prepared with PVA-Ph/chitosan-Ph composite hydrogel shells are highly cytocompatibility with no significant adverse effects on cell viability and proliferation.

3.3 Transfection of cells enclosed in Cell Dome with plasmid DNA

To fabricate the transfection array with non-adherent suspension cells, Cell Domes were prepared from PVA-Ph/chitosan-Ph composite hydrogel, and lipofectamine/pDNA complexes were released from the bottom of the Cell Dome. Cells transfected with Lipofectamine/pDNA complexes within the Cell Dome exhibited red fluorescence, indicating gene expression (Figure. 6-4a). The cells enclosed in each of the Cell Domes on the same glass plate were

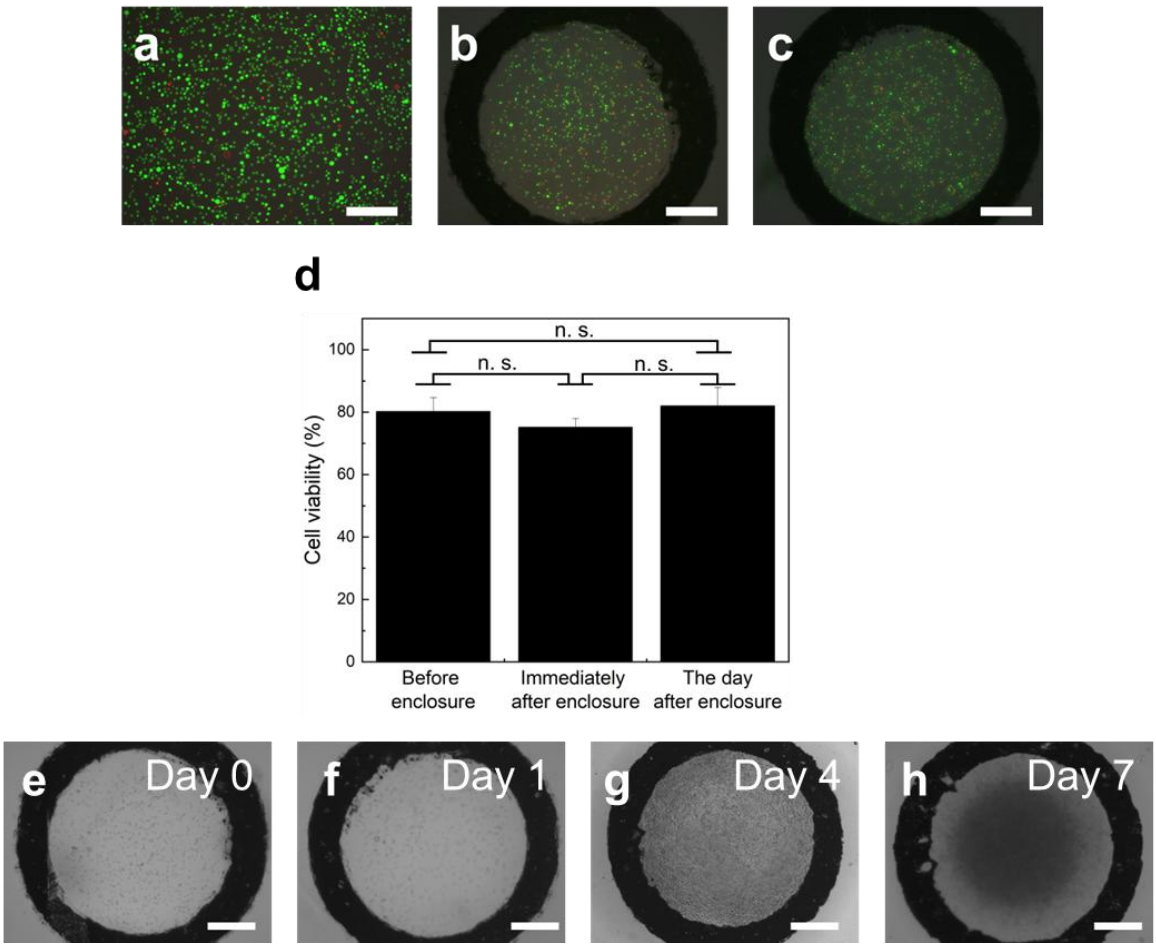

Figure 6-3. (a-c) The fluorescence microscope images of K562 cells before (a), immediately after (b), and the day after (c) enclosure in Cell Domes stained with calcein-AM and PI (Scale Bars: 250 μm). (d) Viability of the cells before, immediately after, and one day after enclosure in Cell Domes. (n = 3, bars: SD, n.s.: no significant difference, *p > 0.05). (e-h) Micrographs of enclosed cells cultured for 0, 1, 4, and 7 days in Cell Domes (Scale bars: 250 μm). Reprinted (adapted) from [218]. Copyright © 2024 Elsevier B.V.

successfully transfected (Figure. 6-4a). Additionally, the enclosed cells in every other alternate Cell Dome were transfected, with no transfection leakage or contamination observed in the adjacent Cell Domes on the same glass plate (Figure. 6-4b). These results demonstrate that use of the PVA-Ph/chitosan-Ph composite hydrogel shell-based Cell Dome facilitated the introduction of genes into suspended K562 cells and enabled the fabrication of a cell-based array with non-adherent cells in suspension.

This Cell Dome-based transfection array overcomes the limitations of conventional cell-based arrays, which are restricted to adherent cells. Additionally, unlike previously proposed cell-based arrays, that require non-adherent cells to adhere to a substrate, necessitating meticulous and gentle solution handling [205], this Cell Dome-based transfection array allows non-adherent cells to be handled easily in suspension using the same solution procedures as adherent cells. Current drawbacks with Cell Dome-based arrays include the size of the Cell

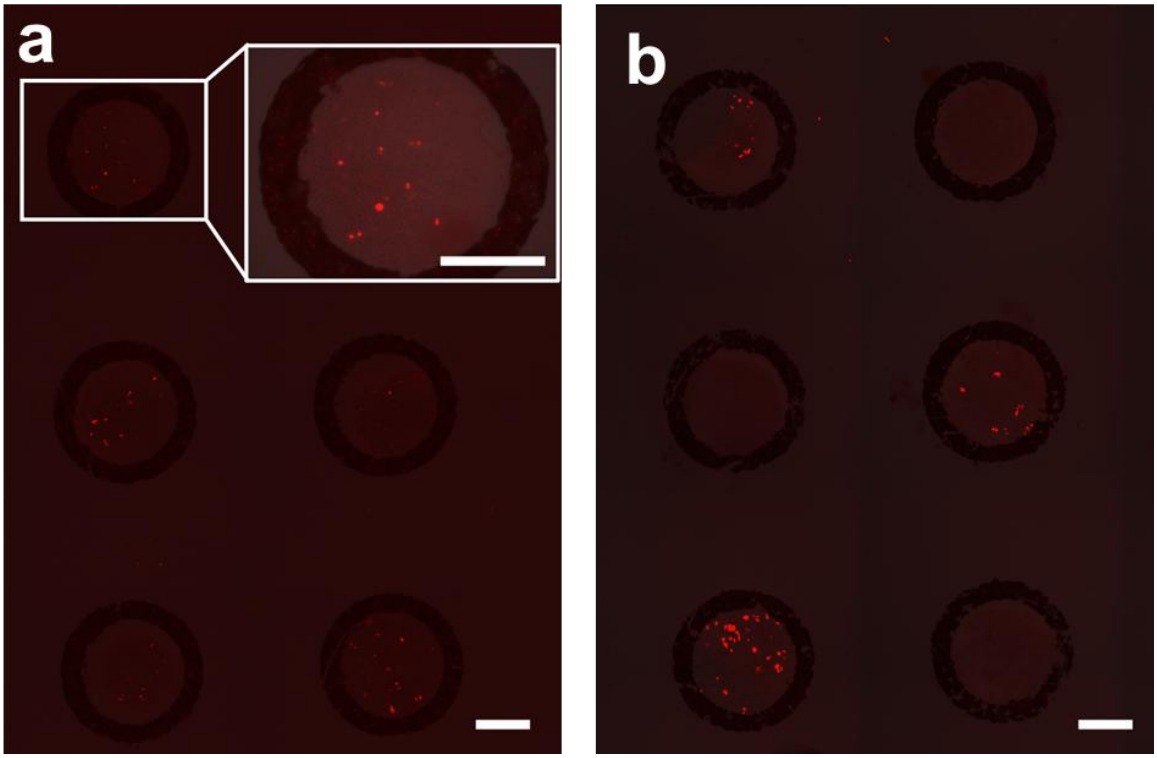

Figure 6-4. (a) K562 cells transfected with Lipofectamine/pDNA complexes released from the bottom of Cell Domes (Scale bars: 500 μm). (b) K562 cells enclosed within Cell Domes alternately transfected into adjacent Cell Domes with Lipofectamine/pDNA complexes (Scale bars: 500 μm). Reprinted (adapted) from [218]. Copyright © 2024 Elsevier B.V.

Dome (diameter: 1 mm) and low gene expression levels. Cell-based array technologies enable the complex characterization of cells in a high-throughput format, providing abundant information from small sample volumes [37, 202, 203, 225]. To efficiently conduct numerous experiments using minimal amounts of reagents, it is essential to reduce the size of the Cell Dome. Although Cell Domes are currently fabricated manually, automating the preparation process could enable the production of smaller Cell Domes. In this regard, a method to fabricate a Cell Dome using an inkjet printer is currently in development. The observed decrease in gene expression levels is attributed to gene transfer using Lipofectamine/pDNA complexes being less efficient, especially with non-adherent cells. Gene transfer methods such as superparamagnetic nanoparticles [226] and RetroNectin® [227] could effectively increase the efficiency of gene transfer to non-adherent cells. By combining these gene transfer methods with a Cell Dome-based transfection array, it may be possible to create cell-based arrays using non-adherent cells with high transfection efficiency.

4. Conclusion

The potential of the Cell Dome as a platform for transfecting non-adherent suspension cells was thoroughly investigated. The PVA-Ph/chitosan-Ph composite hydrogel served as the hydrogel shell of the Cell Dome due to its cytocompatibility and non-interference with transfection by Lipofectamine/pDNA complexes. Lipofectamine/pDNA complexes spotted on the bottom of the Cell Domes on a glass plate could transfect the enclosed cells. No leakage or contamination in the adjacent Cell Domes was observed after transfection with the spotted Lipofectamine/pDNA complexes. This novel Cell Dome-based transfection array has the potential to broaden the scope of cell-based array technologies by facilitating the transfection and evaluation of non-adherent suspension cells.

Some portion of this thesis, including text and figures, have been previously published in the journal article “Cell Dome-based transfection array for non-adherent suspension cells” by Kazama *et al.*, published in *Biochemical Engineering Journal*, 2025, 213, 109554 (Reference No. 218). These sections are reproduced here with permission from © 2024 Elsevier B.V.

Chapter Ⅶ

General Conclusions

This thesis explored the establishment and evaluation of the Cell Dome, a novel bioassay method, covering various aspects: the establishment of standardized Cell Dome (Chapter II), its application for culturing non-adherent (Chapter II) and adherent cells (Chapter III), studies on the effect of hydrogel shell's cell adhesiveness on enclosed cells (Chapter IV), its use in lymphoma modeling (Chapter V), and its application in cell-based transfection arrays (Chapter VI). Thus, this work contributes to advancing the drug development process and provides valuable biological and medical insights into tumors, diseases, and related conditions.

Chapter II described the establishment of a novel, standardized cell culture and evaluation system for bioassay in a dome fabricated with a semi-permeable hydrogel shell obtained through HRP-mediated hydrogelation. This cell-enclosed hydrogel dome was named Cell Dome (1 mm in diameter and almost 300 μm in height). Enclosed K562 cells, as a model of non-adherent cells, grew within the cavity, stained and differentiated with reagents supplied by the surrounding medium, and were easily manipulated in solution without cell loss or damage. Additionally, K562 cells filled in the hemispherical cavities of the Cell Dome (3D microenvironment) were more hypoxic and resistant to mitomycin C than cells cultured in 2D. The Cell Dome system established in this study can greatly improve the culture of non-adherent cells and would be a promising standardization bioassay tool for convenient culture and evaluation of non-adherent cells.

Chapter III focuses on the application of the Cell Dome as an evaluation platform for the 3D culture of adherent cells. HepG2 cells, a type of adherent cells, formed hemispherical cell aggregates that filled the cavity of the Cell Dome by day 18 of culture and remained viable for

up to 29 days. The center of the glass adhesive surface of the hemispherical cell aggregates, which is expected to have an environment similar to that of the center of the spheroid, could be directly observed through the glass plate. Cells cultured in the cell dome for 18 days exhibited higher Pi-class glutathione S transferase enzyme activity, hypoxia-inducible factor-1α gene expression, and resistance to mitomycin C than cells cultured in 2D on tissue culture dishes. These results demonstrate that the Cell Dome is a bioassay that can be applied to adherent as well as non-adherent cells as described in Chapter Ⅱ, suggesting that the Cell Dome is applicable to a wide range of cell-based assays and has the potential to be widely used as a very useful standard platform.

Chapter IV described the effects of the cell adhesion properties of the Cell Dome's hydrogel shell on the enclosed cells. Hydrogel shells with varying degrees of cell adhesion properties were prepared and cell behavior of the human cervical cancer cell line (HeLa), expressing the cell cycle marker fucci2 (HeLa-fucci2 cells), was observed. In adhesive hydrogel shells, cells proliferated along the inner wall of the shell, whereas in non-adhesive hydrogel shells, cells grew uniformly at the bottom of the cavities. Furthermore, cells in non-adhesive hydrogel shells had a higher percentage of cells in the G1/G0 phase compared to those in adhesive shells and exhibited increased resistance to mitomycin when the cavities became filled with cells. These results emphasize the importance of judiciously considering the cell-adhesive properties of the hydrogel shell when selecting material for Cell Domes.

In Chapter V, a 3D lymphoma model was developed by culturing lymphoma-derived TK and KML-1 cells using the Cell Dome system. The central cells in the Cell Dome were hypoxic, and there was an oxygen concentration gradient in the Cell Dome, which more closely mimicked actual lymphoma. To my knowledge, this is the first study to reproduce an oxygen concentration gradient in a 3D culture of lymphoma-derived cells, that more faithfully recapitulates the lymphoma environment than conventional 2D culture methods. CD19

expression did not change in either cell line, while CD20 expression was slightly upregulated in TK cells and downregulated in KML-1 cells cultured within the Cell Dome compared to those cultured in 2D flasks. In addition, both TK and KML-1 cells in the hemispherical structures exhibited higher resistance to doxorubicin than those in 2D flasks. This study demonstrated the utility of the Cell Dome in a 3D lymphoma model and provides valuable insights for studying lymphoma behavior and developing new drugs for lymphoma treatment.

In Chapter Ⅵ, the potential of the Cell Dome as a platform for transfecting non-adherent suspension cells was investigated. The human lymphoma cell line (K562 cells) was used as a model for non-adherent cells to explore suitable hydrogel materials as transfection arrays using Cell Dome (named Cell Dome-based transfection arrays). Gene transfer to suspended non-adherent cells was possible in Cell Domes with PVA-Ph/chitosan-Ph composite hydrogel shells. In other words, the Cell Dome with an appropriate hydrogel shell could be used as a transfection array for non-adherent cells in suspension. This novel Cell-Dome transfection array would be a valuable tool for analyzing the cellular function of non-adherent cells in suspension and showcases the potential for providing important biomedical insights for future research and development.

Overall, this thesis describes the successful establishment of the Cell Dome system as a new bioassay method, providing a platform for standardized cell-based bioassays for both non-adherent and adherent cells. In addition, Cell Dome can be a useful tool for the fabrication and evaluation of 3D lymphoma models and cell-based transfection arrays for suspended non-adherent cells. The findings of this thesis highlight the potential application of Cell Dome in the drug development process for various types of tumors and diseases and provide valuable insights for the biological and medical fields.

Suggestions for Future Works

Based on the findings of this research, the Cell Dome system presents several promising prospects for advancing the fields of biology, medicine, and drug development.

(1) Control of hydrogel shell permeability

The hydrogel shell used in this thesis showed good permeability to low molecular weight compounds and provided nutrients, including oxygen, to the enclosed cells. On the other hand, it is difficult to precisely control the permeation of substances through the hydrogel shell. If it is possible to precisely control the diffusion of substances into and out of the Cell Domes according to the molecular weight and charge of the substance, it is expected to be useful in drug testing and the evaluation using reagents.

(2) 3D Co-culture using Cell Dome

Current research is focused on evaluating the culture of one cell type in the Cell Dome. The next step will be to develop tumor and organ models that better mimic the tissue environment by co-culturing multiple cell types using Cell Dome. In addition to the advantages such as 3D culture of non-adherent cells, the Cell Dome integrates co-culture that recreates the interaction between cells *in vivo*. If both, 3D culture of non-adherent cells and co-culture become possible, it is expected that cell behavior in living tissues can be reproduced more accurately, and responses to drugs can be analyzed with higher precision compared to 2D monoculture.

(3) Mechanization of Cell Dome Fabrication Method

Cell Dome is currently fabricated manually. Mechanizing the Cell Dome fabrication method will enable a large number of assays to be performed simultaneously, contributing to high throughput technology. This will greatly advance the generalized practical application of the

Cell Dome. The study of Cell Dome fabrication using an inkjet printer would be very useful.

(4) Application of Cell Dome system to biochips

It would be very useful to investigate the application of Cell Dome to biochips that mimic *in vivo* interactions to better replicate the *in vivo* environment. Specifically, a biomimetic chip can be attached to the Cell Dome and connected via a flow path can be fabricated. Next, the Cell Dome with 3D co-cultured cells of interest can be placed on the chip and evaluated (for example, pancreatic cancer-derived cells, liver-derived cells, and vasculature-derived cells may be used to evaluate drug action considering drug metabolism in the liver). Various systems can be easily constructed by simply arranging Cell Domes enclosing cells as desired, and this has the potential to create biochips that incorporate 3D culture with greater ease than conventional methods. This is expected to reproduce biological systems that reflect interactions between organs and tumors.

References

[1] C.G. Rousseaux, W.M. Bracken, Overview of Drug Development, (2013) 647-685.
[2] S.A. Langhans, Three-Dimensional in Vitro Cell Culture Models in Drug Discovery and Drug Repositioning, Front Pharmacol 9 (2018) 6.
[3] J.M. Kelm, M. Lal-Nag, G.S. Sittampalam, M. Ferrer, Translational in vitro research: integrating 3D drug discovery and development processes into the drug development pipeline, Drug Discov Today 24(1) (2019) 26-30.
[4] R. Chakravarthy, K. Cotter, J. DiMasi, C.P. Milne, N. Wendel, Public- and Private-Sector Contributions to the Research and Development of the Most Transformational Drugs in the Past 25 Years: From Theory to Therapy, Ther Innov Regul Sci 50(6) (2016) 759-768.
[5] M. Hay, D.W. Thomas, J.L. Craighead, C. Economides, J. Rosenthal, Clinical development success rates for investigational drugs, Nat Biotechnol 32(1) (2014) 40-51.
[6] P.D. Olivo, Bioassays for thyrotropin receptor autoantibodies, Best Pract Res Clin Endocrinol Metab 37(2) (2023) 101744.
[7] T. Tuntland, B. Ethell, T. Kosaka, F. Blasco, R.X. Zang, M. Jain, T. Gould, K. Hoffmaster, Implementation of pharmacokinetic and pharmacodynamic strategies in early research phases of drug discovery and development at Novartis Institute of Biomedical Research, Front Pharmacol 5 (2014) 174.
[8] M.J. Waring, J. Arrowsmith, A.R. Leach, P.D. Leeson, S. Mandrell, R.M. Owen, G. Pairaudeau, W.D. Pennie, S.D. Pickett, J. Wang, O. Wallace, A. Weir, An analysis of the attrition of drug candidates from four major pharmaceutical companies, Nat Rev Drug Discov 14(7) (2015) 475-86.
[9] A. Dove, Drug screening-beyond the bottleneck, Nature America Inc. 17 (1999) 859-863.
[10] K. Han, S.E. Pierce, A. Li, K. Spees, G.R. Anderson, J.A. Seoane, Y.H. Lo, M. Dubreuil, M. Olivas, R.A. Kamber, M. Wainberg, K. Kostyrko, M.R. Kelly, M. Yousefi, S.W. Simpkins, D. Yao, K. Lee, C.J. Kuo, P.K. Jackson, A. Sweet-Cordero, A. Kundaje, A.J. Gentles, C. Curtis, M.M. Winslow, M.C. Bassik, CRISPR screens in cancer spheroids identify 3D growth-specific vulnerabilities, Nature 580(7801) (2020) 136-141.
[11] S. Breslin, L. O'Driscoll, Three-dimensional cell culture: the missing link in drug discovery, Drug Discov Today 18(5-6) (2013) 240-9.
[12] F. Pammolli, L. Magazzini, M. Riccaboni, The productivity crisis in pharmaceutical R&D, Nat Rev Drug Discov 10(6) (2011) 428-38.
[13] K.M. Yamada, E. Cukierman, Modeling tissue morphogenesis and cancer in 3D, Cell 130(4) (2007) 601-10.
[14] G.S. Huang, T.C. Tseng, N.T. Dai, K.Y. Fu, L.G. Dai, S.H. Hsu, Fast isolation and expansion of multipotent cells from adipose tissue based on chitosan-selected primary culture, Biomaterials 65 (2015) 154-62.
[15] H.L. Wong, M.X. Wang, P.T. Cheung, K.M. Yao, B.P. Chan, A 3D collagen microsphere culture system for GDNF-secreting HEK293 cells with enhanced protein productivity, Biomaterials 28(35) (2007) 5369-80.
[16] S. Sakai, K. Inamoto, Y. Liu, S. Tanaka, S. Arii, M. Taya, Multicellular tumor spheroid formation in duplex microcapsules for analysis of chemosensitivity, Cancer Sci 103(3) (2012) 549-54.
[17] Y. Fang, R.M. Eglen, Three-Dimensional Cell Cultures in Drug Discovery and Development, SLAS Discov 22(5) (2017) 456-472.
[18] J. Friedrich, C. Seidel, R. Ebner, L.A. Kunz-Schughart, Spheroid-based drug screen: considerations and practical approach, Nat Protoc 4(3) (2009) 309-24.
[19] Q. Li, C. Chen, A. Kapadia, Q. Zhou, M.K. Harper, J. Schaack, D.V. LaBarbera, 3D

models of epithelial-mesenchymal transition in breast cancer metastasis: high-throughput screening assay development, validation, and pilot screen, J Biomol Screen 16(2) (2011) 141-54.
[20] A. Ivascu, M. Kubbies, Rapid generation of single-tumor spheroids for high-throughput cell function and toxicity analysis, J Biomol Screen 11(8) (2006) 922-32.
[21] R.Z. Lin, H.Y. Chang, Recent advances in three-dimensional multicellular spheroid culture for biomedical research, Biotechnol J 3(9-10) (2008) 1172-84.
[22] A. Khademhosseini, R. Langer, J. Borenstein, J.P. Vacanti, Microscale technologies for tissue engineering and biology, Proc Natl Acad Sci U S A 103(8) (2006) 2480-7.
[23] J. Fukuda, Y. Sakai, K. Nakazawa, Novel hepatocyte culture system developed using microfabrication and collagen/polyethylene glycol microcontact printing, Biomaterials 27(7) (2006) 1061-70.
[24] Y.C. Tung, A.Y. Hsiao, S.G. Allen, Y.S. Torisawa, M. Ho, S. Takayama, High-throughput 3D spheroid culture and drug testing using a 384 hanging drop array, Analyst 136(3) (2011) 473-8.
[25] A.Y. Hsiao, Y.C. Tung, C.H. Kuo, B. Mosadegh, R. Bedenis, K.J. Pienta, S. Takayama, Micro-ring structures stabilize microdroplets to enable long term spheroid culture in 384 hanging drop array plates, Biomed Microdevices 14(2) (2012) 313-23.
[26] M. Khanmohammadi, V. Zolfagharzadeh, Z. Bagher, H. Soltani, J. Ai, Cell encapsulation in core-shell microcapsules through coaxial electrospinning system and horseradish peroxidase-catalyzed crosslinking, Biomed Phys Eng Express 6(1) (2020) 015022.
[27] S. Sakai, H. Inagaki, K. Inamoto, M. Taya, Wrapping tissues with a pre-established cage-like layer composed of living cells, Biomaterials 33(28) (2012) 6721-7.
[28] D. Lv, Z. Hu, L. Lu, H. Lu, X. Xu, Three-dimensional cell culture: A powerful tool in tumor research and drug discovery, Oncol Lett 14(6) (2017) 6999-7010.
[29] C. Jubelin, J. Munoz-Garcia, L. Griscom, D. Cochonneau, E. Ollivier, M.F. Heymann, F.M. Vallette, L. Oliver, D. Heymann, Three-dimensional in vitro culture models in oncology research, Cell Biosci 12(1) (2022) 155.
[30] X.J. Li, A.V. Valadez, P. Zuo, Z. Nie, Microfluidic 3D cell culture: potential application for tissue-based bioassays, Bioanalysis 4(12) (2012) 1509-25.
[31] H.K. Kleinman, G.R. Martin, Matrigel: basement membrane matrix with biological activity, Semin Cancer Biol 15(5) (2005) 378-86.
[32] J.B. Kim, Three-dimensional tissue culture models in cancer biology, Semin Cancer Biol 15(5) (2005) 365-77.
[33] T.R. Sodunke, K.K. Turner, S.A. Caldwell, K.W. McBride, M.J. Reginato, H.M. Noh, Micropatterns of Matrigel for three-dimensional epithelial cultures, Biomaterials 28(27) (2007) 4006-16.
[34] A. Borchers, T. Pieler, Programming pluripotent precursor cells derived from Xenopus embryos to generate specific tissues and organs, Genes (Basel) 1(3) (2010) 413-26.
[35] M. Ravi, V. Paramesh, S.R. Kaviya, E. Anuradha, F.D. Solomon, 3D cell culture systems: advantages and applications, J Cell Physiol 230(1) (2015) 16-26.
[36] J. Ziauddin, D.M. Sabatini, Microarrays of cells expressing defined cDNAs, Nature 411(6833) (2001) 107-110.
[37] K. Papp, Z. Szittner, J. Prechl, Life on a microarray: assessing live cell functions in a microarray format, Cell Mol Life Sci 69(16) (2012) 2717-25.
[38] R. Sato, Bacherlorthesis, (2019).
[39] Y. Qu, Masterthesis, (2021).
[40] I. Smyrek, B. Mathew, S.C. Fischer, S.M. Lissek, S. Becker, E.H.K. Stelzer, E-cadherin, actin, microtubules and FAK dominate different spheroid formation phases and important elements of tissue integrity, Biol Open 8(1) (2019) bio037051.

[41] M.C. Decarli, R. Amaral, D.P.D. Santos, L.B. Tofani, E. Katayama, R.A. Rezende, J. Silva, K. Swiech, C.A.T. Suazo, C. Mota, L. Moroni, A.M. Moraes, Cell spheroids as a versatile research platform: formation mechanisms, high throughput production, characterization and applications, Biofabrication 13(3) (2021) 032002.
[42] A. Backstrom, L. Kugel, C. Gnann, H. Xu, J.E. Aslan, E. Lundberg, C. Stadler, A Sample Preparation Protocol for High Throughput Immunofluorescence of Suspension Cells on an Adherent Surface, J Histochem Cytochem 68(7) (2020) 473-489.
[43] M. Tsang, J. Gantchev, F.M. Ghazawi, I.V. Litvinov, Protocol for adhesion and immunostaining of lymphocytes and other non-adherent cells in culture, Biotechniques 63(5) (2017) 230-233.
[44] B.O. Stokes, Principles of Cytocentrifugation, Laboratory Medicine 35(7) (2004) 434-437.
[45] R. Lamanna, A. Motta, R. Romano, G. Rainaldi, F. Flamma, M. Pentimalli, T. Tancredi, P.L. Indovina, M.T. Santini, Forced adhesive growth of K562 leukemic cells that normally grow in suspension induces variations in membrane lipids and energy metabolism: A proton NMR study, J Biomed Mater Res 46(2) (1999) 171-178.
[46] M. Karimpoor, E. Yebra-Fernandez, M. Parhizkar, M. Orlu, D. Craig, J.S. Khorashad, M. Edirisinghe, Alginate foam-based three-dimensional culture to investigate drug sensitivity in primary leukaemia cells, J R Soc Interface 15(141) (2018).
[47] M. Chatzinikolaidou, Cell spheroids: the new frontiers in in vitro models for cancer drug validation, Drug Discov Today 21(9) (2016) 1553-1560.
[48] F. Hirschhaeuser, H. Menne, C. Dittfeld, J. West, W. Mueller-Klieser, L.A. Kunz-Schughart, Multicellular tumor spheroids: an underestimated tool is catching up again, J Biotechnol 148(1) (2010) 3-15.
[49] J. Friedrich, R. Ebner, L.A. Kunz-Schughart, Experimental anti-tumor therapy in 3-D: spheroids--old hat or new challenge?, Int J Radiat Biol 83(11-12) (2007) 849-71.
[50] M. Hu, R. Deng, K.M. Schumacher, M. Kurisawa, H. Ye, K. Purnamawati, J.Y. Ying, Hydrodynamic spinning of hydrogel fibers, Biomaterials 31(5) (2010) 863-9.
[51] Y. Liu, S. Sakai, M. Taya, Production of endothelial cell-enclosing alginate-based hydrogel fibers with a cell adhesive surface through simultaneous cross-linking by horseradish peroxidase-catalyzed reaction in a hydrodynamic spinning process, J Biosci Bioeng 114(3) (2012) 353-9.
[52] S. Sakai, I. Hashimoto, Y. Ogushi, K. Kawakami, Peroxidase-catalyzed cell encapsulation in subsieve-size capsules of alginate with phenol moieties in water-immiscible fluid dissolving H2O2, Biomacromolecules 8(8) (2007) 2622-6.
[53] S. Sakai, S. Ito, Y. Ogushi, I. Hashimoto, N. Hosoda, Y. Sawae, K. Kawakami, Enzymatically fabricated and degradable microcapsules for production of multicellular spheroids with well-defined diameters of less than 150 μm, Biomaterials 30(30) (2009) 5937-5942.
[54] S. Sakai, K. Mochizuki, Y. Qu, M. Mail, M. Nakahata, M. Taya, Peroxidase-catalyzed microextrusion bioprinting of cell-laden hydrogel constructs in vaporized ppm-level hydrogen peroxide, Biofabrication 10(4) (2018) 045007.
[55] S. Sakai, A. Yoshii, S. Sakurai, K. Horii, O. Nagasuna, Silk fibroin nanofibers: a promising ink additive for extrusion three-dimensional bioprinting, Mater Today Bio 8 (2020) 100078.
[56] E. Gantumur, M. Kimura, M. Taya, M. Horie, M. Nakamura, S. Sakai, Inkjet micropatterning through horseradish peroxidase-mediated hydrogelation for controlled cell immobilization and microtissue fabrication, Biofabrication 12(1) (2019) 011001.
[57] A. Frayssinet, D. Petta, C. Illoul, B. Haye, A. Markitantova, D. Eglin, G. Mosser, M. D'Este, C. Helary, Extracellular matrix-mimetic composite hydrogels of cross-linked hyaluronan and fibrillar collagen with tunable properties and ultrastructure, Carbohyd Polym 236 (2020) 116042.

[58] T. Ashida, S. Sakai, M. Taya, Propagation of human iPS cells in alginate-based microcapsules prepared using reactions catalyzed by horseradish peroxidase and catalase, Artif Cells Nanomed Biotechnol 44(6) (2016) 1406-9.
[59] S. Sakai, S. Ito, H. Inagaki, K. Hirose, T. Matsuyama, M. Taya, K. Kawakami, Cell-enclosing gelatin-based microcapsule production for tissue engineering using a microfluidic flow-focusing system, Biomicrofluidics 5(1) (2011) 13402.
[60] R. Kazama, R. Sato, H. Fujiwara, Y. Qu, M. Nakahata, M. Kojima, S. Fujita, S. Sakai, Development of non-adherent cell-enclosing domes with enzymatically cross-linked hydrogel shell, Biofabrication 15 (2023) 015002.
[61] H. Nagano, E. Kato, S. Yamamura, M. Ueda, Fluorescence studies on nyctinasty which suggest the existence of genus-specific receptors for leaf-movement factor, Org Biomol Chem 1(18) (2003) 3186-3192.
[62] S. Sakai, K. Kawakami, Synthesis and characterization of both ionically and enzymatically cross-linkable alginate, Acta Biomater 3(4) (2007) 495-501.
[63] F. Hofling, T. Franosch, Anomalous transport in the crowded world of biological cells, Rep Prog Phys 76(4) (2013) 046602.
[64] J.A. Rivero, S.E. Adunyah, Sodium butyrate stimulates PKC activation and induces differential expression of certain PKC isoforms during erythroid differentiation, Biochem Biophys Res Commun 248(3) (1998) 664-8.
[65] S. Sakai, S. Ito, K. Kawakami, Calcium alginate microcapsules with spherical liquid cores templated by gelatin microparticles for mass production of multicellular spheroids, Acta Biomater 6(8) (2010) 3132-7.
[66] S.M. Kang, J.H. Lee, Y.S. Huh, S. Takayama, Alginate Microencapsulation for Three-Dimensional In Vitro Cell Culture, ACS Biomater Sci Eng 7(7) (2021) 2864-2879.
[67] J. Sun, H. Tan, Alginate-Based Biomaterials for Regenerative Medicine Applications, Materials (Basel) 6(4) (2013) 1285-1309.
[68] R. Calafiore, G. Basta, G. Luca, M. Calvitti, G. Calabrese, L. Racanicchi, G. Macchiarulo, F. Mancuso, L. Guido, P. Brunetti, Grafts of microencapsulated pancreatic islet cells for the therapy of diabetes mellitus in non-immunosuppressed animals, Biotechnol Appl Biochem 39(Pt 2) (2004) 159-64.
[69] O. Smidsrod, G. Skjak-Braek, Alginate as immobilization matrix for cells, Trends Biotechnol 8(3) (1990) 71-8.
[70] X. Zhang, W. Wang, Y. Xie, Y. Zhang, X. Wang, X. Guo, X. Ma, Proliferation, viability, and metabolism of human tumor and normal cells cultured in microcapsule, Appl Biochem Biotechnol 134(1) (2006) 61-76.
[71] A.D. Augst, H.J. Kong, D.J. Mooney, Alginate hydrogels as biomaterials, Macromol Biosci 6(8) (2006) 623-633.
[72] R. Jin, L.S. Teixeira, P.J. Dijkstra, C.A. van Blitterswijk, M. Karperien, J. Feijen, Enzymatically-crosslinked injectable hydrogels based on biomimetic dextran-hyaluronic acid conjugates for cartilage tissue engineering, Biomaterials 31(11) (2010) 3103-13.
[73] M. Hu, M. Kurisawa, R. Deng, C.M. Teo, A. Schumacher, Y.X. Thong, L. Wang, K.M. Schumacher, J.Y. Ying, Cell immobilization in gelatin-hydroxyphenylpropionic acid hydrogel fibers, Biomaterials 30(21) (2009) 3523-31.
[74] S. Sakai, K. Hirose, K. Taguchi, Y. Ogushi, K. Kawakami, An injectable, *in situ* enzymatically gellable, gelatin derivative for drug delivery and tissue engineering, Biomaterials 30(20) (2009) 3371-7.
[75] M.R. Pandkar, S.G. Dhamdhere, S. Shukla, Oxygen gradient and tumor heterogeneity: The chronicle of a toxic relationship, Biochim Biophys Acta Rev Cancer 1876(1) (2021) 188553.
[76] X.Y. Cui, G. Skretting, Y. Jing, H. Sun, P.M. Sandset, L. Sun, Hypoxia influences stem

cell-like properties in multidrug resistant K562 leukemic cells, Blood Cells Mol Dis 51(3) (2013) 177-84.
[77] N. Rohwer, T. Cramer, Hypoxia-mediated drug resistance: novel insights on the functional interaction of HIFs and cell death pathways, Drug Resist Updat 14(3) (2011) 191-201.
[78] M. Ibarrola-Villava, A. Cervantes, A. Bardelli, Preclinical models for precision oncology, Biochim Biophys Acta Rev Cancer 1870(2) (2018) 239-246.
[79] D.S. Shin, K.S. Anseth, Recent advances in 3D models of tumor invasion, Curr Opin Biomed Eng 19 (2021).
[80] L.L. Berube, K.P. Nickel, M. Iida, S. Ramisetty, P. Kulkarni, R. Salgia, D.L. Wheeler, R.J. Kimple, Radiation Sensitivity: The Rise of Predictive Patient-Derived Cancer Models, Semin Radiat Oncol 33(3) (2023) 279-286.
[81] F. Castro, C. Leite Pereira, M. Helena Macedo, A. Almeida, M. Jose Silveira, S. Dias, A. Patricia Cardoso, M. Jose Oliveira, B. Sarmento, Advances on colorectal cancer 3D models: The needed translational technology for nanomedicine screening, Adv Drug Deliv Rev 175 (2021) 113824.
[82] L. Pierantoni, R.L. Reis, J. Silva-Correia, J.M. Oliveira, S. Heavey, Spatial -omics technologies: the new enterprise in 3D breast cancer models, Trends Biotechnol 41(12) (2023) 1488-1500.
[83] L.S. Costard, R.R. Hosn, H. Ramanayake, F.J. O'Brien, C.M. Curtin, Influences of the 3D microenvironment on cancer cell behaviour and treatment responsiveness: A recent update on lung, breast and prostate cancer models, Acta Biomater 132 (2021) 360-378.
[84] T. Ramirez, A. Strigun, A. Verlohner, H.A. Huener, E. Peter, M. Herold, N. Bordag, W. Mellert, T. Walk, M. Spitzer, X. Jiang, S. Sperber, T. Hofmann, T. Hartung, H. Kamp, B. van Ravenzwaay, Prediction of liver toxicity and mode of action using metabolomics in vitro in HepG2 cells, Arch Toxicol 92(2) (2018) 893-906.
[85] O.A. Almazroo, M.K. Miah, R. Venkataramanan, Drug Metabolism in the Liver, Clin Liver Dis 21(1) (2017) 1-20.
[86] K.M. Beggs, A.R. Maiuri, A.M. Fullerton, K.L. Poulsen, A.B. Breier, P.E. Ganey, R.A. Roth, Trovafloxacin-induced replication stress sensitizes HepG2 cells to tumor necrosis factor-alpha-induced cytotoxicity mediated by extracellular signal-regulated kinase and ataxia telangiectasia and Rad3-related, Toxicology 331 (2015) 35-46.
[87] S.C. Sahu, J. Zheng, J.J. Yourick, R.L. Sprando, X. Gao, Toxicogenomic responses of human liver HepG2 cells to silver nanoparticles, J Appl Toxicol 35(10) (2015) 1160-1168.
[88] K. Mizoi, H. Arakawa, K. Yano, S. Koyama, H. Kojima, T. Ogihara, Utility of Three-Dimensional Cultures of Primary Human Hepatocytes (Spheroids) as Pharmacokinetic Models, Biomedicines 8(10) (2020) 374.
[89] V.M. Lauschke, D.F. Hendriks, C.C. Bell, T.B. Andersson, M. Ingelman-Sundberg, Novel 3D Culture Systems for Studies of Human Liver Function and Assessments of the Hepatotoxicity of Drugs and Drug Candidates, Chem Res Toxicol 29(12) (2016) 1936-1955.
[90] M.T. Donato, L. Tolosa, M.J. Gomez-Lechon, Culture and Functional Characterization of Human Hepatoma HepG2 Cells, Methods Mol Biol 1250 (2015) 77-93.
[91] T. Nii, K. Makino, Y. Tabata, Three-Dimensional Culture System of Cancer Cells Combined with Biomaterials for Drug Screening, Cancers 12(10) (2020) 2754.
[92] M. Bokhari, R.J. Carnachan, N.R. Cameron, S.A. Przyborski, Culture of HepG2 liver cells on three dimensional polystyrene scaffolds enhances cell structure and function during toxicological challenge, J Anat 211(4) (2007) 567-576.
[93] N. Chaicharoenaudomrung, P. Kunhorm, P. Noisa, Three-dimensional cell culture systems as an in vitro platform for cancer and stem cell modeling, World J Stem Cells 11(12) (2019) 1065-1083.
[94] S.C. Ramaiahgari, M.W. den Braver, B. Herpers, V. Terpstra, J.N. Commandeur, B. van

de Water, L.S. Price, A 3D in vitro model of differentiated HepG2 cell spheroids with improved liver-like properties for repeated dose high-throughput toxicity studies, Arch Toxicol 88(5) (2014) 1083-1095.
[95] K. Aritomi, Y. Ishitsuka, Y. Tomishima, D. Shimizu, N. Abe, T. Shuto, M. Irikura, H. Kai, T. Irie, Evaluation of three-dimensional cultured HepG2 cells in a nano culture plate system: an in vitro human model of acetaminophen hepatotoxicity, J Pharmacol Sci 124(2) (2014) 218-229.
[96] T. Yao, Y. Zhang, M. Lv, G. Zang, S.S. Ng, X. Chen, Advances in 3D cell culture for liver preclinical studies, Acta Biochim Biophys Sin (Shanghai) 53(6) (2021) 643-651.
[97] S. Wilkening, F. Stahl, A. Bader, Comparison of primary human hepatocytes and hepatoma cell line Hepg2 with regard to their biotransformation properties, Drug Metab Dispos 31(8) (2003) 1035-1042.
[98] R. Mori, Y. Sakai, K. Nakazawa, Micropatterned organoid culture of rat hepatocytes and HepG2 cells, J Biosci Bioeng 106(3) (2008) 237-242.
[99] W. Liu, M. Sun, B. Lu, M. Yan, K. Han, J. Wang, A microfluidic platform for multi-size 3D tumor culture, monitoring and drug resistance testing, Sensors and Actuators B: Chemical 292 (2019) 111-120.
[100] T. Hurrell, A.A. Ellero, Z.F. Masso, A.D. Cromarty, Characterization and reproducibility of HepG2 hanging drop spheroids toxicology in vitro, Toxicol In Vitro 50 (2018) 86-94.
[101] M. Khanmohammadi, S. Sakai, T. Ashida, M. Taya, Production of hyaluronic-acid-based cell-enclosing microparticles and microcapsules via enzymatic reaction using a microfluidic system, Journal of Applied Polymer Science 133(16) (2016) 43107.
[102] J. Wei, D. Lei, M. Chen, P. Ran, X. Li, Engineering HepG2 spheroids with injectable fiber fragments as predictable models for drug metabolism and tumor infiltration, J Biomed Mater Res B Appl Biomater 108(8) (2020) 3331-3344.
[103] K. Wrzesinski, A. Rogowska-Wrzesinska, R. Kanlaya, K. Borkowski, V. Schwammle, J. Dai, K.E. Joensen, K. Wojdyla, V.B. Carvalho, S.J. Fey, The cultural divide: exponential growth in classical 2D and metabolic equilibrium in 3D environments, PLoS One 9(9) (2014) e106973.
[104] T.M. Achilli, J. Meyer, J.R. Morgan, Advances in the formation, use and understanding of multi-cellular spheroids, Expert Opin Biol Ther 12(10) (2012) 1347-1360.
[105] R. Kazama, S. Fujita, S. Sakai, Cell Dome as an Evaluation Platform for Organized HepG2 Cells, Cells 12(1) (2022) 69.
[106] H. Nagano, E. Kato, S. Yamamura, M. Ueda, Fluorescence studies on nyctinasty which suggest the existence of genus-specific receptors for leaf-movement factor, Rep. Prog. Phys. 76 (2013) 046602.
[107] Y. Liu, S. Sakai, M. Taya, Impact of the composition of alginate and gelatin derivatives in bioconjugated hydrogels on the fabrication of cell sheets and spherical tissues with living cell sheaths, Acta Biomater 9(5) (2013) 6616-6623.
[108] A. Kobayashi, K. Yamakoshi, Y. Yajima, R. Utoh, M. Yamada, M. Seki, Preparation of stripe-patterned heterogeneous hydrogel sheets using microfluidic devices for high-density coculture of hepatocytes and fibroblasts, J Biosci Bioeng 116(6) (2013) 761-767.
[109] J.M. Kim, I.H. Hwang, I.S. Jang, M. Kim, I.S. Bang, S.J. Park, Y.J. Chung, J.C. Joo, M.G. Lee, Houttuynia cordata Thunb Promotes Activation of HIF-1A-FOXO3 and MEF2A Pathways to Induce Apoptosis in Human HepG2 Hepatocellular Carcinoma Cells, Integr Cancer Ther 16(3) (2017) 360-372.
[110] K. Arai, Y. Tsukamoto, H. Yoshida, H. Sanae, T.A. Mir, S. Sakai, T. Yoshida, M. Okabe, T. Nikaido, M. Taya, M. Nakamura, The development of cell-adhesive hydrogel for 3D printing, Int. J. Bioprinting 2(2) (2016) 153-162.
[111] S. Sakai, I. Hashimoto, Y. Ogushi, K. Kawakami, Peroxidase-catalyzed cell encapsulation

in subsieve-size capsules of alginate with phenol moieties in water-immiscible fluid dissolving H_2O_2, Biomacromolecules 8(8) (2007) 2622-2626.
[112] Q. Meng, Three-dimensional culture of hepatocytes for prediction of drug-induced hepatotoxicity, Expert Opin Drug Metab Toxicol 6(6) (2010) 733-746.
[113] A. Basharat, H.E. Rollison, D.P. Williams, D.P. Ivanov, HepG2 (C3A) spheroids show higher sensitivity compared to HepaRG spheroids for drug-induced liver injury (DILI), Toxicol Appl Pharmacol 408 (2020) 115279.
[114] J.M. Kelm, N.E. Timmins, C.J. Brown, M. Fussenegger, L.K. Nielsen, Method for generation of homogeneous multicellular tumor spheroids applicable to a wide variety of cell types, Biotechnol Bioeng 83(2) (2003) 173-80.
[115] C. Eilenberger, M. Rothbauer, E.K. Ehmoser, P. Ertl, S. Kupcu, Effect of Spheroidal Age on Sorafenib Diffusivity and Toxicity in a 3D HepG2 Spheroid Model, Sci Rep 9(1) (2019) 4863.
[116] X. Zhu, Q. Wu, Y. He, M. Gao, Y. Li, W. Peng, S. Li, Y. Liu, R. Zhang, J. Bao, Fabrication of Size-Controllable and Arrangement-Orderly HepG2 Spheroids for Drug Screening via Decellularized Liver Matrix-Derived Micropattern Array Chips, ACS Omega 7(2) (2022) 2364-2376.
[117] J.A. Kyffin, P. Sharma, J. Leedale, H.E. Colley, C. Murdoch, P. Mistry, S.D. Webb, Impact of cell types and culture methods on the functionality of in vitro liver systems - A review of cell systems for hepatotoxicity assessment, Toxicol In Vitro 48 (2018) 262-275.
[118] M. Mori, Y. Fujikawa, M. Kikkawa, M. Shino, M. Sawane, S. Sato, H. Inoue, A highly selective fluorogenic substrate for imaging glutathione S-transferase P1: development and cellular applicability in epigenetic studies, Chem Commun (Camb) 55(56) (2019) 8122-8125.
[119] J.D. Hayes, J.U. Flanagan, I.R. Jowsey, Glutathione transferases, Annu Rev Pharmacol Toxicol 45 (2005) 51-88.
[120] A. Emami Nejad, S. Najafgholian, A. Rostami, A. Sistani, S. Shojaeifar, M. Esparvarinha, R. Nedaeinia, S. Haghjooy Javanmard, M. Taherian, M. Ahmadlou, R. Salehi, B. Sadeghi, M. Manian, The role of hypoxia in the tumor microenvironment and development of cancer stem cell: a novel approach to developing treatment, Cancer Cell Int 21(1) (2021) 62.
[121] H. Chen, X. Wei, H. Chen, H. Wei, Y. Wang, W. Nan, Q. Zhang, X. Wen, The study of establishment of an in vivo tumor model by three-dimensional cells culture systems methods and evaluation of antitumor effect of biotin-conjugated pullulan acetate nanoparticles, Artif Cells Nanomed Biotechnol 47(1) (2019) 123-131.
[122] Xinwei Zhou, Chang Liu, Xinru Zhao, X. Wang, A 3D bioprinting liver umor model for drug screening, World journal of pharmacy and pharmaceutical sciences 5(4) (2016) 196-213.
[123] S. Li, S. Yuan, Q. Zhao, B. Wang, X. Wang, K. Li, Quercetin enhances chemotherapeutic effect of doxorubicin against human breast cancer cells while reducing toxic side effects of it, Biomed Pharmacother 100 (2018) 441-447.
[124] W. Mo, J.T. Zhang, Human ABCG2: structure, function, and its role in multidrug resistance, Int J Biochem Mol Biol 3(1) (2012) 1-27.
[125] L. Gaedtke, L. Thoenes, C. Culmsee, B. Mayer, E. Wagner, Proteomic analysis reveals differences in protein expression in spheroid versus monolayer cultures of low-passage colon carcinoma cells, J Proteome Res 6(11) (2007) 4111-4118.
[126] B. Muz, P. de la Puente, F. Azab, A.K. Azab, The role of hypoxia in cancer progression, angiogenesis, metastasis, and resistance to therapy, Hypoxia (Auckl) 3 (2015) 83-92.
[127] X. Huang, X. Zhang, X. Wang, C. Wang, B. Tang, Microenvironment of alginate-based microcapsules for cell culture and tissue engineering, J Biosci Bioeng 114(1) (2012) 1-8.
[128] L.P. Ferreira, V.M. Gaspar, J.F. Mano, Design of spherically structured 3D *in vitro* tumor models -Advances and prospects, Acta Biomater 75 (2018) 11-34.
[129] B. Gao, C. Jing, K. Ng, B. Pingguan-Murphy, Q. Yang, Fabrication of three-dimensional

islet models by the geometry-controlled hanging-drop method, Acta Mechanica Sinica 35(2) (2019) 329-337.
[130] K. Bialkowska, P. Komorowski, M. Bryszewska, K. Milowska, Spheroids as a Type of Three-Dimensional Cell Cultures-Examples of Methods of Preparation and the Most Important Application, Int J Mol Sci 21(17) (2020) 6225.
[131] K. Froehlich, J.D. Haeger, J. Heger, J. Pastuschek, S.M. Photini, Y. Yan, A. Lupp, C. Pfarrer, R. Mrowka, E. Schleussner, U.R. Markert, A. Schmidt, Generation of Multicellular Breast Cancer Tumor Spheroids: Comparison of Different Protocols, J Mammary Gland Biol Neoplasia 21(3-4) (2016) 89-98.
[132] M.V. Natu, J.P. Sardinha, I.J. Correia, M.H. Gil, Controlled release gelatin hydrogels and lyophilisates with potential application as ocular inserts, Biomed Mater 2(4) (2007) 241-9.
[133] J.Y. Lai, A.C. Hsieh, A gelatin-*g*-poly(*N*-isopropylacrylamide) biodegradable in situ gelling delivery system for the intracameral administration of pilocarpine, Biomaterials 33(7) (2012) 2372-87.
[134] W.-M. Hsu, K.-H. Chen, J.-Y. Lai, G.-H. Hsiue, Transplantation of Human Corneal Endothelial Cells Using Functional Biomaterials: Poly(*N*-isopropylacrylamide) and Gelatin, Journal of Experimental & Clinical Medicine 5(2) (2013) 56-64.
[135] D. Jain, E. Carvalho, A.K. Banthia, R. Banerjee, Development of polyvinyl alcohol-gelatin membranes for antibiotic delivery in the eye, Drug Dev Ind Pharm 37(2) (2011) 167-77.
[136] S. Afewerki, A. Sheikhi, S. Kannan, S. Ahadian, A. Khademhosseini, Gelatin-polysaccharide composite scaffolds for 3D cell culture and tissue engineering: Towards natural therapeutics, Bioeng Transl Med 4(1) (2019) 96-115.
[137] J.B. Rose, S. Pacelli, A.J.E. Haj, H.S. Dua, A. Hopkinson, L.J. White, F. Rose, Gelatin-Based Materials in Ocular Tissue Engineering, Materials (Basel) 7(4) (2014) 3106-3135.
[138] K. Su, C. Wang, Recent advances in the use of gelatin in biomedical research, Biotechnol Lett 37(11) (2015) 2139-45.
[139] M. Khanmohammadi, S. Sakai, M. Taya, Characterization of encapsulated cells within hyaluronic acid and alginate microcapsules produced via horseradish peroxidase-catalyzed crosslinking, J Biomater Sci Polym Ed 30(4) (2019) 295-307.
[140] A.P. McGuigan, M.V. Sefton, Modular tissue engineering: fabrication of a gelatin-based construct, J Tissue Eng Regen Med 1(2) (2007) 136-45.
[141] S.A. Othman, C.F. Soon, N.L. Ma, K.S. Tee, G.P. Lim, M. Morsin, M.K. Ahmad, A.I. Abdulmaged, S.C. Cheong, Alginate-gelatin bioink for bioprinting of hela spheroids in alginate-gelatin hexagon shaped scaffolds, Polymer Bulletin 78(11) (2020) 6115-6135.
[142] M.B. Labowska, K. Cierluk, A.M. Jankowska, J. Kulbacka, J. Detyna, I. Michalak, A Review on the Adaption of Alginate-Gelatin Hydrogels for 3D Cultures and Bioprinting, Materials (Basel) 14(4) (2021) 858.
[143] B. Sarker, D.G. Papageorgiou, R. Silva, T. Zehnder, E.N.F. Gul, M. Bertmer, J. Kaschta, K. Chrissafis, R. Detsch, A.R. Boccaccini, Fabrication of alginate-gelatin crosslinked hydrogel microcapsules and evaluation of the microstructure and physico-chemical properties, J Mater Chem B 2(11) (2014) 1470-1482.
[144] A. Grigore, B. Sarker, B. Fabry, A.R. Boccaccini, R. Detsch, Behavior of encapsulated MG-63 cells in RGD and gelatine-modified alginate hydrogels, Tissue Eng Part A 20(15-16) (2014) 2140-50.
[145] F. Ruther, T. Distler, A.R. Boccaccini, R. Detsch, Biofabrication of vessel-like structures with alginate di-aldehyde-gelatin (ADA-GEL) bioink, J Mater Sci Mater Med 30 (1)(1) (2018) 8.
[146] R. Kazama, S. Sakai, Effect of cell adhesiveness of Cell Dome shell on enclosed HeLa cells, J Biosci Bioeng 137(4) (2024) 313-320.

[147] A. Sakaue-Sawano, T. Kobayashi, K. Ohtawa, A. Miyawaki, Drug-induced cell cycle modulation leading to cell-cycle arrest, nuclear mis-segregation, or endoreplication, BMC Cell Biol 12 (2011) 2.
[148] C.A. Schneider, W.S. Rasband, K.W. Eliceiri, NIH Image to ImageJ: 25 years of image analysis, Nat Methods 9(7) (2012) 671-5.
[149] A. Bonanni, A. d'Aiello, D. Pedicino, M. Di Sario, R. Vinci, M. Ponzo, P. Ciampi, D. Lo Curto, C. Conte, F. Cribari, F. Canonico, G. Russo, R.A. Montone, C. Trani, A. Severino, F. Crea, G. Liuzzo, Molecular Hallmarks of Ischemia with Non-Obstructive Coronary Arteries: The "INOCA versus Obstructive CCS" Challenge, J Clin Med 11(6) (2022) 1711.
[150] A.A. Khalili, M.R. Ahmad, A Review of Cell Adhesion Studies for Biomedical and Biological Applications, Int J Mol Sci 16(8) (2015) 18149-84.
[151] S. Huang, D.E. Ingber, The structural and mechanical complexity of cell-growth control, Nat Cell Biol 1(5) (1999) E131-8.
[152] S.A. Kamranvar, B. Rani, S. Johansson, Cell Cycle Regulation by Integrin-Mediated Adhesion, Cells 11(16) (2022) 2521.
[153] S. Sakai, K. Hirose, K. Moriyama, K. Kawakami, Control of cellular adhesiveness in an alginate-based hydrogel by varying peroxidase and H_2O_2 concentrations during gelation, Acta Biomater 6(4) (2010) 1446-52.
[154] O. Hasturk, K.E. Jordan, J. Choi, D.L. Kaplan, Enzymatically crosslinked silk and silk-gelatin hydrogels with tunable gelation kinetics, mechanical properties and bioactivity for cell culture and encapsulation, Biomaterials 232 (2020) 119720.
[155] J. Bai, Y. Li, G. Zhang, Cell cycle regulation and anticancer drug discovery, Cancer Biol Med 14(4) (2017) 348-362.
[156] Z.A. Stewart, M.D. Westfall, J.A. Pietenpol, Cell-cycle dysregulation and anticancer therapy, Trends Pharmacol Sci 24(3) (2003) 139-45.
[157] P.L. Olive, R.E. Durand, Drug and radiation resistance in spheroids: cell contact and kinetics, Cancer Metastasis Rev 13(2) (1994) 121-38.
[158] A. Sharma, J.F. Arambula, S. Koo, R. Kumar, H. Singh, J.L. Sessler, J.S. Kim, Hypoxia-targeted drug delivery, Chem Soc Rev 48(3) (2019) 771-813.
[159] Z. Chen, F. Han, Y. Du, H. Shi, W. Zhou, Hypoxic microenvironment in cancer: molecular mechanisms and therapeutic interventions, Signal Transduct Target Ther 8(1) (2023) 70.
[160] J.C. Jun, A. Rathore, H. Younas, D. Gilkes, V.Y. Polotsky, Hypoxia-Inducible Factors and Cancer, Curr Sleep Med Rep 3(1) (2017) 1-10.
[161] G.L. Semenza, Hypoxia-inducible factor 1 (HIF-1) pathway, Sci STKE 407 (2007) cm8.
[162] K. Balamurugan, HIF-1 at the crossroads of hypoxia, inflammation, and cancer, Int J Cancer 138(5) (2016) 1058-66.
[163] G.L. Semenza, Targeting HIF-1 for cancer therapy, Nat Rev Cancer 3(10) (2003) 721-32.
[164] T. Wu, Y. Dai, Tumor microenvironment and therapeutic response, Cancer Letters 387 (2017) 61-68.
[165] L. Seguin, J.S. Desgrosellier, S.M. Weis, D.A. Cheresh, Integrins and cancer: regulators of cancer stemness, metastasis, and drug resistance, Trends in Cell Biology 25(4) (2015) 234-240.
[166] X.W. Liu, Y. Su, H. Zhu, J. Cao, W.J. Ding, Y.C. Zhao, Q.J. He, B. Yang, HIF-1alpha-dependent autophagy protects HeLa cells from fenretinide (4-HPR)-induced apoptosis in hypoxia, Pharmacol Res 62(5) (2010) 416-25.
[167] J. Hou, D. Yan, Y. Liu, P. Huang, H. Cui, The Roles of Integrin α5β1 in Human Cancer, OncoTargets and Therapy Volume 13 (2020) 13329-13344.
[168] A. Ambriovic-Ristov, M. Osmak, Integrin-Mediated Drug Resistance, Current Signal Transduction Therapy 1(2) (2006) 227-237.

[169] S.P. Zustiak, S. Dadhwal, C. Medina, S. Steczina, Y. Chehreghanianzabi, A. Ashraf, P. Asuri, Three‐dimensional matrix stiffness and adhesive ligands affect cancer cell response to toxins, Biotechnology and Bioengineering 113(2) (2015) 443-452.
[170] J.O. Armitage, R.D. Gascoyne, M.A. Lunning, F. Cavalli, Non-Hodgkin lymphoma, Lancet 390(10091) (2017) 298-310.
[171] M. Rossi, F. Alviano, S. Righi, E. Sabattini, C. Agostinelli, Three-dimensional models: a novel approach for lymphoma research, J Cancer Res Clin Oncol 148(4) (2022) 753-765.
[172] N. Yanguas-Casas, L. Pedrosa, I. Fernandez-Miranda, M. Sanchez-Beato, An Overview on Diffuse Large B-Cell Lymphoma Models: Towards a Functional Genomics Approach, Cancers (Basel) 13(12) (2021).
[173] C. Eng, Microenvironmental protection in diffuse large-B-cell lymphoma, N Engl J Med 359(22) (2008) 2379-81.
[174] R. Edmondson, J.J. Broglie, A.F. Adcock, L. Yang, Three-dimensional cell culture systems and their applications in drug discovery and cell-based biosensors, Assay Drug Dev Technol 12(4) (2014) 207-18.
[175] Y.-S. Hwang, J. Kim, H.J. Yoon, J.I. Kang, K.-H. Park, H. Bae, Microwell-mediated cell spheroid formation and its applications, Macromolecular Research 26(1) (2017) 1-8.
[176] F. Araujo-Ayala, C. Dobano-Lopez, J.G. Valero, F. Nadeu, F. Gava, C. Faria, M. Norlund, R. Morin, P. Bernes-Lasserre, N. Serrat, H. Playa-Albinyana, R. Gimenez, E. Campo, J.M. Lagarde, A. Lopez-Guillermo, E. Gine, D. Colomer, C. Bezombes, P. Perez-Galan, A novel patient-derived 3D model recapitulates mantle cell lymphoma lymph node signaling, immune profile and in vivo ibrutinib responses, Leukemia 37(6) (2023) 1311-1323.
[177] K. Dus-Szachniewicz, K. Gdesz-Birula, G. Rymkiewicz, Development and Characterization of 3D Hybrid Spheroids for the Investigation of the Crosstalk Between B-Cell Non-Hodgkin Lymphomas and Mesenchymal Stromal Cells, Onco Targets Ther 15 (2022) 683-697.
[178] K. Dus-Szachniewicz, K. Gdesz-Birula, E. Nowosielska, P. Ziolkowski, S. Drobczynski, Formation of Lymphoma Hybrid Spheroids and Drug Testing in Real Time with the Use of Fluorescence Optical Tweezers, Cells 11 (2022) 2113.
[179] R. Kazama, R. Ishikawa, S. Sakai, Development of Hemispherical 3D Models of Human Brain and B Cell Lymphomas Using On-Chip Cell Dome System, Bioengineering 11(12) (2024) 1303.
[180] K. Wang, G. Wei, D. Liu, CD19: a biomarker for B cell development, lymphoma diagnosis and therapy, Exp Hematol Oncol 1(1) (2012) 36.
[181] H.E. Mei, S. Schmidt, T. Dorner, Rationale of anti-CD19 immunotherapy: an option to target autoreactive plasma cells in autoimmunity, Arthritis Res Ther 14 Suppl 5(Suppl 5) (2012) S1.
[182] S. Cang, N. Mukhi, K. Wang, D. Liu, Novel CD20 monoclonal antibodies for lymphoma therapy, J Hematol Oncol 5 (2012) 64.
[183] J. Zeng, J. Wang, W. Gao, A. Mohammadreza, L. Kelbauskas, W. Zhang, R.H. Johnson, D.R. Meldrum, Quantitative single-cell gene expression measurements of multiple genes in response to hypoxia treatment, Anal Bioanal Chem 401(1) (2011) 3-13.
[184] B. Muz, P. de la Puente, F. Azab, M. Luderer, A.K. Azab, Hypoxia promotes stem cell-like phenotype in multiple myeloma cells, Blood Cancer J 4(12) (2014) e262.
[185] S. Ahmed, A.M. Evens, S. Bhalla, A. Singh, C. James, S. Yang, S. Prachand, D. Dokic, R.D. Gascoyne, J.N. Winter, P.T. Schumacker, L.I. Gordon, Hypoxia Inducible Factor 1á (HIF-1á) Regulates CD20 Expression in Lymphoma Cells: Possible Implications for Rituximab Based Therapy in Diffuse Large B Cell Lymphoma (DLBCL), Blood 114(22)(22) (2009) 1698.
[186] E. Decaup, C. Jean, C. Laurent, P. Gravelle, S. Fruchon, F. Capilla, A. Marrot, T. Al Saati, F.X. Frenois, G. Laurent, C. Klein, N. Varoqueaux, A. Savina, J.J. Fournie, C. Bezombes, Anti-

tumor activity of obinutuzumab and rituximab in a follicular lymphoma 3D model, Blood Cancer J 3 (2013) e131.
[187] K. Hayashi, E. Nagasaki, S. Kan, M. Ito, Y. Kamata, S. Homma, K. Aiba, Gemcitabine enhances rituximab-mediated complement-dependent cytotoxicity to B cell lymphoma by CD20 upregulation, Cancer Sci 107(5) (2016) 682-9.
[188] R.P. Taylor, M.A. Lindorfer, Antigenic modulation and rituximab resistance, Semin Hematol 47(2) (2010) 124-32.
[189] M.R. Smith, Rituximab (monoclonal anti-CD20 antibody): mechanisms of action and resistance, Oncogene 22(47) (2003) 7359-68.
[190] S.J. Schuster, L.Y. Huw, C.R. Bolen, V. Maximov, A.G. Polson, K. Hatzi, E.A. Lasater, S.E. Assouline, N.L. Bartlett, L.E. Budde, M.J. Matasar, H. Koeppen, E.C. Piccione, D. Wilson, M.C. Wei, S. Yin, E. Penuel, Loss of CD20 expression as a mechanism of resistance to mosunetuzumab in relapsed/refractory B-cell lymphomas, Blood 143(9) (2024) 822-832.
[191] Y. Li, L. Zhao, X.F. Li, Hypoxia and the Tumor Microenvironment, Technol Cancer Res Treat 20 (2021) 1-9.
[192] A.M. Shannon, D.J. Bouchier-Hayes, C.M. Condron, D. Toomey, Tumour hypoxia, chemotherapeutic resistance and hypoxia-related therapies, Cancer Treat Rev 29(4) (2003) 297-307.
[193] S. Kambayashi, M. Igase, K. Kobayashi, A. Kimura, T. Shimokawa Miyama, K. Baba, S. Noguchi, T. Mizuno, M. Okuda, Hypoxia inducible factor 1alpha expression and effects of its inhibitors in canine lymphoma, J Vet Med Sci 77(11) (2015) 1405-12.
[194] A.M. Evens, L.H. Sehn, P. Farinha, B.P. Nelson, A. Raji, Y. Lu, A. Brakman, V. Parimi, J.N. Winter, P.T. Schumacker, R.D. Gascoyne, L.I. Gordon, Hypoxia-inducible factor-1 alpha expression predicts superior survival in patients with diffuse large B-cell lymphoma treated with R-CHOP, J Clin Oncol 28(6) (2010) 1017-24.
[195] E.A. Pangarsa, P. Wuryantoro, R.M. Naibaho, B. Setiawan, D. Santosa, H. Istiadi, D. Puspasari, C. Suharti, Preliminary study of hypoxia markers in diffuse large B-cell lymphoma, Mol Clin Oncol 17(3) (2022) 140.
[196] X. Jing, F. Yang, C. Shao, K. Wei, M. Xie, H. Shen, Y. Shu, Role of hypoxia in cancer therapy by regulating the tumor microenvironment, Mol Cancer 18(1) (2019) 157.
[197] P. Xu, M. Wang, Y. Jiang, J. Ouyang, B. Chen, The association between expression of hypoxia inducible factor-1α and multi-drug resistance of acute myeloid leukemia, Translational Cancer Research 6(1) (2017) 198-205.
[198] M. Sohail, Z. Sun, Y. Li, X. Gu, H. Xu, Research progress in strategies to improve the efficacy and safety of doxorubicin for cancer chemotherapy, Expert Rev Anticancer Ther 21(12) (2021) 1385-1398.
[199] C. Visco, F. Pregnolato, I. Ferrarini, B. De Marco, V. Bonuomo, E. Sbisa, C. Fraenza, A. Bernardelli, I. Tanasi, F.M. Quaglia, M. Krampera, Efficacy of R-COMP in comparison to R-CHOP in patients with DLBCL: A systematic review and single-arm metanalysis, Crit Rev Oncol Hematol 163 (2021) 103377.
[200] A.L. Correia, M.J. Bissell, The tumor microenvironment is a dominant force in multidrug resistance, Drug Resist Updat 15(1-2) (2012) 39-49.
[201] M. Ikram, Y. Lim, S.Y. Baek, S. Jin, Y.H. Jeong, J.Y. Kwak, S. Yoon, Co-targeting of Tiam1/Rac1 and Notch ameliorates chemoresistance against doxorubicin in a biomimetic 3D lymphoma model, Oncotarget 9(2) (2018) 2058-2075.
[202] O.I. Berthuy, S.K. Muldur, F. Rossi, P. Colpo, L.J. Blum, C.A. Marquette, Multiplex cell microarrays for high-throughput screening, Lab Chip 16(22) (2016) 4248-4262.
[203] H.J. Hong, W.S. Koom, W.G. Koh, Cell Microarray Technologies for High-Throughput Cell-Based Biosensors, Sensors (Basel) 17(6) (2017) 1293.
[204] J.R. Rettig, A. Folch, Large-scale single-cell trapping and imaging using microwell

arrays, Anal Chem 77(17) (2005) 5628-34.
[205] K. Kato, K. Umezawa, M. Miyake, J. Miyake, T. Nagamune, Transfection microarray of nonadherent cells on an oleyl poly(ethylene glycol) ether-modified glass slide, Biotechniques 37(3) (2004) 444-452.
[206] A.M. Raffaele Lamanna, Rocco Romano, Gabriella Rainaldi, Floriana Flamma, Marzia Pentimalli, Teodorico Tancredi, Pietro Luigi Indovina, Maria Teresa Santini, Forced adhesive growth of K562 leukemic cells that normally grow in suspension induces variations in membrane lipids and energy metabolism: A proton NMRstudy, J. Biomed. Mater. Res. 46 (1999) 171-178.
[207] H. Erfle, B. Neumann, U. Liebel, P. Rogers, M. Held, T. Walter, J. Ellenberg, R. Pepperkok, Reverse transfection on cell arrays for high content screening microscopy, Nat Protoc 2(2) (2007) 392-9.
[208] A.L. Hook, H. Thissen, N.H. Voelcker, Advanced substrate fabrication for cell microarrays, Biomacromolecules 10(3) (2009) 573-9.
[209] S. Fujita, R. Onuki-Nagasaki, J. Fukuda, J. Enomoto, S. Yamaguchi, M. Miyake, Development of super-dense transfected cell microarrays generated by piezoelectric inkjet printing, Lab Chip 13(1) (2013) 77-80.
[210] K. Elvitigala, W. Mubarok, S. Sakai, Tuning the crosslinking and degradation of hyaluronic acid/gelatin hydrogels using hydrogen peroxide for muscle cell sheet fabrication, Soft Matter 19(31) (2023) 5880-5887.
[211] S. Gupta, T.J. Webster, A. Sinha, Evolution of PVA gels prepared without crosslinking agents as a cell adhesive surface, J Mater Sci Mater Med 22(7) (2011) 1763-72.
[212] N.E. Vrana, A. O'Grady, E. Kay, P.A. Cahill, G.B. McGuinness, Cell encapsulation within PVA-based hydrogels via freeze-thawing: a one-step scaffold formation and cell storage technique, J Tissue Eng Regen Med 3(7) (2009) 567-72.
[213] C. Peniche, W. Argüelles-Monal, H. Peniche, N. Acosta, Chitosan: An Attractive Biocompatible Polymer for Microencapsulation, Macromolecular Bioscience 3(10) (2003) 511-520.
[214] M. George, T.E. Abraham, Polyionic hydrocolloids for the intestinal delivery of protein drugs: alginate and chitosan--a review, J Control Release 114(1) (2006) 1-14.
[215] S. Sakai, Y. Yamada, T. Zenke, K. Kawakami, Novel chitosan derivative soluble at neutral pH and in-situ gellable via peroxidase-catalyzed enzymatic reaction, Journal of Materials Chemistry 19(2) (2009) 230-235.
[216] H.S. Mansur, E. de S. Costa, A.A.P. Mansur, E.F. Barbosa-Stancioli, Cytocompatibility evaluation in cell-culture systems of chemically crosslinked chitosan/PVA hydrogels, Materials Science and Engineering: C 29(5) (2009) 1574-1583.
[217] M. Koosha, H. Mirzadeh, Electrospinning, mechanical properties, and cell behavior study of chitosan/PVA nanofibers, J Biomed Mater Res A 103(9) (2015) 3081-93.
[218] R. Kazama, S. Fujita, S. Sakai, Cell Dome-based transfection array for non-adherent suspension cells, Biochemical Engineering Journal 213 (2025) 109554.
[219] J. Wu, D. Okamura, M. Li, K. Suzuki, C. Luo, L. Ma, Y. He, Z. Li, C. Benner, I. Tamura, M.N. Krause, J.R. Nery, T. Du, Z. Zhang, T. Hishida, Y. Takahashi, E. Aizawa, N.Y. Kim, J. Lajara, P. Guillen, J.M. Campistol, C.R. Esteban, P.J. Ross, A. Saghatelian, B. Ren, J.R. Ecker, J.C. Izpisua Belmonte, An alternative pluripotent state confers interspecies chimaeric competency, Nature 521(7552) (2015) 316-21.
[220] S. Sakai, M. Tsumura, M. Inoue, Y. Koga, K. Fukano, M. Taya, Polyvinyl alcohol-based hydrogel dressing gellable on-wound via a co-enzymatic reaction triggered by glucose in the wound exudate, J Mater Chem B 1(38) (2013) 5067-5075.
[221] N.A. Patil, B. Kandasubramanian, Functionalized polylysine biomaterials for advanced medical applications: A review, European Polymer Journal 146 (2021) 110248.

[222] S.C. Shukla, A. Singh, A.K. Pandey, A. Mishra, Review on production and medical applications of ε-polylysine, Biochemical Engineering Journal 65 (2012) 70-81.
[223] R. Ramezani Kalmer, M. Mohammadi, A. Karimi, G. Najafpour, Y. Haghighatnia, Fabrication and evaluation of carboxymethylated diethylaminoethyl cellulose microcarriers as support for cellular applications, Carbohydr Polym 226 (2019) 115284.
[224] J.C. Courtenay, M.A. Johns, F. Galembeck, C. Deneke, E.M. Lanzoni, C.A. Costa, J.L. Scott, R.I. Sharma, Surface modified cellulose scaffolds for tissue engineering, Cellulose (Lond) 24(1) (2017) 253-267.
[225] D. Castel, A. Pitaval, M.A. Debily, X. Gidrol, Cell microarrays in drug discovery, Drug Discov Today 11(13-14) (2006) 616-22.
[226] F. Scherer, M. Anton, U. Schillinger, J. Henke, C. Bergemann, A. Kruger, B. Gansbacher, C. Plank, Magnetofection: enhancing and targeting gene delivery by magnetic force in vitro and in vivo, Gene Ther 9(2) (2002) 102-9.
[227] H.J. Lee, Y.S. Lee, H.S. Kim, Y.K. Kim, J.H. Kim, S.H. Jeon, H.W. Lee, S. Kim, H. Miyoshi, H.M. Chung, D.K. Kim, Retronectin enhances lentivirus-mediated gene delivery into hematopoietic progenitor cells, Biologicals 37(4) (2009) 203-9.

List of Publications

Papers:

1. R. Kazama, R. Sato, H. Fujiwara, Y. Qu, M. Nakahata, M. Kojima, S. Fujita*, S. Sakai*, Development of non-adherent cell-enclosing domes with enzymatically cross-linked hydrogel shell, *Biofabrication*, **15(1)**, (2023), 015002.
2. R. Kazama, S. Fujita*, S. Sakai*, Cell Dome as an Evaluation Platform for Organized HepG2 cells, *Cells*, **12(1)**, (2023), 69.
3. R. Kazama, S. Sakai*, Effect of cell adhesiveness of Cell Dome shell on enclosed HeLa cells, *Journal of Bioscience and Bioengineering*, **137**, (2024), 313-320.
4. R. Kazama, S. Fujita, S. Sakai*, Cell Dome-based transfection array for non-adherent suspension cells, *Biochemical Engineering Journal*, **213**, (2025), 109554.
5. R. Kazama, R. Ishikawa, S. Sakai*, Development of Hemispherical 3D Models of Human Brain and B Cell Lymphomas Using On-Chip Cell Dome System, *Bioengineering,* **11(12)**, (2024), 1303.

International Conference/Symposium:

6. Ryotaro Kazama, Ikki Horigchi, Masaru Kojima, Satoshi Fujita, Shinji Sakai, "The development of hemispherical cell-enclosing domes for culture and evaluation of non-adherent cells", 3rd Asian Congress; Alternatives to Animal Experiments (ACAAE 2022), 14^{th} - 16^{th}, December 2022, Jeju, Republic of Korea, (Poster).
7. Ryotaro Kazama, Shinji Sakai, "Cell Adhesiveness of Hydrogel Shell Composing Cell Dome: Effect on the Cells Cultured in Cell Dome", 16th Asian Congress on Biotechnology, 15^{th} - 19^{th} October 2023, Ho Chi Minh City, Vietnam, (Poster).
8. Ryotaro Kazama, Shinji Sakai, "3D co-culture of lymphoma-derived cells and vascular endothelial cells in Cell Dome", 12th World Biomaterials Congress (WBC 2024), 26^{th} -

31st May 2024, Daegu, Republic of Korea, (Oral Presentation).

9. Ryotaro Kazama, Shinji Sakai, "Novel Transfection array for non-adherent cells in suspension utilizing Cell Dome", 2024 8th International Conference on Nanomaterials and Biomaterials (8th ICNB 2024), 25th - 28th November 2024, Phuket, Thailand, (Oral Presentation).

Award:

10. "Silber Award" 3rd Asian Congress; Alternatives to Animal Experiments (ACAAE 2022), 14th - 16th, December 2022, Jeju, Republic of Korea.

Acknowledgments

The author is deeply grateful to Professor Shinji Sakai (Division of Chemical Engineering, Graduate School of Engineering Science, Osaka University) for his constant guidance, helpful advice, and encouragement throughout this study. The author would like to express her sincere gratitude to Associate Professor Masaru Kojima (Division of Chemical Engineering, Graduate School of Engineering Science, Osaka University), Assistant Professor Masaki Nakahata (Graduate School of Science, Osaka University), and Assistant Professor Ikki Horiguchi (Division of Chemical Engineering, Graduate School of Engineering Science, Osaka University) for their valuable advice and encouragement during this work.

The author is also grateful to Dr. Satoshi Fujita (AIST-Osaka University Advanced Photonics and Biosensing Open Innovation Laboratory, National Institute of Advanced Industrial Science and Technology (AIST)), and Professor Keiichiro Suzuki (Graduate School of Engineering Science, Osaka University) for their valuable advice and comments on this dissertation.

The author would like to thank Professor Atsushi Shono (Department of Industrial Chemistry, Faculty of Engineering, Tokyo University of Science) and Lecturer Yuya Murakami (Applied Chemistry and Biochemical Engineering, Shizuoka University) for their kind cooperation.

The author would like to thank all the members of Sakai Laboratory for their experimental encouragement and friendship.

The author gratefully acknowledges the financial support for this study by the fellowship of the JST SPRING and Japan Society for the Promotion of Science (JSPS).